

# The Application of Liquid- Scintillation Counting to Radionuclide Metrology <sup>1st</sup>

edition 1980





---

**Bureau International  
des Poids et Mesures**

**1<sup>st</sup> edition      1980**

---

#### Copyright statement

This document is distributed under the terms of the Creative Commons Attribution 4.0 International License (<http://creativecommons.org/licenses/by/4.0/>), which permits unrestricted use, distribution, and reproduction in any medium, provided you give appropriate credit to the original author(s) and the source, provide a link to the Creative Commons license, and indicate if changes were made.

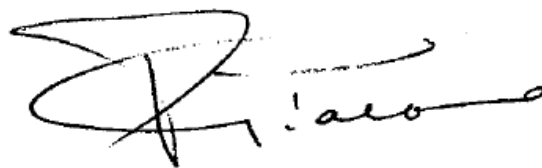
## Foreword

This monograph is one of several to be published by the Bureau International des Poids et Mesures (BIPM) on behalf of the Comité Consultatif pour les Etalons de Mesure des Rayonnements Ionisants (CCEMRI). The aim of this series of publications is to review various topics which are of importance for the measurement of ionizing radiation and radioactivity, in particular those techniques normally used by participants in international comparisons. It is hoped that these publications will prove to be useful reference volumes both for those who are already engaged in this field and for those who are approaching such measurements for the first time.

It is the purpose of this monograph to discuss the special problems that arise when liquid-scintillation counting is used for radionuclide metrology where the requirements are more exacting than for the routine counting of samples in biomedical and related fields for which the technique is so widely used. The contributions were solicited by a working group of Section II of the CCEMRI and edited by W.B. Mann and J.G.V. Taylor, with comments on the final draft from J. Steyn.



E. Ambler  
Chairman of the CCEMRI



P. Giacomo  
Director of the BIPM

# The Application of Liquid-Scintillation Counting to Radionuclide Metrology

## Contents

<b>1. Introduction</b>	<b>8</b>
<b>2. Applications of Liquid Scintillation Counting in Science and Technology</b>	<b>10</b>
2.1. Introduction	10
2.2. Experimental biochemistry	10
2.3. Pharmacological, medical and biological applications	10
2.4. Geophysical and related applications	11
2.5. Archaeology	11
2.6. Miscellaneous applications	12
2.7. Possible future trends	12
<b>3. The Preparation of Counting Samples</b>	<b>13</b>
3.1. Introduction	13
3.2. Ideal solution counting samples	17
3.3. Real solution counting samples	20
3.4. Emulsion counting samples	23
<b>4. Design of High-Efficiency Liquid-Scintillation Counting Systems</b>	<b>27</b>
4.1. Introduction	27
4.2. Methods of comparing liquid-scintillation counting systems	27
4.3. Considerations for optimizing the figure of merit	30
4.4. Designs for high-efficiency liquid-scintillation counting systems	34
4.5. Conclusions	39
<b>5. The Statistics of the Scintillation Process and Determination of the Counting Efficiency</b>	<b>41</b>
5.1. Introduction	41
5.2. Theoretical pulse-height distributions	42
5.3. The counting efficiency	51
5.4. Non-linear effects	52
5.5. System design and testing	58
5.6. Conclusions	59
<b>6. The Use of Liquid Scintillators in Radionuclide Metrology</b>	<b>60</b>
6.1. Introduction	60
6.2. Characteristics of metrology equipment	60
6.3. The methods	62
6.4. Conclusion	67

<b>7. The Problem of Afterpulses</b>	<b>68</b>
7.1. Introduction	<b>68</b>
7.2. Afterpulses in electron-multiplier phototubes	<b>68</b>
7.3. The effect of $\gamma$ rays on electron-multiplier phototubes	<b>71</b>
7.4. The decay of excited liquid scintillation	<b>72</b>
7.5. Phosphorescence problems	<b>72</b>
7.6. Some quantitative measurements of afterpulses	<b>73</b>
7.7. Conclusion	<b>75</b>
<b>8. Intercomparison of <math>^{134}\text{Cs}</math> by Liquid-Scintillation Counting</b>	<b>76</b>
8.1. Introduction	<b>76</b>
8.2. Counting equipment and conditions	<b>77</b>
8.3. Results	<b>78</b>
8.4. Non liquid-scintillation results	<b>79</b>
8.5. Conclusion	<b>80</b>
<b>References</b>	<b>81</b>

# 1. Introduction

In 1970 Section II, CCEMRI, set up a small working group to look into the “feasibility of liquid-scintillation counting for the metrology of radionuclides which decay by the emission of low-energy radiation”.

At the time, liquid-scintillation (LS) counting was already well established as the counting method of choice for the routine assay of biological and medical samples labelled with  $^3\text{H}$  and  $^{14}\text{C}$ . One large university reported processing  $3 \times 10^6$  samples per year. This popularity had resulted in the development of commercial instruments fitted with high-capacity sample changers and sophisticated data-processing electronics.

The major attraction of LS counting for metrologists, essentially  $4\pi$  geometry for even relatively low-specific-activity sources, had been found to be partially offset by problems and pitfalls related to its major drawback, a very low scintillation efficiency. In general these problems cannot be overcome to the extent required for highly accurate direct activity measurements with unmodified commercial instruments. With the aim of bringing discussions of the salient points together with a useful bibliography under one cover, the working group solicited the reviews that make up this volume. Unfortunately this has taken much longer than first anticipated and these editors who took up the task in 1977 are particularly grateful to Dr. B.W. Fox and Dr. J.A.B. Gibson who prepared first drafts promptly and then agreed to bring them up to date several years later. No attempt has been made to impose uniformity of style or treatment and, since the topics are by no means independent, it has not been practical to eliminate completely some duplication of subject matter from one part to another. In this respect we wish to acknowledge the help of Dr. B.W. Fox and Dr. B.M. Coursey in eliminating considerable duplication between Chapter 2 and Chapter 3.

In summary, Chapter 2 is the least directly concerned with metrology. It serves as a useful introduction to the subject with emphasis on the ubiquity of LS counting in the life and earth sciences. Despite its title, Chapter 3 is not a repetition of the material in several recent reviews on LS sample preparation; it stresses procedures to be followed to obtain sources for standardization with the highest possible efficiency and stability. Chapter 4 explains the physical principles underlying the special configurations that distinguish instruments optimized for metrology from commercial models designed for high throughput with minimal user intervention. Chapter 5 outlines the statistical analysis and calibration procedure required to compensate for the zero-detection probability resulting from the very low scintillation efficiency of LS systems. The published accounts of radioactivity standardizations made with systems using liquid scintillators are reviewed in Chapter 6. A general review of spurious pulses was given in an earlier monograph in this series, and Chapter 7 deals specifically with afterpulses to which LS systems employing sensitive phototubes at high gains are particularly susceptible.

The final part Chapter 8 gives the results of an intercomparison arranged by the working group in which the participants measured  $^{134}\text{Cs}$  by  $4\pi\beta(\text{LS})\text{-}\gamma$  coincidence counting. It should be noted that the coincidence method does not involve explicit consideration of the zero-detection probability Chapter 5. The efficiency-extrapolation problems in the two cases are quite different. In the preparation of Chapter 8 the editors wish to acknowledge the assistance of Dr. D. Smith and Dr. L.L. Lucas.

---

J.G. V. Taylor  
Atomic Energy of Canada Limited

W.B. Mann  
National Bureau of Standards



Chalk River, Ontario

Washington, D.C.

---

## 2. Applications of Liquid Scintillation Counting in Science and Technology

B.W. Fox<sup>(1)</sup>

<sup>(1)</sup> Christie Hospital and Holt Radium Institute, Withington, Manchester M20 9BX, UK.

### 2.1. Introduction

The introduction of liquid-scintillation (LS) counting in the mid 1950's revolutionized the use of soft  $\beta$ -emitting radionuclides in a wide diversity of applications. The most extensive application has undoubtedly been in the field of experimental biochemistry concerned with drug metabolism and basic biochemical investigations associated with problems in molecular biology.

In addition, the availability of many radionuclides, already formulated into pure inorganic and organic chemicals, has enabled a wider diversity of disciplines to employ LS counting in their investigations. Some 80 of these radionuclides are listed in Table 1. Clinical biochemistry has seen the development of body-fluid assays and of radioimmunoassay methods. Considerable improvements in the assay of  $\beta$ -particle emitters in very low radioactivity concentrations in aqueous solution has also led to a wider application within such fields as hydrology, climatology and archaeology.

As the modern LS spectrometer has been developed into an automated, high-precision photon detector, capable of providing data in a form suitable for computer analysis, its use has been extended to applications (not involving liquid scintillators) such as the study of chemiluminescence, bioluminescence and the measurement of Čerenkov radiation.

### 2.2. Experimental biochemistry

Many precursors of macromolecular synthesis, such as amino acids, nucleic acid bases and their corresponding nucleosides and nucleotides, lipids, steroids as well as short-chain macromolecules such as peptides and oligonucleotides are now readily available from commercial sources, often with the radioactive label in highly specific sites. Almost all types of tissues can now be processed rapidly to a form suitable for efficient assay in the LS spectrometer. Early reviews of particular value are those of Rapkin [83] (covering the years 1957 to 1963), Parmentier and ten Haaf [142] (from 1963 to 1968), Price [208] (up to 1972), and Fox [253] (1973-1974). There are several publications of International Symposia [27], [147], [175], [192], [214], [233], [265] dealing with this subject, as well as monographs [69], [168], [254], [275] covering the field of sample-preparation techniques. A large part of this literature deals with specialized procedures developed to assay specific biological materials, some of which were adapted to metrology studies. Basic sample preparation techniques with emphasis on their application to radionuclide metrology are described in Chapter 3 of this Monograph.

### 2.3. Pharmacological, medical and biological applications

The use of radioactively labelled drugs in pharmacological studies has contributed, to a considerable extent, to our knowledge of the disposition and metabolism of such drugs in

both animals and man. Many techniques have been described for the radioassay of whole blood, plasma, urine and other body fluids as well as the tissues themselves [254]. The advent of radioimmunoassay procedures [181] has still further advanced our knowledge of physiological functions, avoiding the problems associated with the administration of radioactively labelled substances to patients. The accidental ingestion of soft  $\beta$ -emitters can be monitored more accurately, e.g.  $^3\text{H}$  in urine. A survey [72] of 300 000 samples over a tenyear period to 1964 showed that the lower detection limit was approximately  $18 \text{ kBq ml}^{-1}$ . Also by measuring  $^3\text{H}$  levels in blood samples and in urine at prescribed times after injection of trace levels of tritiated water, the total body water in patients can be calculated, an important parameter in certain chronic disease states [184]. Iron-absorption efficiency by the gut can also be measured by injection of  $^{55}\text{Fe}$  intravenously, followed one hour later by an orally administered dose of  $^{59}\text{Fe}$ , and measuring the relative levels of the two isotopes in the blood twelve to fourteen days later [99].  $^{129}\text{I}$  and  $^{125}\text{I}$  have been used in similar fashion to study thyroid function [67].

The detection and measurement of a variety of radionuclides derived from the environment, such as fall-out from nuclear explosions, is exemplified by the assay of  $^{147}\text{Pr}$  in urine [82],  $^{32}\text{P}$  in foodstuffs [100] and  $^{239}\text{Pu}$  in tissue [140]. The incorporation of organo-tin [145], thallium and lead compounds [258] into scintillator mixtures has increased the absorption of soft  $\gamma$  rays so that they can be detected more efficiently in LS counters. A small volume of aqueous sample is placed in a separate vial suspended in the scintillator. Thus total recovery of the sample is possible.

## 2.4. Geophysical and related applications

The sensitive assay of  $^3\text{H}$  at low concentrations is of considerable importance in those hydro-geological problems associated with the tracing of underground water supplies and the direction of movement of water and brine in oil fields [118]. Also, the movement and age of water in surface waters in ponds and lakes [93], as well as the problems of water movement in estuaries in connection with sewage disposal, can be determined.

The radioassay of natural  $^3\text{H}$  has been much improved [212] by initially converting water into acetic acid by reaction with acetic anhydride. The resulting  $^3\text{H}$ -acetic acid is then reacted with calcium carbide to prepare acetylene which is further polymerized to benzene. Detection limits using this procedure are reported to be as low as one tritium atom per  $10^{18}$  hydrogen atoms.

## 2.5. Archaeology

Carbon-14, with a 5730-year half-life, is continuously being introduced into the biosphere at a relatively constant rate (except for nuclear explosions) by particle reactions in the upper atmosphere. The carbon laid down in plant growth therefore has a characteristic  $^{14}\text{C}$  to  $^{12}\text{C}$  ratio. Hence a measurement of the proportion of the two isotopes present in a piece of ancient carbonaceous material gives an estimate of the age of the sample.

The conventional method [248] of radiocarbon dating using LS counting is to combust the sample in oxygen and trap the evolved  $\text{CO}_2$ . The  $\text{CO}_2$  formed is then converted to lithium carbide. Water is used to convert the carbide into acetylene gas which is then polymerised to benzene for assay. Contemporary carbon as benzene gives a count rate of  $0.123 \text{ s}^{-1}$  per gram of carbon, corresponding to 95% of the 1962 National Bureau of Standards (NBS) oxalic-

acid- $^{14}\text{C}$  standard, with an overall chemical yield of 96 to 98% and a counting efficiency of 65 to 70%. A bomb combustion method has also been described [235] to process up to 12 g of sample.

## 2.6. Miscellaneous applications

Spectral resolutions attainable in LS counters for  $\alpha$ -emitting nuclides have been studied in some detail by Horrocks [81] and by McDowell [183], using such nuclides individually and in mixtures. By means of pulse-shape discrimination techniques [236], a more accurate discrimination of particle type can be made, extending considerably the range of complexity of mixtures which can be analysed.

LS counting has also been applied to the study of oil distribution in petrol and diesel engines [201], as well as in leaks of gas-containing equipment [200]. The “assimilation” and “mineralisation” of sea-water samples have also been measured [220] by the conversion of  $^{14}\text{C}$ -glucose into  $^{14}\text{CO}_2$ .

## 2.7. Possible future trends

Further applications of the techniques of LS counting are inevitable, especially as the on-line and off-line processing of data become more sophisticated. A more detailed study of colloid-scintillation counting may lead to new ways of attacking problems associated with biological membranes. The use of solvents with high refractive indices or regions of anomalous dispersion may extend the application of LS systems for Čerenkov counting (with its freedom from chemical quenching) to radionuclides with maximum  $\beta$ -particle energies far below the 0.26 MeV Čerenkov threshold in water [289], [163]. Although the advent of microprocessor technology may allow for more rapid acquisition and processing of data, it will still be necessary to ensure that raw data are also available for checking or for alternative treatment.

### 3. The Preparation of Counting Samples

B.M. Coursey<sup>(1)</sup> and A.A. Moghissi<sup>(2)</sup>

<sup>(1)</sup> Radioactivity Group,  
National Bureau of  
Standards, Washington,  
D.C. 20234, USA.

<sup>(2)</sup> Georgia Institute of  
Technology, Atlanta,  
Georgia 30332, USA.

#### 3.1. Introduction

This part is intended as a guide to sample preparation for radionuclide metrology techniques employing LS counting. This material should also be useful to those engaged in applied-science studies, such as radioimmunoassay or environmental monitoring, which generally involve comparative rather than direct activity measurements.

The physical and chemical properties are examined for the three types of counting sample most often employed in standards work. A counting sample is defined here as a sealed source containing the organic scintillator solution plus sample. Examples are given for the preparation of such samples for a number of radionuclides which differ in their chemical behaviour as well as in their nuclear-decay schemes.

The most often stated advantage of LS counting over other counting techniques is that the sample may be incorporated into the detector and  $4\pi$  geometry is thereby obtained. The ease of sample preparation and the high  $\beta$ -particle counting efficiencies attainable for  $^3\text{H}$  and  $^{14}\text{C}$ -labelled biological samples have made LS counting a major tool in life-sciences research. Lowenthal [227] reported that more than  $10^7$  LS counting measurements were made annually.

By comparison, very few LS measurements are made in the field of radionuclide metrology, the subject of the present report. It is not surprising then that most of the problems discussed in the literature on sample preparation for LS counting arise because an organic sample containing  $^3\text{H}$  or  $^{14}\text{C}$  is not in a suitable chemical or physical form for dissolution in an organic-liquid scintillator. Several review articles on sample preparation are available: Parmentier and ten Haaf [142], Turner [188], Rapkin [209], Kobayashi and Maudsley [224], Fox [254], Peng [275]. Most of the several hundred references cited in these reviews deal with the specifics of how to oxidize, combust, or solubilize organic materials so that they may be incorporated into a scintillating matrix for a comparative assay.

In radionuclide metrology, however, the choice of the composition for the counting sample depends not so much on the organic chemistry of the sample as it does on the chemical behavior and decay scheme of the radionuclide to be measured. Table 1 lists radionuclides, grouped according to their chemical behavior, which may be of interest in radionuclide metrology. Many of the references in the table were taken from earlier reviews on this subject by Dyer [193], Horrocks [223] and Peng [242]. Figure 1 is a periodic chart showing the 57 different elements which have been incorporated into LS counting samples.

METALS																		NONMETALS																				
IA																		III A	IV A	V A	VI A	VII A	He															
(H)	II A	TRANSITION METALS																B	(C)	N	O	F	Ne															
Li	Be																	Al	(Si)	P	(S)	(Cl)	(Ar)															
Na	Mg	III B	IV B	V B	VI B	VII B	VIII			IB	II B							Ga	Ge	As	Se	Br	(Kr)															
K	Ca	Sc	Ti	V	Cr	Mn	Fe	Co	Ni	Cu	Zn							In	Sn	Sb	Te	(I)	(Xe)															
Rb	Sr	Y	Zr	Nb	Mo	Tc	Ru	Rh	Pd	Ag	Cd							Tl	Pb	Bi	Po	At	(Rn)															
Cs	Ba																	Hf	Ta	W	Re	Os	Ir	Pt	Au	Hg	Tl	Pb	Bi	Po	At	(Rn)						
Fr	Ra																																					
LANTHANIDE SERIES		La	Ce	Pr	Nd	Pm	Sm	Eu	Gd	Tb	Dy	Ho	Er	Tm	Yb	Lu																						
ACTINIDE SERIES		Ac	Th	Pa	U	Np	Pu	Am	Cm	Bk	Cf	Es	Fm	Md	No	Lw																						

Ar

IDEAL  
SOLUTION  
SCINTILLATOR

Be

REAL  
SOLUTION  
SCINTILLATOR

Sc

EMULSION  
SCINTILLATOR

Figure 1 — Periodic chart of the elements showing the liquid-scintillator formulations that have been used for radioisotopes of the indicated elements.

Table 1. Radionuclides which have been assayed by liquid-scintillation counting

Group I A (except $^3\text{H}$ )	
$^{22}\text{Na}$	[56], [74], [88], [95]
$^{24}\text{Na}$	[31], [49]
$^{40}\text{K}$	[57], [56]
$^{42}\text{K}$	[154]
$^{86}\text{Rb}$	[154], [205]
$^{87}\text{Rb}$	[36]
$^{134}\text{Cs}$	[245]
$^{137}\text{Cs}$	[64], [77], [95]
Group II A	
$^7\text{Be}$	[95]
$^{10}\text{Be}$	[102]
$^{45}\text{Ca}$	[38], [95]
$^{85}\text{Sr}$	[95], [213]
$^{89}\text{Sr}$	[243]
$^{90}\text{Sr}$	[95], [94], [243]
$^{133}\text{Ba}$	[202]
$^{226}\text{Ra}$	[77], [286]

## Group III A

$^{114}\text{In}^{\text{m}}$	[77]
$^{204}\text{Tl}$	[74], [95], [91]

## Group IV A (except carbon)

$^{32}\text{Si}$	[71]
$^{113}\text{Sn}$	[77], [203]
$^{121}\text{Sn}^{\text{m}}$	[281]
$^{210}\text{Pb}$	[131]

## Group V A

$^{32}\text{P}$	[23], [48], [95]
$^{124}\text{Sb}$	[88]
$^{207}\text{Bi}$	[77]
$^{210}\text{Bi}$	[131]

## Group VI A

$^{35}\text{S}$	[52], [95]
$^{210}\text{Po}$	[77], [131], [95]

## Group VII A

$^{36}\text{Cl}$	[95], [105], [202]
$^{125}\text{I}$	[67], [92], [213], [257]
$^{129}\text{I}$	[92], [222]
$^{131}\text{I}$	[23], [48], [95], [92], [213]
$^{211}\text{At}$	[20]

## Noble gases

$^{37}\text{Ar}$	[240]
$^{85}\text{Kr}$	[79], [98], [143], [241]
$^{131}\text{Xe}^{\text{m}}$	[79]
$^{133}\text{Xe}$	[240], [241]
$^{135}\text{Xe}$	[241]
$^{222}\text{Rn}$	[79], [286]

## Groups I Band II B

$^{110}\text{Ag}^{\text{m}}$	[74]
$^{198}\text{Au}$	[48], [49], [95], [88]
$^{65}\text{Zn}$	[122], [202]
$^{109}\text{Cd}$	[80], [256]
$^{203}\text{Hg}$	[80]

## Groups III B, IV B, V B

$^{46}\text{Sc}$	[205]
$^{90}\text{Y}$	[243]
$^{95}\text{Zr}$ - $^{95}\text{Nb}$	[45], [88]
$^{95}\text{Nb}$	[45], [156]

## Groups VI B and VII B

---

$^{51}\text{Cr}$	[122], [186], [239]
$^{54}\text{Mn}$	[95], [122]
$^{56}\text{Mn}$	[95]
$^{99}\text{Tc}$	[91], [300]

## Group VIII

---

$^{55}\text{Fe}$	[122], [128], [174]
$^{59}\text{Fe}$	[205]
$^{57}\text{Co}$	[122], [213]
$^{60}\text{Co}$	[23], [48], [95], [88], [169], [202]
$^{63}\text{Ni}$	[59]
$^{106}\text{Ru}$	[53], [169]

## Lanthanides

---

$^{139}\text{Ce}$	[276]
$^{144}\text{Ce}$	[75], [88], [202]
$^{147}\text{Pm}$	[82], [74]
$^{147}\text{Sm}$	[77], [73]
$^{151}\text{Sm}$	[53]
$^{176}\text{Lu}$	[73]

## Actinides

---

$^{230}\text{Th}$	[77]
$^{232}\text{Th}$	[51], [77]
$^{233}\text{U}$	[81], [256]
$^{238}\text{U}$	[47], [221]
$^{238}\text{Pu}$	[81]
$^{239}\text{Pu}$	[77], [182], [225]
$^{241}\text{Pu}$	[129]
$^{241}\text{Am}$	[95], [183], [191], [189], [182], [283]
$^{243}\text{Am}$	[183]
$^{244}\text{Cm}$	[183], [283]
$^{249}\text{Bk}$	[183]
$^{252}\text{Cf}$	[183], [283]
$^{253}\text{Es}$	[183]

---

The list given in this table differs from those given in previous reviews on this subject. No attempt was made to list all radionuclides ever counted in an LS spectrometer. The emphasis was on the assembling of as many references as possible which would aid the reader in preparing high-efficiency liquid scintillators.

References are not given to Čerenkov counting or counting using suspended or gel scintillators. Short half-life daughters, such as  $^{113}\text{In}^m$  and  $^{144}\text{Pr}$ , were not listed except in those instances where the daughter activity was measured after chemical separation from the parent radionuclide. References were not included to metrology studies in which the scintillator was not specified (e.g.  $^{67}\text{Ga}$  and  $^{87}\text{Y}$  [210], see p. 93) and one extensive list [218] (containing among others  $^{47}\text{Ca}$ ,  $^{58}\text{Co}$ ,  $^{64}\text{Cu}$ ,  $^{75}\text{Se}$ ,  $^{82}\text{Br}$ ,  $^{99}\text{Tc}^m$ ,  $^{169}\text{Yb}$ ) was not included because the sample preparations described there, for use in biological studies, were considered



to be inappropriate for use in radionuclide metrology. Twelve radionuclides not given here are included in a list published recently by Joy [282]. They were not included here because no references were given to the original work.

Most of the counting samples used in standards work fall into one of the following three categories:

1. **“Ideal” solutions**—Ideal counting samples are those consisting of an efficient aromatic solvent and one or more scintillators at optimum concentrations. The sample to be assayed is a simple nonquenching organic compound such as  $^3\text{H}$ -toluene. Calibrated sealed sources of this type are often sold as “unquenched standards”.
2. **“Real” solutions**—More often, the sample is only sparingly soluble in the aromatic solvent and other agents must be added to increase the solubility. Two common ways of doing this are to add a second polar solvent such as ethanol, or to add a chelating agent which binds the radionuclide in a soluble complex.
3. **“Liquid-liquid emulsions”**—These are the most popular counting samples in use today. They consist of small water droplets or micelles uniformly dispersed in the organic solvent. Non-ionic detergents are used as the dispersing agent. The radionuclide to be measured is usually in the aqueous phase whereas the scintillation process occurs in the organic phase.

In the remainder of the present work, these three categories are examined in greater detail. For each of these types of samples, sections are included dealing with general considerations, uses, and methods of preparing stable counting samples.

## 3.2. Ideal solution counting samples

### 3.2.1. General considerations of ideal solution counting samples

Most of the advances in LS counters over the past twenty years—at least those that resulted in greater counting efficiency—have been due to improvements in the phototubes and in the optical and electronic design. Scintillator formulations, by comparison, have changed very little. Now, as twenty years ago, an example of an unquenched counting sample is  $^3\text{H}$ -toluene in toluene containing 3 g/l PPO and 0.5 g/l POPOP<sup>(1)</sup>.

Different formulations can be compared using the figure of merit given by Birks [69]. The figure of merit is the number of photoelectrons arriving at the first dynode of the phototube per kiloelectronvolt of energy deposited in the scintillator. Its use in radionuclide metrology is discussed in Chapter 4 and Chapter 5 of this Monograph. More recently Birks [238] has isolated those terms from the figure of merit over which the chemist has some control and defined the product of those terms as the scintillator figure of merit which depends upon

1. the choice of the solvent,
2. the solvent-solute energy transfer efficiency,
3. the solute quantum yield and concentration, and
4. the matching between solute fluorescence and phototube absorption.

<sup>(1)</sup> A list of scintillators referred to in this Monograph is given in Table 2

**Table 2. Abbreviations, chemical formulae and wavelengths ( $\lambda$ ) at fluorescence-emission maxima for organic scintillators referred to in this Monograph<sup>2</sup>**

2

Chemical structures for these scintillators, except for PPD and BIBUQ are given in Table 6 of [284]. (2)

Abbreviation	Formula	Fluorescence-emission maximum $\lambda$ (nm)
<b>Primary scintillators</b>		
TP	p-terphenyl	342
PPD	2, 5-diphenyl-1, 3, 4-oxadiazole	360
PPO	2, 5-diphenyloxazole	375
PBD	2-phenyl-5-(4-biphenyl)-1, 3, 4-oxadiazole	375
t-butyl-PBD	2-(4'-t-butylphenyl)-5-(4''-biphenyl)-1, 3, 4-oxadiazole	385
BIBUQ	4, 4'''-bis-(2-butyloctyloxy)-p-quaterphenyl	366, 385
<b>Secondary scintillators</b>		
POPOP	1, 4-di-(2-(5-phenyloxazolyl))-benzene	415
DM-POPOP	1, 4-di-(2-(4-methyl-5-phenyloxazolyl))-benzene	427
bis-MSB	p-bis-(o-methylstyryl)-benzene	425

Following procedures given in Birks [238], one can arrive at scintillator combinations which give slightly higher scintillator figures of merit than the toluene solution of PPO and POPOP. Tables comparing the most frequently used LS solvents are given in Birks [69]. Simple aromatic compounds such as benzene, toluene and p-xylene have long been recognized as the most efficient solvents, for reasons described in Fuchs et al. [170] and Laustriat et al. [158].

The choice of scintillators is often governed by the spectral response of the phototube. Response curves for the current alkali phototubes, such as the RCA 8850, Philips 56 DUVP, and EMI 9813-B, are given in the manufacturers' literature, and fluorescence spectra and quantum yields for a large number of scintillators are given in Berlan [166]. Although PPO is still the most common primary solute, terphenyl, PBD and tert-butyl-PBD are also used for some applications [209]. For many of these solutes there is an optimum concentration beyond which the scintillation yield decreases due to "self quenching". Optimum concentrations for primary solutes are given in Birks [69] and Horrocks [223]. Details of quenching caused by excimers (excited complexes containing two solute molecules) are discussed by Horrocks [176], [223].

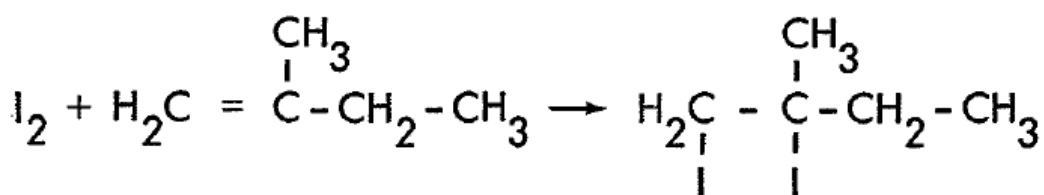
In the latest alkali tubes, the absorption spectra sufficiently overlap the PPO fluorescence spectrum that there is little need for a wavelength shifter. Nevertheless, most workers continue to add the secondary solute, particularly if color quenching due to the sample is anticipated. The three most often used are POPOP, dimethyl-POPOP and bis-MSB. Bis-MSB is slightly more soluble in the common solvents than the oxazoles and solubility is often the determining factor.

<sup>2</sup> Chemical structures for these scintillators, except for PPD and BIBUQ are given in Table 6 of [284].

### 3.2.2. Uses of ideal solution counting samples

**Nobles gases**—As may be seen from the periodic table in Figure 1, noble gas radionuclides are among the few which have been assayed in unquenched or ideal counting samples. At one symposium on the noble gases [247], several papers were devoted to LS counting. For accurate work the solubility of the noble gas in the scintillator must be determined at the temperature at which measurements will be made [79]. The solubility of these gases in toluene increases with atomic weight, so the proportion of activity in the gas phase is relatively larger for lighter gases, such as  $^{37}\text{Ar}$  and  $^{85}\text{Kr}$ , than it is for heavier members of the group, such as  $^{133}\text{Xe}$  and  $^{222}\text{Rn}$ .

**Group VII A—The halides**—The halides, such as  $^{36}\text{Cl}$  and  $^{125}\text{I}$ , are normally assayed as salts in alkaline solution. If it is necessary to prepare unquenched samples, however, they may be converted to organic halides. An often cited example is that of Yerick and Ross [67], who reacted molecular iodine, as both  $^{125}\text{I}$  and  $^{129}\text{I}$ , with an olefin by the reaction

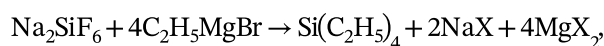


The alkyl halide obtained is only a mild quenching agent and is quite stable except in alkaline solution, where the iodide groups may be replaced by -OH groups.

Ronzani and Tamers [105] report that unquenched samples containing  $^{36}\text{Cl}$  may be prepared by synthesizing silicon tetrachloride ( $\text{SiCl}_4$ ) which is then dissolved in a toluene-PBD liquid scintillator.

**Groups II B and III A—VI A**—If it is necessary to dissolve radionuclides from these groups in unquenched counting samples, there are a number of organometallic compounds available. Dimethyl-Hg, for instance, could be used for  $^{203}\text{Hg}$ . Many organometallic compounds of gallium, indium, and selenium are available commercially because of their usefulness in semiconductor research [250]. Organometallic compounds of heavy elements, such as tetrabutyltin and tetraethyl lead, are often used to increase the detection efficiency for  $\gamma$  rays [69].

Most of these organometallic compounds are synthesized by Grignard reactions. A useful example is the work of Brodzinski et al. [71] with  $^{32}\text{Si}$ . They prepared a nonquenching tetralkyl silicon compound by the reaction



where X = Br or F.

The magnesium compound on the left is called a Grignard reagent. Such agents are widely used for attaching alkyl groups to metals and some non-metals in groups III A–VI A. In the work cited above, the  $^{32}\text{Si}$ -tetraethyl silane was introduced into a toluene solution scintillator.

### 3.2.3. Preparation of ideal solution counting samples

Pure solvents and scintillators must be used to avoid quenching caused by impurities [229]. One can buy scintillators individually, as premixed blends, or as concentrates, which are

diluted with additional solvent to the optimum concentration. These optimum concentrations are typically 5 to 10 g/l for the primary solute and 1 to 2 g/l for the secondary solute.

In metrology studies two preparation methods are used for these types of samples. The most prevalent method is to pipet the scintillator solution into the counting vial and then to dispense an aliquot of the sample material into the vial. There are two drawbacks to this straightforward technique. First, it is desirable to remove oxygen from the counting sample, to minimize quenching, and one cannot easily purge the vial after a volatile sample has been added. Second, errors in dispensing volatile samples will be greater than those incurred in dispensing aqueous samples in the same mass range.

Merritt [207] and BIPM [237] describe in detail the inaccuracies involved in dispensing aqueous samples in the range 20 to 70 mg. It is exceedingly difficult to dispense  $^3\text{H}$ -toluene with comparable accuracy.

The more accurate method is to spike a large quantity of the solvent (of the order of one litre) with a small sample (1 to 5 g). Aliquots of the large batch are then dispensed into the cells. See, for example, Garfinkel et al. [90]. In this procedure weighing errors are much less than 0.1% because of the relatively large masses being transferred. Deoxygenating however is still a formidable problem.

The oxygen may be removed by purging with a nonquenching gas, usually nitrogen or argon, or by vacuum techniques. Despite the simple principles involved in these two operations, a great deal of care is necessary to insure that part of the sample is not removed with the oxygen. An example of a vacuum system used for LS sample preparation is given by Johns [241]. In this system, an LS vial with a Luer fitting is placed on a vacuum rack, the gaseous sample ( $^{85}\text{Kr}$ ,  $^{133}\text{Xe}$ ,  $^3\text{H}$ -methane) is cryogenically transferred to the vial, and then de gassed scintillator is introduced.

In another method described by Shuping et al. [143], the solvent is refluxed for about fifteen minutes to remove oxygen. Subsequently, the system is enclosed and the solvent permitted to cool. The solvent may then be transferred either in a manifold or by using an inert gas atmosphere.

### 3.3. Real solution counting samples

#### 3.3.1. General considerations of real solution counting samples

Most measurements in LS metrology before 1970 were made using what we have called real solutions. That is, some other agent was added to insure the solubility of the sample radionuclide in the solvent. The five predominant types of real solutions are

1. those containing labelled cation salts of organic acids, such as  $^{87}\text{Rb}$ -octoate [36],
2. those containing labelled cations complexed by alkyl phosphate chelating agents, such as  $^{147}\text{Pm}$ -diethyl hexyl phosphoric acid [82],
3. binary liquid solutions, such as 8% toluene-15% ethanol, which will tolerate small quantities of water containing the sample radionuclide as an inorganic salt,
4. dioxane-naphthalene solutions, which may also be used with small aqueous samples, and lastly

5. those scintillator solutions in which organic amines are used as trapping agents for labelled anions.

Item 5) will not be dealt with here, as the use of amines for trapping  $^{14}\text{CO}_2$  and  $^{35}\text{SO}_2$  is a widely used technique and thorough reviews are available [224], [242], [275].

For most radionuclides present as cations, the choice among the first four types of solutions is somewhat arbitrary. As a general rule the counting efficiency would be slightly less for types 3) and 4) as ethanol is a mild quenching agent [223] and dioxane-naphthalene is a poor solvent relative to xylene or toluene [284]. The quenching in solutions prepared using the organic acids (types 1) and 2) will be dependent for the most part on the purity of the scintillators and reagents used.

Horrocks [223] notes that the most often used organic acids (solution type 1) are octoic and naphthenic acids. A method of preparing cadmium, bismuth, and lead octoates suitable for use in liquid scintillators is described by Ronzio [40]. Many metal salts of these acids are commercially available as they are often used as catalysts in the petrochemical industry.

The most often used chelating agent is “diethylhexyl phosphoric acid, normally abbreviated as HDEHP. Horrocks [174], [221], for example, has used HDEHP for such diverse nuclides as  $^{55}\text{Fe}$ ,  $^{113}\text{Sn}$ , and natural uranium, while Erdtmann [75] and Erdtmann and Herrmann [88] have used the same agent for  $^{22}\text{Na}$ ,  $^{60}\text{Co}$ ,  $^{95}\text{Zr}$ - $^{95}\text{Nb}$ ,  $^{124}\text{Sb}$ ,  $^{144}\text{Ce}$ - $^{144}\text{Pr}$  and  $^{198}\text{Au}$ . HDEHP is also widely used by inorganic and nuclear chemists for solvent extraction studies [126], [180], [183]. Mason et al. [261], for example, used HDEHP to extract  $^{91}\text{Y}$ ,  $^{147}\text{Pm}$ ,  $^{152}\text{Eu}$ ,  $^{170}\text{Tm}$ , and  $^{177}\text{Lu}$  from acid solutions into benzene. After equilibration of the two phases, aliquots were taken from each, evaporated to dryness, and counted with a proportional counter. Mason [274] reports that in more recent work, they have introduced the sample aliquot from each phase directly into an emulsion scintillator for LS counting.

Many other alkyl phosphates have, of course, been used for extracting radionuclides into liquid scintillators. Ludwick [45] used dibutyl phosphate to introduce  $^{95}\text{Zr}$ - $^{90}\text{Nb}$  into a xylene scintillator, while Horrocks and Harkness [59] used  $^{63}\text{Ni}$  labelled dioctyl phosphate, also in a xylene scintillator. Reference to other useful complexing agents may be found in [193] and [242].

Too few articles in the literature on LS metrology give detailed descriptions of the scintillator formulation used. Six papers which do contain a wealth of detail are listed here, along with the type of solution scintillator employed and the number of radionuclides studied (in parentheses):

Flynn et al. [77]	toluene-ethanol-octoic acid: (10)
Dyer et al. [74]	toluene-ethanol: (4)
Vaninbroukx and Spagnol [95]	toluene-ethanol: (15) dioxane-naphthalene: (13)
Erdtmann [75], Erdtmann and Herrmann [88]	toluene-ethanol-HDEHP: (6) dioxane-naphthalene: (6)
Steyn [122]	xylene-ethanol: (5)

The relative amounts of primary and secondary solvents differ significantly in these works. The solvent used by Vaninbroukx and Spagnol contained 89% toluene and 11% ethanol by volume while some of those used by Dyer et al. contain over 50% ethanol. It is also interesting to compare in this regard the types of solution scintillators used by the participants in the 1963

BIPM international comparison of  $^{241}\text{Am}$  [84]. This report contains details of the scintillators used by the six laboratories who used LS counting methods (Toluene, xylene and dioxane solution scintillators were used).

The real key to stability in these solution scintillators probably lies in selecting the proper chemical form of the radionuclide and concentration of carrier.

Dioxane-naphthalene scintillators were developed by Furst et al. [17] over twenty years ago, as a means of dissolving aqueous samples in an organic solvent. In addition to the precision metrology studies cited above, these scintillators have also been widely used for environmental measurements [141] and for biological samples [148]. There seems, however, to be little reason for their continued use. Dioxane is more toxic than toluene and p-xylene has a lower flash point, and its naphthalene solutions are less efficient solvents. For practical applications, the dioxane-naphthalene systems have been largely replaced by emulsion scintillators.

### 3.3.2. Uses of real solution counting samples

It is evident from Figure 1 that most radionuclides can be incorporated into real-solution counting samples. For noble gas radionuclides, however, there is no particular advantage to adding solubilizing agents, as the noble gases are most soluble in pure aromatic hydrocarbons [151].

Sufficient examples have already been given for real-solution scintillators used for radionuclides present as cations ( $^{22}\text{Na}$ ,  $^{87}\text{Rb}$ ,  $^{60}\text{Co}$ , etc.). Some radionuclides normally counted as anions are  $^{14}\text{C}$  ( $\text{CO}_3^-$ ),  $^{35}\text{S}$  ( $\text{SO}_3^-$ ),  $^{32}\text{P}$  ( $\text{HPO}_4^-$ ), and the halides ( $\text{Cl}^-$ ,  $\text{I}^-$ , etc.). Such solutions are usually made basic (with  $\text{KOH}$ , for example) to prevent escape of volatile labelled material. Solution scintillators used for radioiodines are described by Rhodes [92].

### 3.3.3. Preparation of real solution counting samples

In most experiments, the counting samples are prepared by first pipetting the scintillator solution into the vial and then transferring an aliquot of an aqueous solution into the vial. For accurate work, gravimetric techniques are used, such as those described by Merritt [207] and Vaninbroukx and Spagnol [95].

The procedures described in those works are too lengthy to be reproduced here in full. We should like to mention, however, one technique described there [95] for insuring that the sample and solution scintillator are thoroughly mixed. First, about 0.1 ml of the aqueous sample (containing the radionuclide and appropriate carriers) is weighed into an open 100-ml bottle. Then the sample is dissolved in 6 ml of ethanol, 44 ml of toluene-based scintillator is added, and the bottle is closed and shaken mechanically for 10 minutes. Individual counting samples are then weighed into counting cells.

The main limitation to the use of toluene-ethanol scintillators is that the counting samples are often unstable and the radionuclide may precipitate or become adsorbed on the surface of the vial. The first point to consider when instability is recognized is the homogeneity of the solution. If the sample is indeed a true solution (one in which the relative proportions of constituents are the same in any differential volume element as they are in the total sample), then several steps may be taken to prevent the radioactive cation from being adsorbed on the container walls. The most effective means of keeping the sample in solution is to add sufficient inactive carrier to insure that the reactive sites on the glass surface are occupied by

inactive ions. Several examples are given by Erdtmann [75], in which the stability is studied as a function of carrier concentration. The amount of carrier necessary to prevent adsorption will depend on the temperature, sample pH, and concentrations of complexing agents.

In other work Vaninbrouckx and Spornol [95] added ethylene glycol with solutions of  $\text{SrCl}_2$  to prevent adsorption while Smith and Stuart [245] reported adding a drop of concentrated acid to the sample, a technique also mentioned in Monographie BIPM-I [237]. One should exercise caution, however, in adding strong acid to these solutions. Nitric and perchloric acids, in particular, may produce explosive compounds. Concentrated acids may also accelerate oxidation and decomposition of the fluors. A reasonable limit to the acid concentration for these solutions would be that obtained on adding 150 mg of an aqueous solution of 4 mol HCl per  $\text{dm}^3$  to 10 ml of solution (90% toluene-10% ethanol, by volume).

Smith and Stuart [245] have also mentioned using a silicone treatment on the surface of the glass vials. Physical and chemical models for these wall-surface treatments are given in recent work by Harding and Dixon [267] and techniques for applying such treatments are described in Monographie BIPM-I [237].

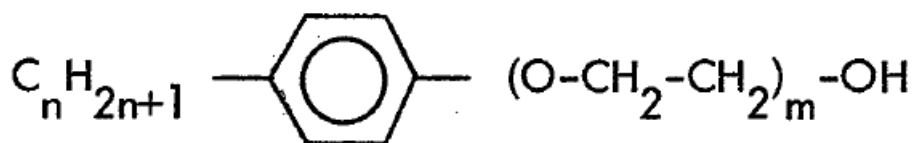
### 3.4. Emulsion counting samples

#### 3.4.1. General considerations of emulsion counting samples

The commercial emulsion scintillators in use today have evolved from the work of many investigators over the past fifteen years. The history of the development of these scintillators and their practical applications were discussed recently by Benson [251]. As Fox has demonstrated in a series of papers [216], [217], [254], the chief advantage of emulsion scintillators is that one may incorporate relatively large proportions of aqueous sample, and still maintain reasonable counting efficiencies. His figure of merit for low-level  $^3\text{H}$  counting is proportional to the product of counting efficiency and volume fraction of water.

The present treatment, however, will be limited to high-efficiency emulsion counting samples, which contain less than 5% water by volume. In such systems, water micelles are dispersed in the organic phase consisting of a solvent and a dispersing agent. Dispersing agents are also called emulsifiers, detergents, and surfactants. The tenn surfactant is used here since “surface-active” agent best describes their function in these ternary mixtures.

Reference works on emulsion technology [127], [226] reveal that a large number of surfactants can be used to form stable emulsions. Lieberman and Moghissi [159] evaluated many of these and found certain non-ionic surfactants best suited for use in emulsion scintillators. The most popular of these, which are known by the Röhm and Haas trademark Triton, are formed by the reaction of an alkyl phenol with ethylene oxide and have the general formula



Generally  $m$ , the number of ethylene oxide groups, is about the same as  $n$ , the number of methyl groups. For Triton-X 100,  $m = 9$  and  $n = 8$ , while for Triton N101,  $m = 10$  and  $n = 9$ . Another useful agent is BBS-3, a proprietary compound distributed by Beckman [256]. When a small amount of water is dispersed in a large volume of solvent, the surfactant molecules

stabilize the two-phase system by orienting themselves with the alkyl chain, or hydrophobic end, in the organic phase and the hydrophilic end (containing the ether groups with the unbound electrons on oxygen) in the aqueous phase.

The proportions of solvent, surfactant, and water necessary to form a stable emulsion will depend on variables such as temperature, pH and salt concentrations [118], [188], [216], [217]. For the small samples used in metrology studies, it is only necessary to establish the minimum amount of surfactant required to form a stable system. Excess surfactant will serve only to lower the scintillation yield (although recent work [231] has shown that the aromatic surfactants do behave as scintillators, to a limited extent). Few references are available on emulsion scintillators which are specifically formulated to give high counting efficiency for small samples. One such system, reported by Horrocks [256], consists of 16% BBS-3 and 84% toluene by volume. This seems to be a reasonable lower limit to the amount of surfactant required to prevent phase separation. Most of the commercial products on the market contain 20 to 33% surfactant by volume.

An intriguing question about these emulsion systems is whether the micelle diameters are small compared to the range of particles emitted in the nuclear decay (or transition) process. As early as 1967, van der Laarse [118] showed that there was a small but significant difference in  $\beta$ -particle counting efficiency depending upon whether the activity was in the organic scintillator phase ( $^3\text{H}$ -toluene) or inside the micelles ( $^3\text{H}$ -water).

In a recent work devoted to this topic, Horrocks [256] determined counting efficiency as a function of water concentration for samples of  $^3\text{H}$ ,  $^{109}\text{Cd}$ - $^{109}\text{Ag}^{\text{m}}$ , and  $^{233}\text{U}$ . Gibson [255] at the same symposium suggested that (at least for systems described by Horrocks [256], see p. 96) the micelle diameters are of the order of 10 nm or less and, therefore, energy loss within the micelles will only be significant for a few radionuclides such as  $^3\text{H}$  and  $^{55}\text{Fe}$ . Gibson has suggested more recently [291] that emulsion scintillators should not be used in metrology studies until the question of energy loss within the micelles has been resolved.

It is usually assumed that when samples containing dissolved salts are dispersed in these two-phase systems, the ionic species will be in the aqueous phase. The extent to which radioactive species are extracted into the organic phase has received little attention. It is clear however that when one adds an extractant such as HDEHP to these emulsion systems, the radioactive sample is extracted to some extent from the water micelles. This is similar in fact to McDowell's work [183] with actinides, in which aqueous samples are introduced into a toluene-HDEHP "extractive scintillator". With plutonium the HDEHP serves two purposes. First it extracts plutonium from the acidic aqueous phase and second it prevents  $\text{Pu}^{+4}$  from polymerizing in the weak acid environment of the organic phase [63], [183].

In recent work at NBS,  $^{239}\text{Pu}$  solution samples (100 to 300 mg in an aqueous solution of  $5\text{ mol l}^{-1}\text{ HNO}_3$  were introduced directly into 10 ml of a commercial emulsion scintillator and a rapid loss in count rate was observed (5% per day). Stable samples were obtained however when the emulsion was made 0.05 molar in HDEHP.

Another "extractive scintillator" for curium, californium and americium has been described by Miglio [283].

### 3.4.2. Uses of emulsion counting samples

Radionuclides of at least 22 of the elements shown in Figure 1 have already been incorporated into emulsion scintillators. Several extensive works are listed here, together with the



brandname-emulsion scintillator employed and the number of radionuclides examined (in parentheses):

Horrocks [221], [222], [256], [257]	Ready-Solv VI: (6)
Handler and Romberger [202]	Insta-Gel: (7)
Ishikawa and Takiue [205]	Insta-Gel: (4)
Bransome and Sharpe [213]	BBS-3—toluene: (4)

Only recently have precise radionuclide metrology results been reported in which emulsion scintillators were used. In the international comparison on  $^{139}\text{Ce}$  [276], sponsored by the Bureau International des Poids et Mesures (BIPM), the three laboratories who used LS counting (IBJ, NAC, and NPL) <sup>(1)</sup> all used commercial emulsion scintillators. Several of the participants in the  $^{134}\text{Cs}$  international comparison (the results of which are presented in Chapter 8 of this Monograph) also used commercial emulsion scintillators.

<sup>(1)</sup> IBJ—Instytut Badan Jadrowych, Świerk, Poland  
NAC (formerly NPRL)  
—National Accelerator Centre, Pretoria, South Africa  
NPL—National Physical Laboratory, Teddington, United Kingdom.

### 3.4.3. Preparation of emulsion counting samples

Many of the procedures given in previous sections, for preparing solution counting samples, are also applicable for preparing emulsions. When using commercial products, however, one should heed suggestions given by the supplier as many of these products are formulated for specific types of samples. Some of the emulsions may appear cloudy at first and then clear after standing for several hours. If samples are to be counted at reduced temperature, they should be stored at that temperature and examined before counting to insure that phase separation has not occurred.

Chemiluminescence and phosphorescence are often observed with emulsion systems [251]. Presumably these problems are associated with impurities in the surfactants. Some workers report reducing the chemiluminescence by pretreating the surfactant [251], while others find that warming the sample to 40 °C reduces this component of the background [159]. Many workers also advise doing as much of the sample preparation as possible under red light to avoid unnecessary photoactivation.

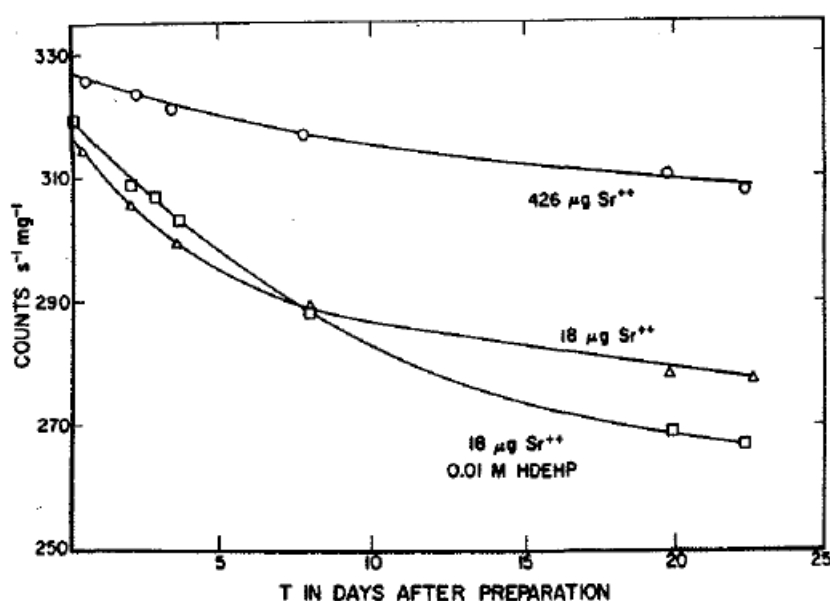
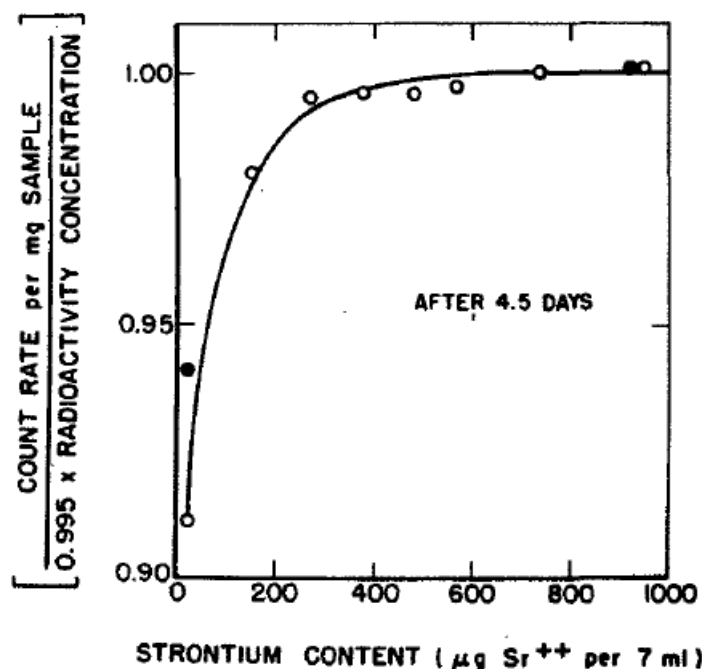


Figure 2 — Loss in count rate observed for some  $^{89}\text{Sr}$  counting samples prepared using a commercial emulsion scintillator. Measurements were made at

6 °C using a Packard TriCarb, with a window fixed by a single low-level discriminator. The counting efficiency in this window was 0.995. The counting samples consisted of  $\approx 75$  mg of aqueous solution ( $\text{SrCl}_2$  in an aqueous solution of 0.1 mol HCl per  $\text{dm}^3$ )  $\in$  stem: [15 ml of emulsion scintillator in borosilicate-glass vials (from measurements made at NBS).



**Figure 3 —** Relative loss in count rate due to sample adsorption for ten counting samples containing different amounts of strontium carrier and chelating agent: ○ strontium only, ● strontium + 0.2 mmol HDEHP. Each vial contained  $\approx 75$  ml of aqueous sample in 7 ml of a commercial emulsion scintillator (from measurements made at NBS).

The stability of counting samples can still be a problem with emulsion systems. Figure 2, for instance, shows the loss in count rate for some  $^{89}\text{Sr}$  samples dispersed in a commercial emulsion scintillator. Note that the addition of chelating agent alone was not sufficient to prevent the sample from being adsorbed on the wall of the glass vial. A series of vials having different carrier concentrations was then prepared and 1 mg of strontium per 7 ml of emulsion was found sufficient to give a stable sample. Figure 3 shows the response for this series of samples as a function of added carrier after 4.5 days.

Volatility of the sample is another problem that still has to be considered when using emulsion scintillators. The commercial formulations are usually supplied in acid form in order to inhibit chemiluminescence reactions [150], which may occur when strongly alkaline clinical samples are mixed with the scintillator. A problem occurs if a slightly alkaline sample, such as  $^{14}\text{C}$ -labelled  $\text{Na}_2\text{CO}_3$ , is added to a commercial product which is acidic. In this case volatile  $^{14}\text{CO}_2$  may escape into the void space above the scintillator, as shown in recent work by Herbland [268] and Huskisson and Ward [280]. This problem can be avoided for carbonate samples by first adding sufficient basic carrier solution to neutralize the scintillator emulsion, before adding the sample.

## 4. Design of High-Efficiency Liquid-Scintillation Counting Systems

B.M. Coursey and W.B. Mann<sup>(1)</sup>

<sup>(1)</sup> Radioactivity Section,  
National Bureau of  
Standards, Washington, D.  
C. 20234, USA.

### 4.1. Introduction

In order to compare LS counting systems of different design, we must first refer to some figures of merit which have been used in this field. The most useful of these for design purposes is the figure of merit,  $\eta$  [32], [69], which is the number of photoelectrons arriving at the first dynode per kiloelectronvolt of energy deposited in the scintillator. By way of comparison  $\eta$  is of the order of 6 photoelectrons/keV for a conventional  $7.6 \times 7.6$  cm NaI(Tl) detector, while for a single-phototube LS system  $\eta$  will be between 0.2 and 2 photoelectrons/keV depending on the design of the system. In the second part of this section we consider methods of optimizing  $\eta$ , and finally a review is given on the LS systems that have been used in radionuclide metrology.

### 4.2. Methods of comparing liquid-scintillation counting systems

It is essential to the many instrument manufacturers that they have some agreed basis for rating the sensitivity of different counting systems. Most commercial counting systems consist of two phototubes and a screw-cap vial in the arrangement shown in Figure 4. One index often used to compare these systems is the  $^3\text{H}$  counting efficiency for the two tubes in coincidence,  $\epsilon(^3\text{H})$ , for a so-called unquenched sealed standard. These standards [297] usually consist of fifteen milliliters of deaerated liquid scintillator consisting of  $^3\text{H}$ -toluene, PPO and POPOP in toluene<sup>(1)</sup>.

<sup>(1)</sup> Chemical formulae for scintillators mentioned in this Monograph are given in Table 2.

In a recent intercomparison of six commercial instruments, Patterson et al. [287] found  $\epsilon(^3\text{H})$  ranged from 42% to 57%. Presumably these values were slightly low because air-saturated samples were used. With unquenched standards the manufacturers usually claim to obtain  $\epsilon(^3\text{H})$  of 60 to 65%.

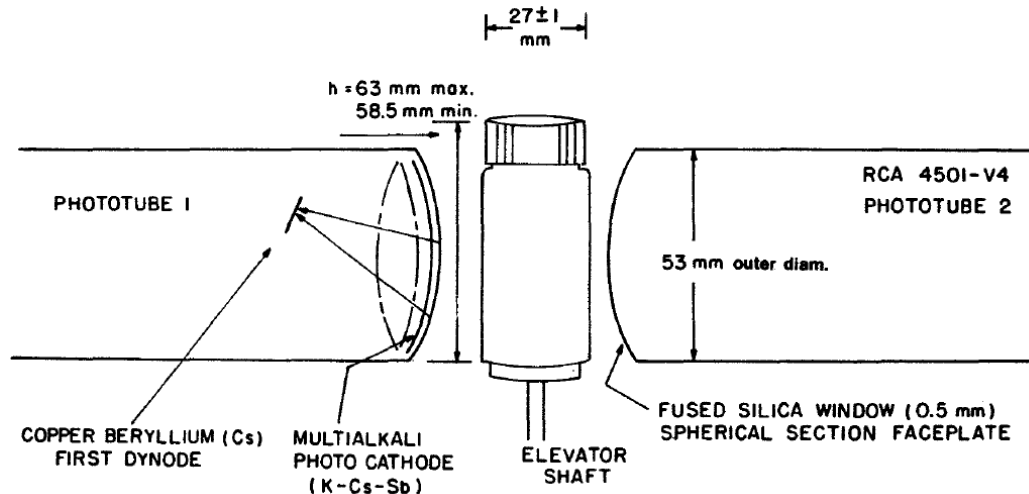
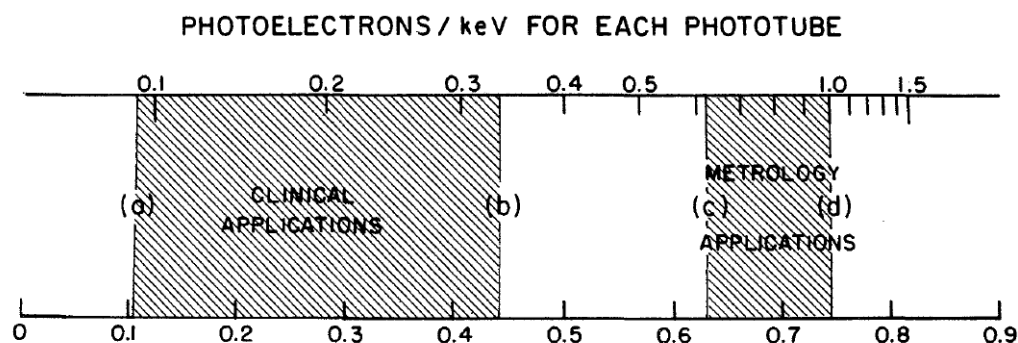


**Figure 4 — Schematic diagram of standard counting vial and phototubes used for typical commercial LS counter (Packard TriCarb 3320).**

- Dimensions of vial are given in IEC standard 582 [269]. Reviews of the various properties of commercial vials (and smaller inserts called “minivials”) are available [242], [285], [288].
- “Minivials” have an outer diameter of 14 mm, and fit inside glass holders which have essentially the same dimensions as the larger vials.
- The optimum volume of scintillator depends on the system, since the stop position on the elevator shaft influences the optical geometry [288].
- Other phototubes used in commercial counting systems include EMI QB9635 and Philips 56 DUVP.

There are some problems with using  $^3\text{H}$  counting efficiency as the sole gauge of sensitivity and for radionuclide metrology work in particular it is much more informative to specify the figure of merit  $\eta$  for the counting system. The relationship between  $\varepsilon(^3\text{H})$  and  $\eta_0$ , the merit figure uncorrected for ionization quenching, is shown in Figure 5. See also Section 5.4.1.

Almost all of the millions of measurements made annually with LS counting systems fall in the region on the left of the figure. To reach  $\varepsilon(^3\text{H})$  in excess of 70%, however, requires a great deal of effort. It is this high-efficiency region though that offers the greatest promise for standardization techniques for low-energy  $\beta$ -particle emitters and electron-capture (EC) radionuclides. Moreover, the results reported by Kolarov et al. [157] and the Monte-Carlo calculations presented in a series of six papers by Malcolm and Stanley [228], [259], [260], [271], [272], [273] suggest that the limits have not yet been reached in LS-system design and further improvements are likely.



### $\epsilon(^3\text{H})$ , $^3\text{H}$ COUNTING EFFICIENCY FOR TWO PHOTOTUBES IN COINCIDENCE

**Figure 5 — Comparison of figure of merit  $\eta_0$  and  $^3\text{H}$  counting efficiency from Gibson and Marshall [195] and Gibson [291].**

This figure was constructed by overlaying the upper and lower scales in Fig. 4 from Gibson and Marshall [195] and was extended to higher counting efficiency based on more recent calculations by Gibson [291].

The special conditions under which a quantitative relationship exists between these two scales are discussed by Gibson and coworkers [89], [172], [195], [255] and in Chapter 5 of this Monograph.

1. Counting efficiency observed for severely quenched samples.
2. Typical efficiency observed for  $^3\text{H}$ -water samples in commercial emulsion scintillators with the type of counting system shown in Figure 4.
3. Nominal upper limit for  $^3\text{H}$ -toluene unquenched standards in commercial counting systems.
4. Kolarov et al. [157] reported  $\epsilon(^3\text{H}) = 73\%$  for  $^3\text{H}$ -toluene in unquenched samples in a system specially designed to give high counting efficiency.

Before proceeding one other figure of merit should be mentioned, namely  $\epsilon(^3\text{H})^2/B$ ; where  $B$  is the background count rate expressed in counts per minute. A good value for a commercial system would be  $\epsilon(^3\text{H})^2/B = 250$ , where  $\epsilon(^3\text{H}) = 62\%$  and  $B = 15.4$  counts per minute. Although it is clearly desirable to keep the background low, the magnitude of the total background count rate is often less important than the way the background is distributed with pulse height, or energy. For example, below approximately 10 keV, the background will include a contribution from the “monos” peak (see [204] and Figure 10 and Figure 11 of this Monograph). To reduce the background in this region it is usually necessary to cool the tubes, which reduces therm ionic emissions.

In the region above 10 keV,  $B$  depends on shielding, construction materials used for counting cell and detector, scintillator volume, and other factors as discussed in NCRP Report 58 [284]. Useful recent work on reduction of the background caused by cosmic radiation is given by Alessio et al. [249], [279].

In the following section we will focus on design considerations for obtaining high values for the figure of merit.

### 4.3. Considerations for optimizing the figure of merit

In this treatment we will not consider explicitly the processes of light production and quenching in the liquid scintillator, because they have been discussed in detail elsewhere [146], [153], [144]. Similarly we will not consider the statistical nature of the photoelectric response process at the phototube, as that subject is addressed in Chapter 5 of this Monograph.

Although  $\eta$  is a function of electron energy ( $E_e$ ), it is convenient to describe the system response arbitrarily for 5-keV monoenergetic electrons. In the remainder of this discussion,  $\eta$  values will be for  $E_e = 5$  keV unless otherwise stated.

Following the treatment of Birks [69], [146], Equation (1) gives  $\eta_E$  in terms of the three basic elements of the scintillation process:

1. the production of primary photons by excitation of the liquid scintillator,
2. the light-collection efficiency, and
3. the phototube response.

$$\eta_E = \frac{\left[ \frac{S_e E_e}{h\bar{\nu}} \right] G [m C_{pe} g_c]}{E_e}, \quad (1)$$

where

$S_E$  scintillation yield, the fraction of electron energy which is converted to light energy [223],

$h\bar{\nu}$  average energy of emitted photons,

$G$  light-collection efficiency, that fraction of the photons generated in step Section 4.3, 1) that arrive at the photocathode,

$m C_{pe} g_c$  phototube response, the fraction of photons arriving at the photocathode, which result in photoelectrons arriving at the first dynode,

where

$m$  spectral matching factor, which has a value between 0 and 1 and is a measure of the overlap of the emission spectrum of the scintillator and the absorption spectrum of photocathode (see Section 6.3.3,

$C_{pe}$  maximum photoelectric efficiency of the photocathode, also called the “quantum efficiency”, and

$g_c$  photoelectron-collection efficiency at the first dynode.

Equation (1) is interesting from a design standpoint because all three terms in brackets have to be optimized to obtain values of  $\eta_0$  in excess of 1 photoelectron/keV. The first term is a function of the chemical composition of the sample and the third term is more or less fixed by the choice of the phototube. The light-collection efficiency, however, depends on the selection of the counting vial and optical arrangement and represents an important parameter under the control of the investigator.

### 4.3.1. The scintillation yield

The scintillation yield is about 4.5% for 5-keV electrons in the best liquid scintillators. Some of the problems that limit direct measurements of  $S_E$  are:

1. the yield depends on the nature of the ionizing particle; for example, the yield for an  $\alpha$  particle is only about one-tenth that of a  $\beta$  particle of the same energy, due to differences in ionization density along the particle track [69],
2. the yield depends on the energy of the particle; for  $\alpha$  and  $\beta$  particles, the energy loss per unit length of path is inversely proportional to the square of the particle velocity [9] (see also Section 5.4.1, ionization quenching),
3. finally the yield depends on the chemical composition of the sample [238].

Given the difficulties involved it is perhaps not too surprising that there are few data available on scintillation yields. Most workers rely on the absolute-scintillation- yield measurements of Hastings and Weber [65] with  $^3\text{H}$  and  $^{14}\text{C}$  in a liquid scintillator composed of PPO and POPOP in toluene, and those of Skarstad et al. [137] with  $^{14}\text{C}$  in a solution of terphenyl in benzene.

Malcolm and Stanley [259] have combined these yield data with Horrocks' [80] relative yield vs. electron-energy data to arrive at an empirical expression giving  $S_E$  as a function of  $E_e$ . Using their value of  $S_E = 0.04$  for 5 keV, and comparative data for different solvents [69], [238] one would expect  $S_e \approx 0.045$  for p-xylene with an efficient scintillator such as PPO or t-butyl PBD. Using 3.2 eV as the average photon energy (385 nm), one finds that a 5-keV electron will produce 71 primary photons. This is the first term in brackets in Equation (1).

### 4.3.2. Light-collection efficiency

Estimates of the fraction  $G$  of these 71 primary photons that reach the phototube have been very crude and range from as low as 10% to as high as 100%. Before addressing the problem of estimating  $G$  we will discuss some of the design factors that must be considered in optimizing light-collection efficiency, namely:

- average photon light-path length,
- shape of sample container,
- interfaces,
- reflecting surfaces, and
- light guides.

**Photon light-path length**—The further the photons have to travel through the scintillator, the greater the attenuation on the photon pulse before it reaches the boundaries of the container. The two major processes in this attenuation are

- absorption of the photons by other scintillator molecules, and
- absorption of the photons by colored impurities in the solution (referred to as color quenching).

Sipp and Miehe [232] have studied time resolution and fluorescence—absorption in liquid-scintillator cells between two RCA 8850 phototubes. Their results clearly show the

dependence of these two parameters on the path length in the cell, which was varied from 0.2 to 5 cm.

**Shape of the container**—It has long been recognized that certain geometrical shapes, rectangular cells [2] and spherical vials [120], [259], for example, are better suited for photon measurements than the cylindrical vials used in most commercial instruments. Further evidence of light losses in the cylindrical geometry is presented by Stanley [234]. Figure 6 in that reference is a photograph of the bottom of a vial, in which the exposure is due only to the fluorescence from the cell. The cylindrical symmetry there is shown to have a collimating effect (a bright ring near the edge is observed) which results in excessive losses at the bottom of the cylinder.

**Interfaces**—Clearly every interface between the scintillator and the photocathode represents a potential reflection for the photons [134]. There are two usual ways to reduce losses at these interfaces. First, one can sandblast the outer surface of the container [106], to make a more diffuse surface and reduce internal reflection. Second, one can employ optical coupling greases or fluids which have a refractive index close to that of the cell and phototube face. The refractive index of the liquid scintillators is about 1.50, while that for borosilicate glass, which is used for many counting vials and is also used in the envelope for the RCA 8850, is 1.47. One useful silicone coupling grease is “Dow Corning Optical Couplant Q2-3067” for which  $n_D = 1.4648$ .

**Reflective surfaces**—Materials most often used for reflecting surfaces are polished aluminum,  $\text{TiO}_2$  (such as NE 560 from Nuclear Enterprises),  $\text{MgO}$  and  $\text{BaO}$ . In some very early work Hayes et al. [21] looked at the efficacy of Al and  $\text{TiO}_2$  reflectors for scintillators which emit at different wavelengths. Some of the results rearranged by Birks [69] are given here.

Scintillator	Relative pulse height		$\lambda_{\max}$ nm
	Al	$\text{TiO}_2$	
TP	0.91	0.76	342
PPO	1.02	0.97	375
POPOP	1.21	1.45	415

It appears then that polished aluminum is superior if only the primary scintillator is used. If wavelength shifters are employed however, (see Section 3.2.1,  $\text{TiO}_2$  would be better due to its better reflecting properties at longer wavelengths.

**Light guides**—Materials most often employed in light guides [32], [69] are cylindrical rods of polymethylmethacrylate (Perspex, Lucite, Plexiglas), although quartz rods or fiber optics [296] also exhibit very high transmission. In the close geometries employed in LS counters, however, the light guide most often is a hollow Lucite container filled with a light-weight silicone oil of matching refractive index, for example, Dow Corning 550 Silicone Fluid, which has a  $n_D = 1.50$  and a kinematic viscosity of  $1.15 \text{ cm}^2\text{s}^{-1}$  [290].

**Monte-Carlo methods for calculating light-collection efficiency**—While the details presented in the last five subsections are useful in optimizing the light-collection efficiency, we have still not addressed the problem of how one makes a quantitative estimate of  $G$  to use in Equation (1).

One could obtain estimates of  $G$  using the Monte-Carlo calculations of Malcolm and Stanley [271]. Their computer program allows them to simulate photon emission, attenuation and collection processes for a given geometrical arrangement of vial, reflector and phototubes.



Thus far they have reported results for only two arrangements, namely, for the IEC standard vial containing 20 ml of liquid scintillator, and for a spherical vial containing, for example, 5 ml of scintillator.

Rather than use their estimates here we have elected to estimate all other parameters in Equation (1) and then to solve for  $G$  as the unknown. With this objective in mind we consider now the phototube response.

#### 4.3.3. Phototube response

The bracket term in Equation (1),  $[m C_{pe} g_c]$  which we have called the phototube response, gives the fraction of photons arriving at the photocathode which result in photoelectrons arriving at the first dynode, and is about 0.25 for the typical scintillator/phototube combinations used in radionuclide metrology. We consider now in a little more detail the three terms that make up this response.

The spectral matching factor  $m$  is given by

$$m = \frac{\int_0^\infty I(\lambda) \Phi(\lambda) d\lambda}{\int_0^\infty I(\lambda) d\lambda}, \quad (2)$$

where  $I(\lambda)$  is the fluorescence spectrum of the scintillator, normalized such that  $\int_0^\infty I(\lambda) d\lambda = 1$ , and  $\Phi(\lambda)$  is the photocathode response function, normalized such that the maximum value of  $\Phi(\lambda) = 1$ .

According to Birks [238] spectral matching factors are quite high for the usual primary scintillators with alkali photocathodes. For instance,  $m = 0.97$  for PPO with an alkali tube.

The second term  $C_{pe}$  is the actual maximum photoelectric efficiency, or “quantum efficiency” reported by the tube manufacturer, and does not include  $g_c$ , the photoelectron collection efficiency at the first dynode [196].

Details of the construction of phototubes often used in LS counting are given by Coates [149], Krall and Persyk [198] and Persyk and Lewis [230]. Typical values for  $m$ ,  $C_{pe}$  and  $g$  are given in Table 3. Of these three the  $g_c$  value is the most difficult to measure and it causes the greatest uncertainty in the phototube response [162], [292].

**Table 3.** Typical figures of merit for commercial counting system<sup>1</sup> and for high-efficiency LS counting system for  $E_e = 5$  keV

1

Similar systems have been reported using EMI phototubes, e.g. EMI QB9635 for a commercial system [234], and EMI 95145/A for a high-efficiency LS counting system [122]. (1)

<sup>1</sup> Similar systems have been reported using EMI phototubes, e.g. EMI QB9635 for a commercial system [234], and EMI 95145/A for a high-efficiency LS counting system [122].

System characteristics	Commercial system	High-efficiency LS system
phototube	2 RCA 4501-V4	2 RCA 8850
tube face	quartz, spherical	Pyrex, piano-concave
first dynode	CuBe (Cs)	GaP (Cs)
light coupling	air	silicone grease
vial volume	15 cm <sup>3</sup>	2.8 cm <sup>3</sup>
vial material	glass	quartz
number of primary photons per 5 keV electron	71	71
$G$ value for each phototube	0.11	0.18
$m$	0.97	0.97
$C_{pe}$	0.32	0.32
$g_c$	0.80	0.80
$\eta$ : 5 keV for each phototube <sup>(a)</sup>	0.37	0.38
$\epsilon(^3\text{H})$ for two phototubes in coincidence	62%	73%

(a)  $\eta_0$  values taken from Figure 5 were corrected for ionization quenching using  $Q(E) = 0.63$  (see Figure 14).

#### 4.3.4. Comparison of figures of merit for two liquid-scintillation counting systems

In Table 3 we give some typical values for the parameters in Equation (1), which allow an interesting comparison to be made between the commercial system and a high-efficiency LS system. To arrive at estimates of the light-collection efficiency, Equation (1) was solved for  $G$ , using the values for other parameters shown in the table. This result indicates that about 11% of the primary photons emitted are incident on each phototube in an arrangement such as the one shown in Figure 4, which compares well with about 14% given by the Monte-Carlo program for a similar geometry [271], Table 2b).

#### 4.4. Designs for high-efficiency liquid-scintillation counting systems

Figure 6 illustrates schematically some of the most commonly used geometrical arrangements of phototubes and sample containers. Most workers use some variation of the design used in the commercial system Figure 6-1 which consists of two phototubes and an economical cylindrical vial of glass or plastic. In another popular design shown in Figure 6-4, a vial is coupled to the face of a vertically mounted phototube. This geometry is particularly well suited for  $4\pi\beta-\gamma$  coincidence counters [245], because a NaI(Tl) re-entrant well crystal can be positioned around the sample from above to give greater than  $2\pi$  geometry for the  $\gamma$ -ray detector. Small rectangular vials, such as the ones shown in Figure 6-3, are seldom used in LS counting<sup>(1)</sup>.

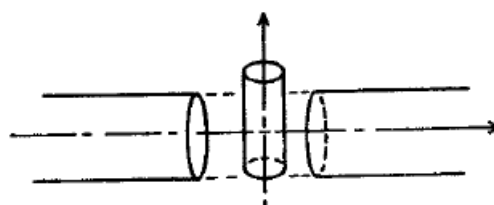
<sup>(1)</sup> Large-volume rectangular liquid scintillators have been used, however, for diverse studies such as neutrino-detection experiments and whole-body counting of small animals and humans. Useful data on the construction of such detectors may be found in Shureliff and Jones [2] and Smith [244].

In the following paragraphs we give some additional details for three geometrical arrangements, which, provided everything is optimized properly, should give figures of merit  $\eta_0$  in excess of 1 photoelectron/keV. The three are:

1. right-circular cylinders, in which the axis of the cylinder is perpendicular to that of the phototubes Figure 6-1, Figure 6-2,
2. right-circular cylinders in which the axis of the cell is parallel to the axis of the phototubes Figure 6-4, Figure 6-5, and
3. spherical vials Figure 6-6.

#### 4.4.1. Cylindrical vials perpendicular to phototube

Sensitivity can be optimized in this geometry by using small-diameter tubing for the container. An efficient light guide is then used between the sample container and the phototube face [45], [79]. McDowell and Weiss [262], in a system designed for assaying  $\alpha$  particles, use a silicone oil-filled container as the light guide. The inner surfaces of the light guide are painted with reflecting paint.



(1)(1)  
(2)(2)  
(3)(3)  
(4)(4)  
(5)(5)  
(6)(6)

Figure 6-1 — Cylinder with axis perpendicular to axis of phototubes<sup>(1)(1)</sup>

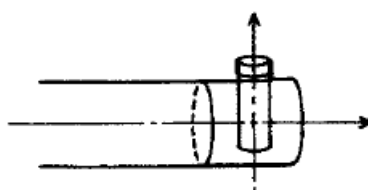


Figure 6-2 — Cylinder with axis perpendicular to axis of phototube<sup>(2)(2)</sup>

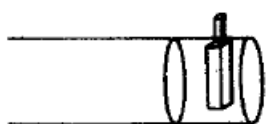


Figure 6-3 — Rectilinear cell with single phototube<sup>(3)(3)</sup>

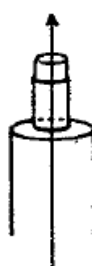
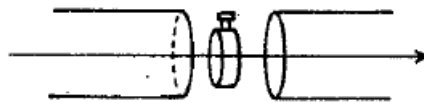
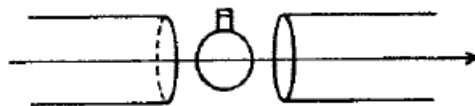


Figure 6-4 — Cylinder with axis parallel to axis of phototube<sup>(4)(4)</sup>



**Figure 6-5 — Cylinder with axis parallel to axis of phototubes<sup>(5)(5)</sup>**



**Figure 6-6 — Spherical cell between two phototubes<sup>(6)(6)</sup>**

#### Key

- (1) [45],[53],[249],[288]
- (2) [79],[183],[262]
- (3) [190]
- (4) [20],[28],[46],[71],[77],[85],[86],[95],[114],[177],[122],[197],[245],[270]
- (5) [44],[61],[122],[157],[232],[278],[279],[281]
- (6) [120],[273]

**Figure 6 — Geometrical arrangements of sample containers and phototubes often used in high-efficiency LS systems.**

The light-collection efficiency will be better for small-radius cylinders [81] and this results in higher counting efficiency for low-energy  $\beta$  particles and better energy resolution for  $\alpha$  particles. The resolution for  $\alpha$  particles, expressed as  $\text{FWHM}/E_\alpha$  (full width at half maximum divided by  $\alpha$ -particle energy), is 20 to 25% for a 25-mm diameter cylinder, while Horrocks reported 10.7% using vials constructed from 6-mm diameter thin-walled Pyrex tubing.

#### 4.4.2. Cylindrical vials with axis of cylinder parallel to that of phototube

The single phototube arrangements in Figure 6-4 have been used extensively in metrology work and current systems used at NPL and at NBS are of this design. Light-collection efficiency here depends markedly on the dimensions of the scintillator. The NPL samples, for instance, consist of 5 ml of scintillator in a cylindrical vial, while the NBS sources consist of 3 ml in a hemispherical vial.

The light-collection efficiency is, as expected, inversely proportional to the height of scintillator in the vial. This was demonstrated by Vaninbroukx and Spornol [95] by observing the width of the  $\alpha$ -particle peak from  $^{210}\text{Po}$  as a function of the height of scintillator in the vial.

The second very useful arrangement Figure 6-5 allows one to couple the flat ends of a cylinder directly to the faces of two phototubes [122]. Kolarov et al. [157] used a quartz-spectrophotometer cell with two RCA 8850 phototubes and obtained  $\epsilon(^3\text{H}) = 73\%$  for the tubes in coincidence, and 89% in summation. These cells are available in both glass and quartz, with specified light paths of from 0.1 cm to 5 cm.

Although there are no data on the  $\varepsilon(^3\text{H})$  as a function of path length in these spectrophotometer cells, there are some useful results published by Kaufman and coworkers 20 years ago [44], [61], using a cylindrical container made by connecting the faces of the two phototubes with an aluminum tube, which was polished on the inner surface. The curves shown in Figure 7 give efficiency as a function of separation distance of the phototubes. The fact that the three curves have different slopes is evidence of differences in the attenuation of light in the scintillators. As we mentioned before, different concentrations of solute molecules or colored impurities will give rise to different attenuation characteristics [266].

#### 4.4.3. Spherical vials

Malcolm and Stanley [273], using the Monte-Carlo method, derived a design for a system employing a spherical 5-ml vial, in which the  $\varepsilon(^3\text{H})$  for an unquenched sample was as high as 86%.

There is some early experimental work for this geometry, but since the work was published in Russian it appears to have received little notice in reviews on this subject. Two of the most interesting drawings from this work by Paligorić et al. [120] are included here in Figure 8. They did not report  $\varepsilon(^3\text{H})$  directly, so we cannot compare their results with those derived by the Monte-Carlo method. The figures of merit  $\eta_{49}$  keV of about 0.3 photoelectron/keV for each tube suggest, however, that even though the light-collection efficiency was high, the scintillation yield and phototube response were less than optimum. According to the English translation, the scintillator used was composed of PPO and POPOP in dioxane. In the usual formulations, this scintillator contains 60 grams of naphthalene per liter of dioxane. If naphthalene is omitted from this formulation, the scintillation yield is considerably less than that found with PPO in toluene.

It can be seen in Figure 8-1 that the efficiency begins to decrease for  $^{32}\text{P}$  in the small vials due to the wall effect. This means that in designing a system for general use in metrology one has to consider which radionuclides are to be assayed, so that the dimensions of the container will be large compared to the range of the  $\alpha$  or  $\beta$  particles. For the spherical vials it appears the 5 ml vial suggested by Malcolm and Stanley [273] is close to optimum for low-energy  $\beta$  emitters.

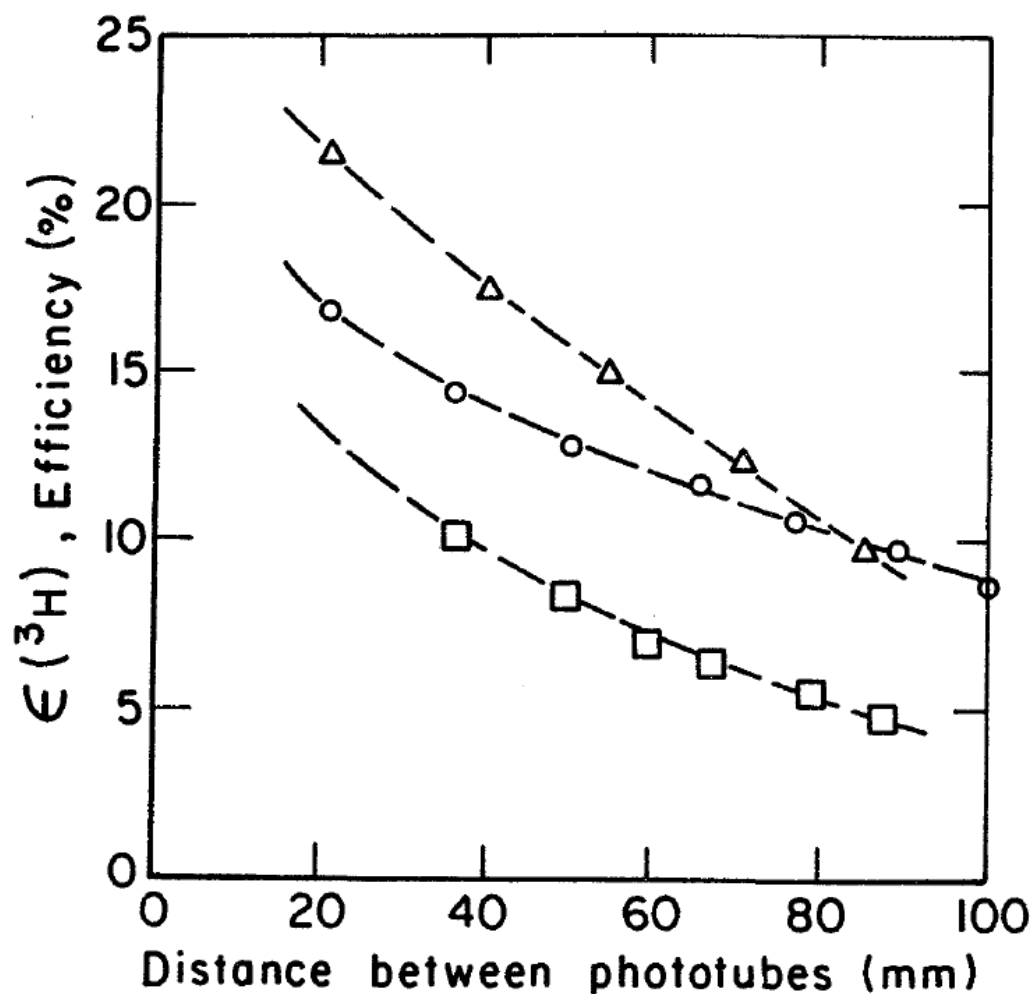


Figure 7 —  $^3\text{H}$  counting efficiency as a function of separation distance between the phototubes, after Kaufman et al. [44].

In this system (see also Figure 6-5, the DuMont phototube face plates formed the ends of a cylindrical cavity containing the scintillator. The three curves are for different scintillator formulations, and demonstrate the effect of color quenching at longer light-path lengths.

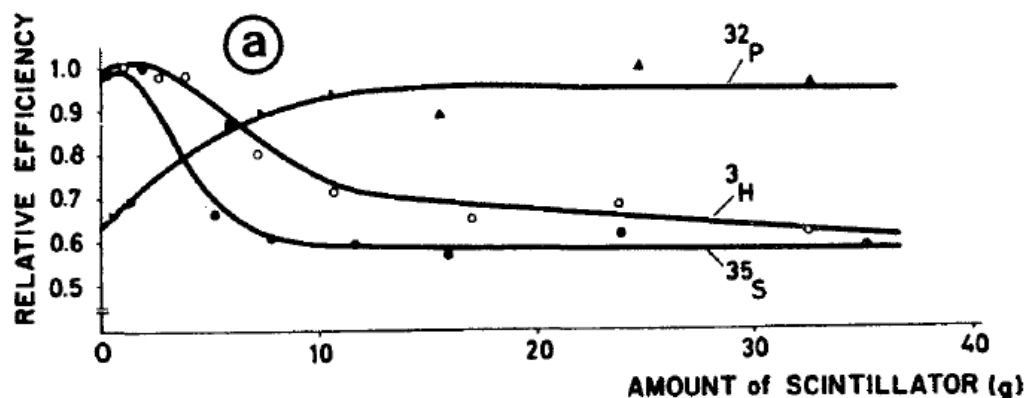
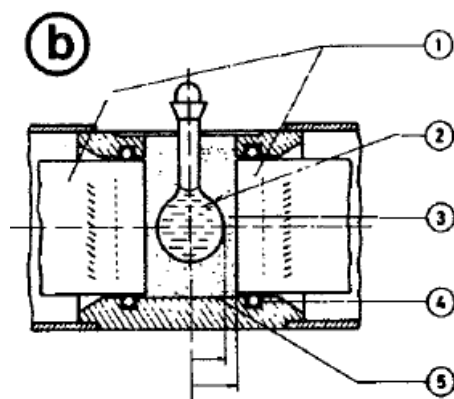


Figure 8-1 — Relative counting efficiency as a function of mass of scintillator for system employing spherical vials.



**Figure 8-2 — Schematic arrangement of system employing spherical vial.**

Nine vials of different diameters were used: 10 to 42 mm corresponding to 0.3 to 35 g of scintillator.

1. phototubes,
2. scintillator solution 7 g PPO and 50 mg POPOP in 1 l dioxane,
3. silicone oil,
4. rubber seal,
5. counter casing with  $\text{TiO}_2$  reflector.

Figures are adapted from [120], originally in Russian, and are based on an English translation provided by the authors (courtesy IAEA, Vienna).

#### 4.4.4. Other systems

Another rather unique design of an LS counting system for use in radionuclide metrology has been reported by Pochwalski and Radoszewski [293]. In this system, three phototubes are arranged symmetrically about the axis of a cylindrical glass vial, and triple coincidence events, as well as single and dual coincidence events, may be recorded.

Several systems are also in use which employ optical filters between the cell and phototube to allow one to vary the counting efficiency for a single sample [190], [294], [299].

## 4.5. Conclusions

From this review it may be concluded that there is no single design for an LS counting system that is clearly superior to others. Rather it seems that most of the simple arrangements shown in Figure 6 can be incorporated into very high-efficiency systems, suitable for use in radionuclide metrology, providing care is taken to optimize all of the factors in system design that we have mentioned here.

The three major requirements for a high-efficiency system design are correct scintillator composition, good optical coupling and sensitive, matching phototubes. When all of these are optimized as in the system used by Kolarov et al. [157], a superior counting system results. With currently available phototubes and good liquid scintillators the early two-phototube

designs reported by Kaufman et al. [61], Horrocks and Studier [79], and Paligorić et al. [120] should also give a figure of merit  $\eta_0$  in excess of 1 photoelectron/keV for each phototube.



## 5. The Statistics of the Scintillation Process and Determination of the Counting Efficiency

J. A. B. Gibson<sup>(1)</sup>

<sup>(1)</sup> Environmental and Medical Sciences Division, AERE, Harwell, Oxon, UK.

### 5.1. Introduction

As has been indicated in earlier parts, the great advantage of the LS counter is the absence of any source of self-absorption for truly homogeneous solutions. However there are two serious limitations which stem from the low scintillation efficiency of such systems and therefore limit the accuracy with which  $\beta$ -ray and electron-capture nuclides of low maximum energy can be determined. The limitations are

1. the pulse-height distribution obtained with a liquid scintillator does not correspond directly to the input spectrum because of poor resolution and a non-linear response at low energies which results in a steep rise in the distribution at these energies,
2. even if the extrapolation of integral bias curves to zero bias is feasible theoretically, then the intercepts on the ordinate do not correspond to the total number of charged particles losing energy in the scintillator and there will always be a finite probability of non-detection called the “zero-detection probability”.

The poor resolution of the system also means that it is not possible to set a suitable detection threshold which corresponds to a known electron energy. For example, a 5-keV electron depositing energy in the scintillator will produce only about three photoelectrons at the input to the first dynode of the electron-multiplier phototube. This is a very small number of events which have large statistical variations about this mean of three. Subsequent amplification cannot reduce these variations and it is found that the observed pulse-height distributions are such that integral curves cannot be extrapolated directly to zero bias. The theoretical analysis of such curves will demonstrate the need to fit the observations over the full pulse-height distribution.

The detailed theory of an ideal scintillation counter was reviewed by Gale and Gibson [101] who provided a detailed study of the statistical processes involved in converting electron energy in a scintillator to a pulse-height distribution from an electron-multiplier phototube. Subsequent papers by Gibson and Gale [133], Gibson [195], [255] and Gale [219] established the models required for determining this distribution both exactly and by use of mathematical models based upon Beta and Gamma functions. The introduction of the high-gain phototube (RCA type 8850) has largely removed the need for such functions and a model based upon the Poisson distribution with small corrections should be adequate for the analysis of the pulse-height distributions. As Houtermans [204] has pointed out, “any extrapolation method is just as good as the physical model justifying the adopted shape of the extrapolated function”. The arbitrary choice of linear or logarithmic extrapolations cannot be justified just because the result obtained agrees with that obtained by other direct methods. However, each method must be justified independently without reference to another method. Intercomparisons came later.

This part is mainly concerned with outlining the methods used for calculating the pulse-height distribution and the zero-detection probability including a discussion of non-linear influences on this calculation. Brief comments will be made on the effect of these statistical limitations

on system design and hence the type of additional measurement required to overcome these problems will be discussed.

## 5.2. Theoretical pulse-height distributions

Practically, the scintillation counter can be thought of as a converter (electron energy into light), an attenuator (light into photoelectrons at the cathode of the phototube) and an amplifier (the dynodes). Each stage of the whole process of converting energy into an electronic pulse involves some distortion or uncertainty so that an input of  $E$  keV will produce, on average, a pulse of height  $\bar{V}$  volts with an uncertainty of  $(\sigma_V)$  where  $\sigma_V$  can be 50 or 100% of  $\bar{V}$ . In addition, an input of  $2E$  will not necessarily produce an output of  $2\bar{V}$  because the system is non-linear. These distortions and non-linearities can be measured and explained by mathematical models.

Starting with a single photon of light the number of electrons produced at the first stage of the phototube by conversion in the photocathode will be  $\bar{r}$ , where  $\bar{r} < 1$ , i.e., only a proportion of the light pulses produce an electron. In the latest phototubes, the quantum efficiency of the photocathode is about 30%. The deposition of energy along the track of a 5-keV electron in the scintillator, if totally converted into light at 425 nm (maximum emission of a typical scintillator), would produce 1 700 quanta. Typically, however, between 95 and 99% of the energy goes into heating the scintillator, and only the remaining 1 to 5% is produced as light. In a typical liquid scintillator, this scintillation yield is approximately 1%, so that a 5-keV electron would produce about seventeen light quanta, with about five photoelectrons at the input to the first dynode.

This is not quite the complete story because the linear rate of energy deposition in the scintillator will also reduce the efficiency of conversion into light. At 5 keV this “ionization-quenching” effect [69] amounts to about 4%, so that a mean number of about three photoelectrons will strike the first dynode for 5 keV of energy deposited in the scintillator. These three electrons will be amplified into a pulse of perhaps  $10^7$  electrons at the anode of the phototube with further amplification by external electronics. However, three is the mean,  $\bar{r}$ , of a Poisson distribution in which 0, 1, 2, 3, ...,  $r$ , photoelectrons may strike the first dynode. The probability that no photoelectron will strike the first dynode is, therefore,  $e^{-3} = 0.050$  which is the zero-detection probability for this energy in the system. The probability of obtaining  $r$  photoelectrons at the input of the first dynode is

$$P_0(\bar{r}, r) = e^{-\bar{r}} \frac{(\bar{r})^r}{r!}. \quad (3)$$

This simple theory will be developed further in subsequent sections.

### 5.2.1. The statistics of the scintillation counter

The pulse-height distribution from a scintillation counter is not a simple function of the input energy except at high energies ( $> 500$  keV) where a simple Gaussian distribution gives an adequate representation of the output. In considering radiations from radionuclides such as  $^3\text{H}$ ,  $^{55}\text{Fe}$ ,  $^{63}\text{Ni}$  and  $^{14}\text{C}$ , such an approach is not correct. Neither can the output be considered as a Poisson distribution at low energies because the phototube modifies this distribution at the input and produces a variance in excess of that expected from the Poisson distribution. This additional distortion is small for the modern high-gain phototubes.

Gale and Gibson [101] reviewed the mathematical methods used to describe the pulse-height distribution for a single-electron input to the first dynode and produced generating functions for any number of electrons and also for an input with a Poisson distribution. The formulae developed in an earlier paper [89] are as follows. The probability of obtaining  $n$  electrons from the  $k$ th stage of the phototube from an input to the first dynode of exactly  $r$  electrons is

$$P_k(r, n) = \frac{m_k^r}{n!} \sum_{i=0}^{n-1} (n-i) P_k(r, i) P_{k-1}(1, n-i), \text{ for } n \neq 0, k > 1, \quad (4)$$

and

$$P_k(r, 0) = \{P_k(1, 0)\}^r \quad (5)$$

is the zero-detection probability. Now

$$P_k(1, 0) = \exp(-m_1) \exp\{m_k P_{k-1}(1, 0)\}, \quad (6)$$

where  $m_k$  = gain of the  $k$ th stage ( $k = 1, 2, 3, 4, \dots$ ).

It will be noted that the probability distribution is calculated from the single-electron output from the  $(k-1)$ th stage and can be calculated directly for any particular value of  $r$ , independent of a calculation of any other value of  $r$ .

$P_k(1, 0)$  and  $P_k(r, 0)$  are the zero-detection probabilities and the generating functions are based upon the Poisson distribution Equation (3). The pulse-height distribution from an input to the first dynode distributed with a Poisson mean of  $\bar{r}$  electrons is

$$P_k(\bar{r}, n) = \frac{\bar{r}^n}{n!} \sum_{i=0}^{n-1} (n-i) \cdot P_k(r, i) \cdot P_k(1, n-i), \text{ for } n \neq 0, \text{ and } k \geq 1, \quad (7)$$

and

$$P_k(\bar{r}, 0) = \exp(-\bar{r}) \cdot \exp\{\bar{r} \cdot P_k(1, 0)\}. \quad (8)$$

The output is again derived from the single-electron input, but this time at the  $k$ th stage. Similar generating functions have been derived by Prescott [104] to take account of non-uniformity in the dynodes of the phototube and they contain the Poisson distribution as a special case. However, as has been shown by Coates [149], this additional complication is unnecessary if a high-gain phototube is used.

The major problem with this exact model is the amount of computer time required to produce a pulse-height distribution and Gale and Gibson [101] proposed an algebraic approximation in the form of a Gamma function to reduce the computing time. However the introduction of the RCA phototube with a first stage gain of between 30 and 35 has reduced the necessity for such an approach because the distortion introduced by the dynodes is small. For example the mean and variance calculated using the generating functions above are:

Mean  $\mu = \bar{r} \cdot m_1 \cdot m_2^{k-1},$

Variance  $\sigma^2 = \bar{r} \cdot m_1^2 \cdot m_2^{2(k-1)} \left\{ 1 + \frac{m_2}{m_1(m_2-1)} \right\}.$

An initial stage with a gain of  $m_1$  and subsequent stages of gain  $m_2 = m_3 = m_4 = \dots = m_k$  are assumed. The relative variance is

$$\frac{\sigma^2}{\mu^2} = \frac{1}{\bar{r}} \left\{ 1 + \frac{m_2}{m_1(m_2-1)} \right\}. \quad (9)$$

At the input of the first stage, the relative variance is  $1/\bar{r}$  so that the term in the brackets in Equation (9) represents the additional distortion introduced by the dynodes. Now if  $m_1 = 35$  and  $m_2 = 4$ , the relative variance is  $1.038/\bar{r}$  and the relative standard deviation is  $1.019/\sqrt{\bar{r}}$ . This means that the width of the peak from a single (mono) or multielectron input is increased by less than 2% over that expected for a Poisson distribution. The effects on the zero-detection probability are not detectable ( $\approx 10^{-14}$ ) and so it is reasonable to assume that a Poisson distribution can be used to represent the pulse-height distribution from this type of phototube. Other tubes with a lower first-stage gain require the more exact approach discussed above.

### 5.2.2. Pulse-height distributions

An excellent review of the output from the RCA 8850 phototube was prepared by Houtermans [204] and he shows the pulse-height distribution from single photons for this phototube Figure 9. The relative peak width at half maximum (FWHM) is 41%, which is a function of the relative variance such that, for a Gaussian distribution,

$$(\text{FWHM})^2 = \frac{\sigma^2}{\mu^2} \cdot 8 \ln 2 = \frac{8}{\bar{r}} \ln 2.$$

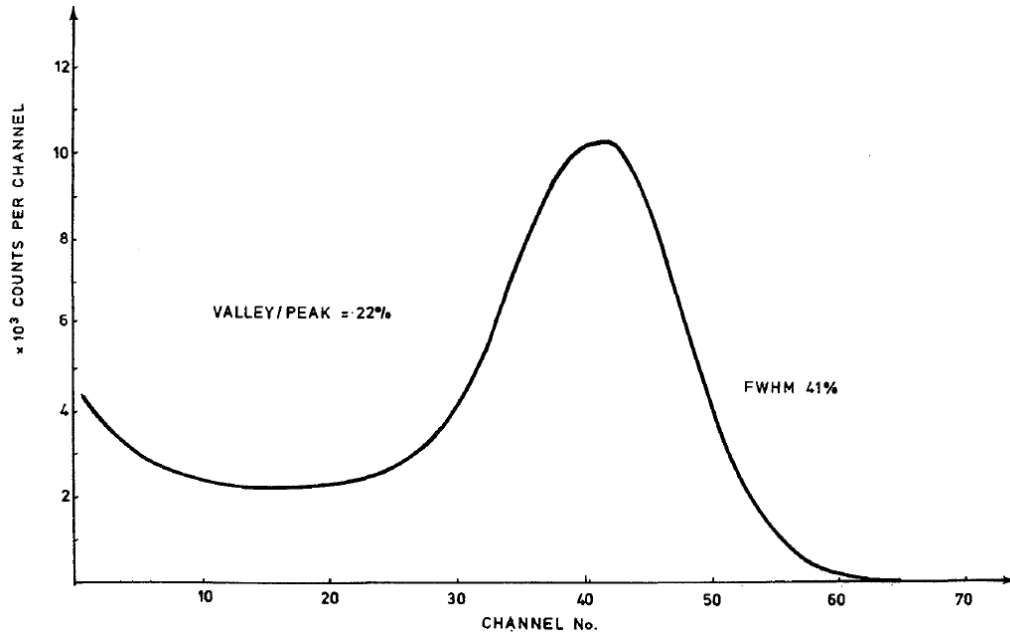


**Figure 9 — Mono spectrum for an electron-multiplier phototube of type RCA 8850 [204] (courtesy North-Holland Publishing Company, Amsterdam).**

Thus  $\bar{r} = (8 \ln 2) / 0.41^2 = 33$ , which is equal to the first stage gain ( $m_1$ ) as given in the manufacturers' specification. The distribution below the peak is due to edge effects [149] but, by careful choice of the tube, these can be reduced to a minimum (peak to valley  $> 5$ ). The dark noise should also be minimised and it is important to have a high quantum efficiency for the photocathode.

In the ideal situation, the distribution would be purely Poissonian and the result of having  $r = 2, 3, 4, \dots$  electrons incident at the same time would produce a series of distributions with means of 66, 99, 132, and so on. If an input to the first stage is itself distributed according to the Poisson distribution, then it is necessary to add together the contributions such that the final distribution may be approximated by the distribution at the output of the first stage, viz,

$$P_k(\bar{r}, n) \approx P_1(\bar{r}, n) = \sum_{i=1}^{\infty} P_0(\bar{r}, i) \cdot P_0(\overline{m_1}i, n),$$

where  $m_1$  is the gain of the first stage and  $P_0$  is the Poisson distribution as defined by Equation (3). Thus

$$P_k(\bar{r}, n) \approx P_0(\bar{1}, n) \cdot \exp(m_1 - \bar{r}) \cdot \sum_{i=1}^{\infty} \frac{\bar{r}^n}{i!} (\bar{r})^i \exp(-m_1 i). \quad (10)$$

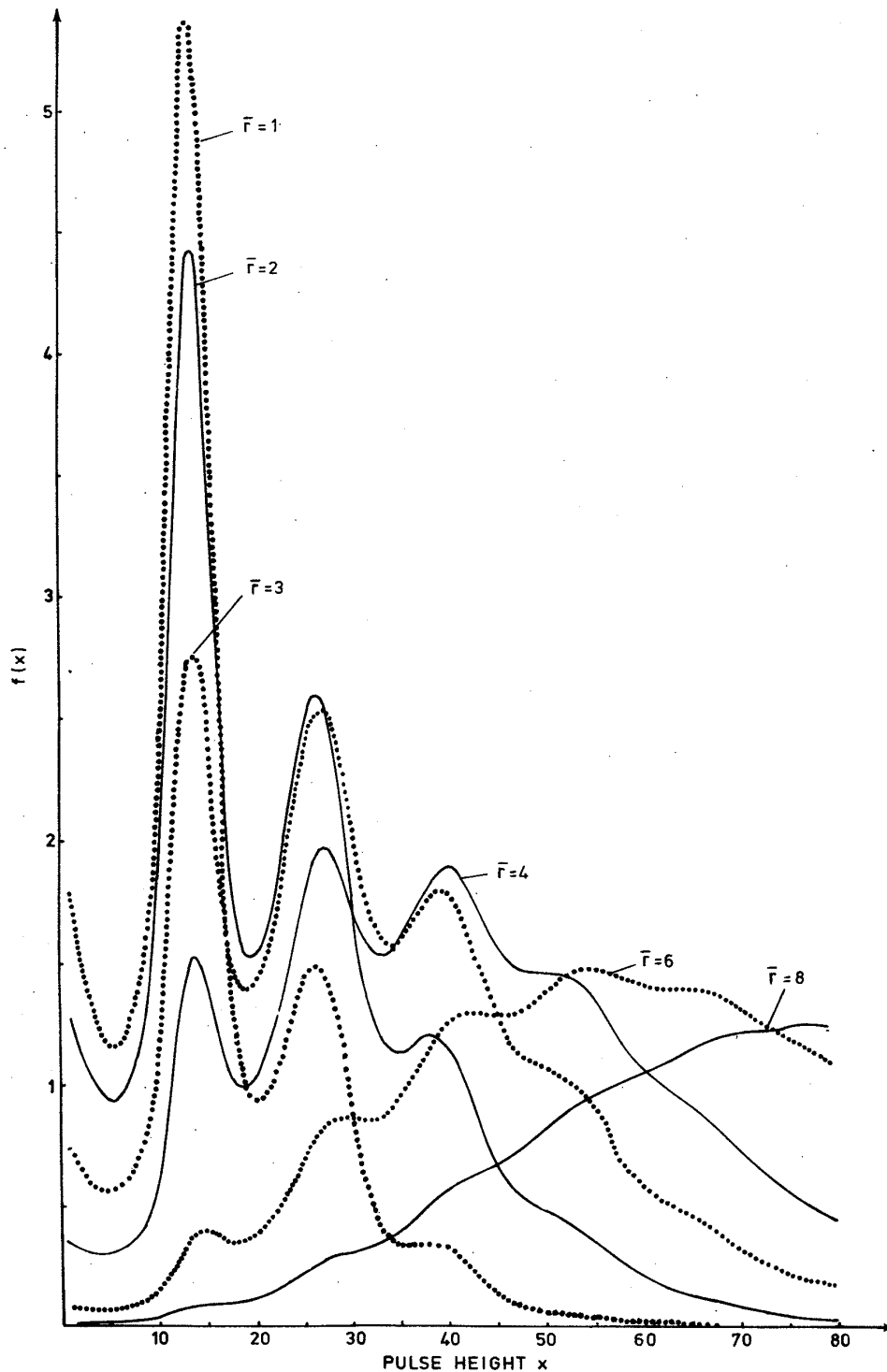


**Figure 10 — Calculated pulse-height distributions for an input to the first dynode distributed according to Poisson statistics with means of  $\bar{r}$  from 1 to 8 [204] (courtesy North-Holland Publishing Company, Amsterdam).**

For a more exact calculation, to allow for the edge effects on the dynodes, the generating functions produced in Section 5.2.1 can be used. The spectrum of monos that is measured can be used instead of the Poisson distribution. The zero-detection probability is unchanged because the major contribution (>99.99%) is due to the input distribution to the first dynode.

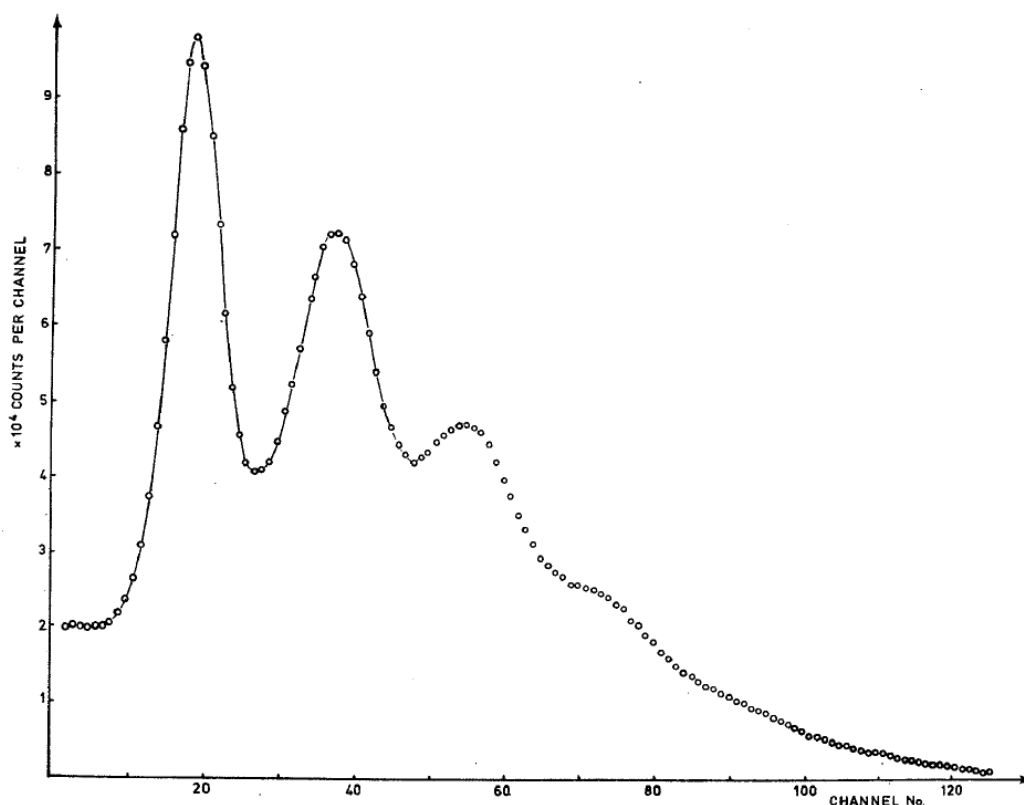


**Figure 11 — Measured pulse-height distribution of  $^{55}\text{Fe}$  [204] (courtesy North-Holland Publishing Company, Amsterdam).**

Houtermans [204] used the measured mono-electron distribution to calculate the spectra expected and these are shown in Figure 10. The actual observed spectrum for  $^{55}\text{Fe}$  given in Figure 11 shows the peaks from 1, 2, 3 and 4 monos as expected by the theory. The value of  $\bar{\tau}$  in this figure is between 2 and 3 [204].

This distribution demonstrates the difficulty of defining an equivalent energy threshold. At higher energies the input will be a Gaussian distribution and the resolution into quantised peaks will not be observed. An example is also shown by Houtermans for  $^{113}\text{Sn} + ^{113}\text{In}^m$  Figure 12, with an input energy of about 380 keV. The FWHM is 15.5%, which corresponds to a mean number of monos of 231. In the actual determination of  $\bar{\tau}$ , it is necessary to allow for the double peak at 368 and 392 keV and this partially accounts for the difference from a value of  $\bar{\tau} = 264$  calculated from the peak position.

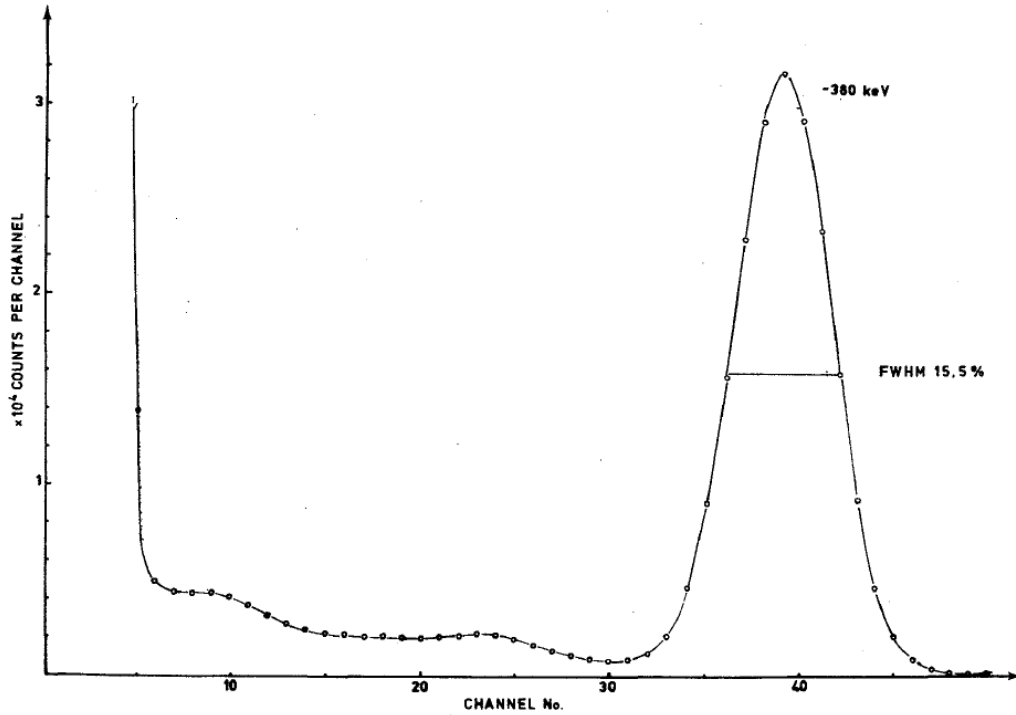


Figure 12 — Measured pulse-height distribution of  $^{113}\text{Sn} + ^{113}\text{In}^m$  [204] (courtesy North-Holland Publishing Company, Amsterdam).

Thus it is possible to calculate the pulse-height distribution from a single phototube for the measured parameters in the system. However, in order to do this, the non-linear effects must be included and these are considered in Section 5.4.

### 5.2.3. The pulse-height distribution for a coincidence system

Most modern systems are arranged so that the outputs of the two phototubes are added when a pulse is observed in both tubes (see for example Gibson and Lally [173], see p. 91). Thus since both tubes are required to produce a pulse, then there will be the equivalent of at least two photoelectrons in each detected event. For an input of exactly  $i$  electrons shared randomly between the two phototubes the output is reduced by a factor corresponding to the probability of all  $i$  electrons being detected by one of the phototubes. The factor is  $(1 - 2^{1-i})$  as quoted by Swank [32], but it can be deduced simply from the binomial distribution.

Thus, in calculating the spectrum from a Poisson-distributed input to the first dynode Equation (10), this factor must be included, i.e.

$$P_k^c(\bar{r}, n) \approx \sum_{i=2}^{\infty} P_0(\bar{r}, i) \cdot P_0(\bar{m}_1 i, n) \cdot (1 - 2^{1-i}). \quad (11)$$

As discussed by Jordan [178],  $\bar{r}$  can be less than 2 or less than 1 and there is still a finite probability of detection with a coincidence system.



#### 5.2.4. The pulse-height distribution for a $\beta$ -ray spectrum

The distribution for a spectrum of electrons can be calculated by dividing it up into a sufficient number of discrete energy bands of mean energy,  $E_j$ , which, when multiplied by the appropriate figure of merit ( $\eta$  electrons/keV, give a value of  $\bar{r}$  such that

$$\bar{r} = \eta E_j. \quad (12)$$

$\bar{r}$  can be used with Equation (9) or Equation (10) and weighted according to the proportion of the spectrum in the energy band  $E_j - \Delta E/2$  to  $E_j + \Delta E/2$ . The weighting factors,  $H(j)$ , when integrated over the spectrum, are equal to unity. Thus the pulse-height distribution is obtained from

$$S(\eta) = \sum_{j=1}^J H(j) P(\eta E_j, n), \quad (13)$$

where  $J$ , the number of elements in the spectrum, is normally about twenty depending upon the degree of precision required. There is little point in using element widths,  $\Delta E$ , much less than the resolution of the system. It should be noted that  $\eta$  is not independent of  $E$  at low energies (see Section 5.4.1).

#### 5.2.5. Electron capture and internal conversion

X rays and electrons from electron-capturing (EC) nuclides and internal-conversion (IC) transitions can usefully be used to measure the figure of merit,  $\eta$ , for the system and as was shown in Figure 11, they also are used to demonstrate the validity of the theoretical calculation of the pulse-height distributions. However to calculate the complete distribution it is necessary to consider all possible modes of decay involving the production of cascades of Auger electrons and X rays (from the L, M, N, ... shells) which may escape from the scintillator without interacting. In some cases, fifteen or more alternative modes of decay are possible and Figure 13 indicates the sort of analysis required for the calculation. IC transitions often do not occur singly either because of the ejection of both K and L electrons with appropriate probabilities or because two or more transitions produce electrons of similar energy. Consideration of these effects is important in assessing the peak position and vital in using the resolution of the peak to determine the figure of merit. This point was discussed above for the decay of  $^{113}\text{Sn} + ^{131}\text{In}^m$  Figure 12.

Having decided upon the input spectrum, the same approach can be adopted as for  $\beta$ -ray emitters and values of  $H(j)$ , based upon this assumed spectrum, inserted into Equation (13).

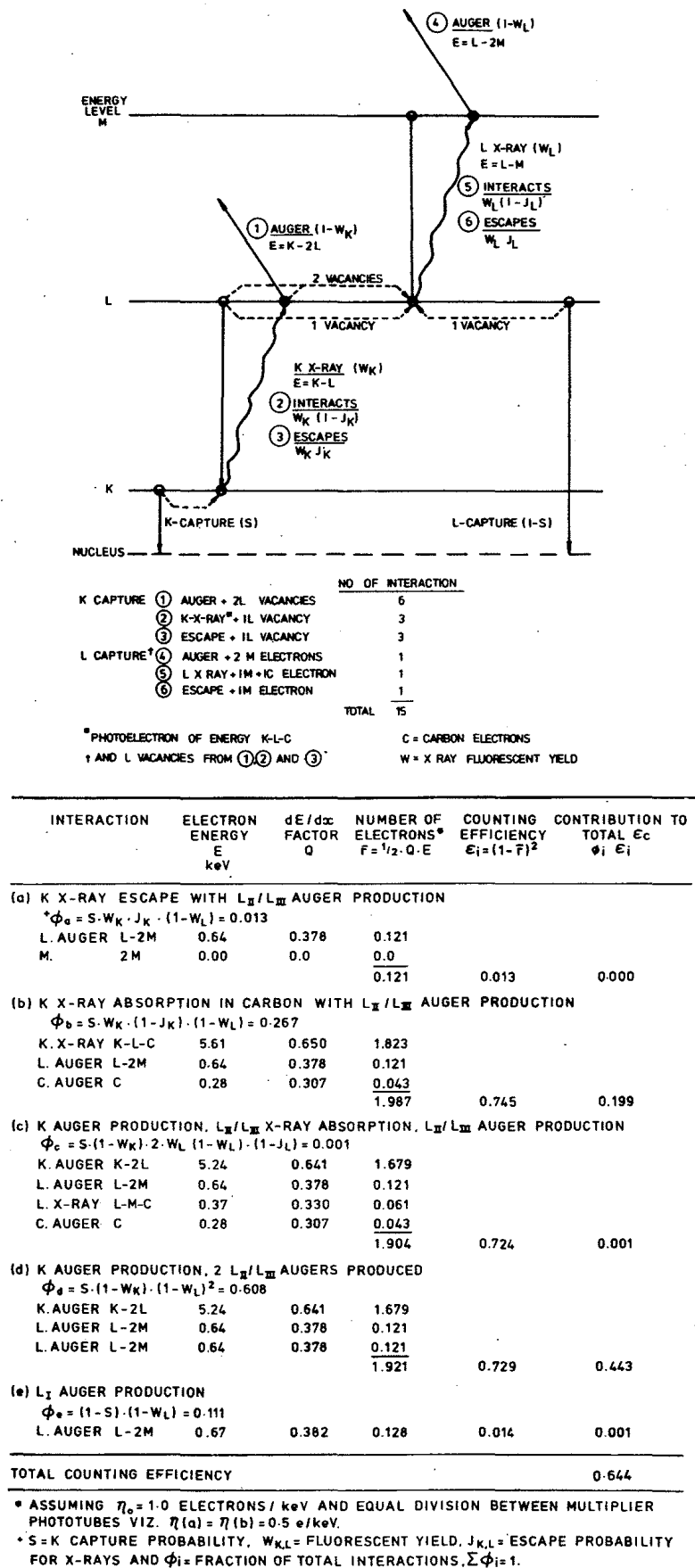


Figure 13 — Selected interactions for EC nuclides and a calculation of the efficiency for <sup>55</sup>Fe in a coincidence system at figures of merit of η<sub>0</sub> = 1.0 and 0.5 photoelectron/keV [195] (courtesy Pergamon Press Ltd., Oxford).

### 5.2.6. The Compton edge

It is necessary to measure the response of the system to a wide range of energies in order to determine the extent of the non-linear response of the scintillator. There are insufficient nuclides decaying by isomeric transitions, with the ejection of monoenergetic electrons, so that it is necessary to use Compton-recoil electrons of maximum energy (the Compton edge) from a series of external  $\gamma$ -ray sources. The energy for the maximum transference of energy to the scintillator is given by

$$E = E_\gamma [1 + E_\gamma / (m_0 c^2)]^{-1},$$

where  $E_\gamma$  equals the incident  $\gamma$ -ray energy and  $m_0 c^2$  is the rest mass of the electron in appropriate energy units, such that  $E_\gamma / m_0 c^2$  is dimensionless. The shape of the Compton spectrum is a function of the energy, and the appropriate function is given in various sources (e.g. [130], see p. 88). This theoretical spectrum can also be divided up into energy bands, weighted by  $H(j)$ , and the output distribution calculated using Equation (13).

It is conventional to take the point corresponding to half the maximum height as the position of the Compton edge. This may lead to small errors in calibration but this should not affect the calculation of the overall counting efficiency.

The position of the Compton edge is also used by Horrocks [256] as a means of determining the degree of quenching in a liquid scintillator. His method is relative, but it is very useful for checking that a particular sample conforms to the operating parameters of the system.

## 5.3. The counting efficiency

In Section 5.2 it has been shown that the pulse-height distribution can be calculated and compared with measured distributions. Integrating this distribution, including all monos, will give the total of all detected events  $N$ . As mentioned earlier, the efficiency,  $\varepsilon$ , will not be 100% and it is now necessary to demonstrate how it can be calculated so that  $N_0 = N/\varepsilon$  can be deduced.

### 5.3.1. The counting efficiency for a single phototube

Starting with a monoenergetic source of electrons in the scintillator, the number of electrons at the input to the first dynode will follow a Poisson distribution of mean  $\bar{r}$ . The zero-detection probability,  $Z$ , is  $e^{-\bar{r}}$  and the efficiency

$$\varepsilon = 1 - Z = 1 - e^{-\bar{r}}.$$

With the RCA tube, there is no further reduction in efficiency in the phototube. The presence of the low-energy tail on the mono distribution has less than a 0.01% effect. Unfortunately no radionuclide decays with a single electron energy, so it is always necessary to determine the counting efficiency by means of an integral, or a summation. It is also necessary in the practical case to use a summation as discussed in Section 5.2.4, Equation (13). The efficiency  $\varepsilon_1(\beta)$  for a single phototube is then given by

$$\varepsilon_1(\beta) = 1 - \sum_{j=1}^J H(j) \cdot \exp\{-\eta \cdot E(j)\}, \quad (14)$$

where  $\eta$  is the figure of merit (photoelectrons/keV) and  $E$  is the energy in keV.

The spectral characteristics of most  $\beta$  emitters are known and calculation methods based upon the Fermi theory can be used [16] to evaluate  $H(j)$ . A similar approach can be made for EC nuclides where the contributions from the Auger electrons and X rays need to be included [195].

### 5.3.2. The counting efficiency for two phototubes in coincidence

Again starting with a monoenergetic source of electrons and two phototubes in coincidence, if the zero-detection probability for phototube  $A$  is  $Z(a)$  and for phototube  $B$  is  $Z(b)$ , then the efficiency is

$$\begin{aligned}\varepsilon_c &= \{1 - Z(a)\}\{1 - Z(b)\} \\ &= \{1 - Z(a) - Z(b) + Z(a + b)\} \\ &= \{1 - e^{-\tau(a)} - e^{-\tau(b)} + e^{-[\tau(a) + \tau(b)]}\}\end{aligned}$$

The efficiency for counting a  $\beta$ -ray emitter is then obtained by summation,

$$\varepsilon_c(\beta) = 1 - \sum_{j=1}^J H_j \{ \exp[-\eta(a)E(j)] + \exp[-\eta(b)E(j)] - \exp[-(\eta(a) + \eta(b)) \cdot E(j)] \},$$

where  $\eta(a)$  and  $\eta(b)$  are the figures of merit for phototubes  $A$  and  $B$  respectively.

The counts from the two phototubes separately and then in coincidence can be expressed as three independent simultaneous equations

$$\begin{aligned}N_1 &= N_0 \cdot \varepsilon_1 = N_0 \{1 - F(a)\}, \\ N_2 &= N_0 \cdot \varepsilon_2 = N_0 \{1 - F(b)\} \text{ and} \\ N_c &= N_0 \cdot \varepsilon_c = N_0 \{1 - F(a) - F(b) + F(a + b)\},\end{aligned}$$

where  $F(y) = \sum_{j=1}^J H(j) \exp[\eta(y)E(j)]$ , with  $y = a, b$  or  $a + b$ .

Thus with the measured values  $N_1$ ,  $N_2$  and  $N_c$  and three unknowns,  $a$ ,  $b$  and  $N_0$ , Tissen [33] and, later, Kolarov et al. [157] suggested that  $N_0$  could be determined. However it is necessary to know the form of the summation  $F$  since for a  $\beta$ -ray spectrum  $F(a) \cdot F(b) \neq F(a + b)$ .

In general, it will be better to compare the calculated and measured distributions before calculating the counting efficiency by one of the above methods.

## 5.4. Non-linear effects

There are various effects in a scintillation counter which can lead to the output not being proportional to the input. The statistical variations have been discussed above and some of the non-linear effects have already been mentioned including ionization quenching, boundary losses and non-uniformity in the phototube cathode and dynodes. These effects will be discussed below.

### 5.4.1. Ionization quenching

As mentioned in the introduction to this chapter, the energy transfer from the initial energy deposition in the scintillator to light output is very inefficient (1 to 5%). If the ionizing particle

deposits energy in a very short track length (high  $dE/dx$ ) as is observed for  $\alpha$  particles and low-energy electrons then, as Birks [69] has shown, there is a further reduction in the scintillation efficiency. Birks used the term “ionization quenching” to describe this loss and produced an equation which can be derived from the Stern-Volmer [1] theory of quenching, for a first-order effect, as the rate of light output per unit track length,

$$\frac{dL}{dx} = \frac{\eta_s dE/dx}{1 + kB dE/dx}, \quad (15)$$

where  $dE/dx$  is the specific energy loss (normally expressed in  $\text{MeV cm}^{-2}\text{g}^{-1}$ ),  $k$  is a rate constant and  $BdE/dx$  is the concentration of ionizing events. Other workers have included a further term  $C(dE/dx)^2$  in the denominator and Voltz [144] proposed an equation of the form

$$\frac{dL}{dx} = \eta_s \frac{dE}{dx} \exp\left\{-\frac{kBdE}{dx}\right\}. \quad (16)$$

Equation (15) due to Birks [69] is to be preferred but the use of alternatives may be necessary if an appropriate fit to the observed data cannot be obtained. The meaning of the terms in Equation (15) will now be explained. The value of the constant  $kB$  is about  $9 \text{ mgcm}^{-2}\text{MeV}^{-1}$  and thus for  $\beta$  particles and electrons with energies greater than about 1 keV, where  $dE/dx = 100 \text{ MeVcm}^{-2}\text{g}^{-1}$ , the Equation (15) and Equation (16) give similar results ( $53\eta_s$  and  $40\eta_s$ , respectively). Here  $\eta_s$  is defined as the figure of merit for the scintillator when  $dE/dx$  tends to zero (i.e. high  $\beta$ -ray energies). If  $kB dE/dx$  is small compared to 1, then the light output from an electron of energy  $E$  is

$$L = \eta_s \int_0^R \left(\frac{dE}{dx}\right) dx = \eta_s \int_0^E dE = \eta_s E, \quad (17)$$

and  $\eta_s = L/E$  is the light output per unit energy input. A second figure of merit for the complete system is  $\eta_0 = \lambda L/E$ , where  $\lambda$  is the photocathode efficiency. In the general case when  $kB dE/dx$  is not small compared to 1, then

$$L(E) = \eta_s \int_0^E \frac{dE}{1 + kB dE/dx} = \eta_s \cdot E \cdot Q(E),$$

where  $Q(E)$  is obtained by numerical integration. Thus in general

$$\eta_E = \frac{\lambda \cdot L(E)}{E} = \eta_0 Q(E).$$

The shape of  $Q(E)$  is dependent upon the value chosen for  $kB$  and an example with  $kB = 9 \text{ mgcm}^{-2}\text{MeV}^{-1}$  is given in Figure 14, which was calculated using a modified form of the Bethe-Bloch theory for  $dE/dx$  [22], with  $dE/dx$  proportional to  $E^{-0.5}$  below 400 eV [160].

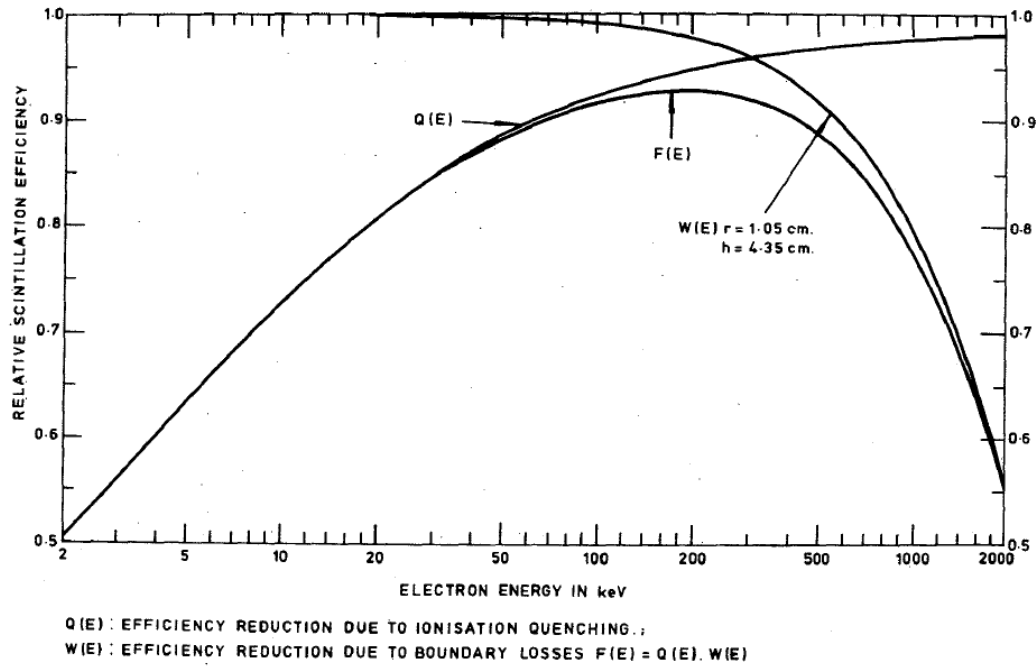


**Figure 14 — Variations of scintillation efficiency with electron energy due to ionization quenching and wall effects [133] (courtesy Institute of Physics, London).**

It should be noted that for  $\alpha$  and other charged particles, when  $kB \, dE/dx \gg 1$ , Equation (15) reduces to

$$\frac{dL}{dx} = \frac{\eta_s}{kB}$$

and

$$L = \frac{\eta_s}{kB} \int_0^R dx = \frac{\eta_s}{kB} \cdot R(E)$$

and the light output is proportional to the range of the particle, not to its energy.

#### 5.4.2. Boundary losses at high electron energies

One major difficulty in determining  $\eta_0$  at high electron energies is that a significant proportion of the energy may be lost into the walls of the scintillator cell and out of the surface of the scintillator. This will distort the spectrum and may give misleading results. Benjamin et al. [55] derived a formula for the fraction of energy deposited within a cylinder of radius  $r$  and height  $h$ , such that

$$W(E) = 1 - 0.5 \left\{ \frac{1}{r} + \frac{1}{h} \right\} R(E),$$

where  $R(E)$  is the range of an electron of energy  $E$  [22]. As far as possible the energy lost to the boundaries should be reduced to a minimum so that corrections to the observed spectrum are unnecessary. Normally this boundary loss is not sufficient to reduce the counting efficiency as enough energy will be deposited in the scintillator to produce a detectable output from the phototube and this effect is only important in setting up a system. Illustrative values of  $W(E)$  are shown in Figure 14.

### 5.4.3. Loss of photon radiation from the scintillator without interaction

This problem arises in three cases:

1. in the loss of X rays after electron capture,
2. where a nuclide decays by an isomeric transition without emitting a  $\beta$  particle or an electron and only  $\gamma$  rays are produced (e.g.  $^{137}\text{Ba}^m$ ) and
3. where the liquid scintillator is used as the  $\beta$ -ray detector in the  $4\pi\beta-\gamma$  coincidence method (e.g. [88], see p. 86).

Gibson and Marshall [195] calculated the probability of escape for a right circular cylinder of radius  $a = 10.5$  mm and half length,  $l = 27.75$  mm, based upon the following integral for the total probability of escape

$$J(E) = \frac{\int \int e^{-\mu d} d\Omega dV}{\int \int d\Omega dV},$$

where the solid angle  $d\Omega = \sin\theta d\theta d\psi$  with the integral of  $\theta$  from 0 to  $\pi$  and  $\psi$  from 0 to  $\pi$  as well. The volume element  $dV = x dx dz$  Figure 15 where the radial term,  $x$ , is integrated from 0 to  $a$  and the axial term,  $z$ , from 0 to  $l$ , the half length of the scintillator. The divisor can be integrated analytically to give  $\pi a^2 l$  ( $= V/2$ ) and the numerator integral must be solved numerically using tabulated values of the mass attenuation coefficient,  $\mu_a$ , for different photon energies (e. g. [130]). The distance,  $d$ , from the point of origin of the X ray to the boundaries of the scintillator is complicated to calculate. Thus the escape is considered in three parts:

1. top of the cylinder,  
 $\mu_a d = \mu_a (l - z) \cos\theta$ ,  
 with integration limits for  $\theta$  from  $\theta = 0$  to  $\theta = \theta_1 = \tan^{-1}\left\{\frac{-x \cos\psi \pm f}{1-z}\right\}$ ,
2. curved section,  
 $\mu_a d = -\mu_a (x \cos\psi \pm f) / \sin\theta$ ,  
 with integration limits for  $\theta$  from  $\theta = \theta_1$  to  $\theta = \theta_2 = \tan^{-1}\left\{\frac{-x \cos\psi \pm f}{-1-z}\right\}$ ,
3. bottom of the cylinder,  
 $\mu_a d = -\mu_a (1 + z) / \cos\theta$ ,  
 with integration limits for  $\theta$  from  $\theta = \theta_2$  to  $\theta = \pi$ .

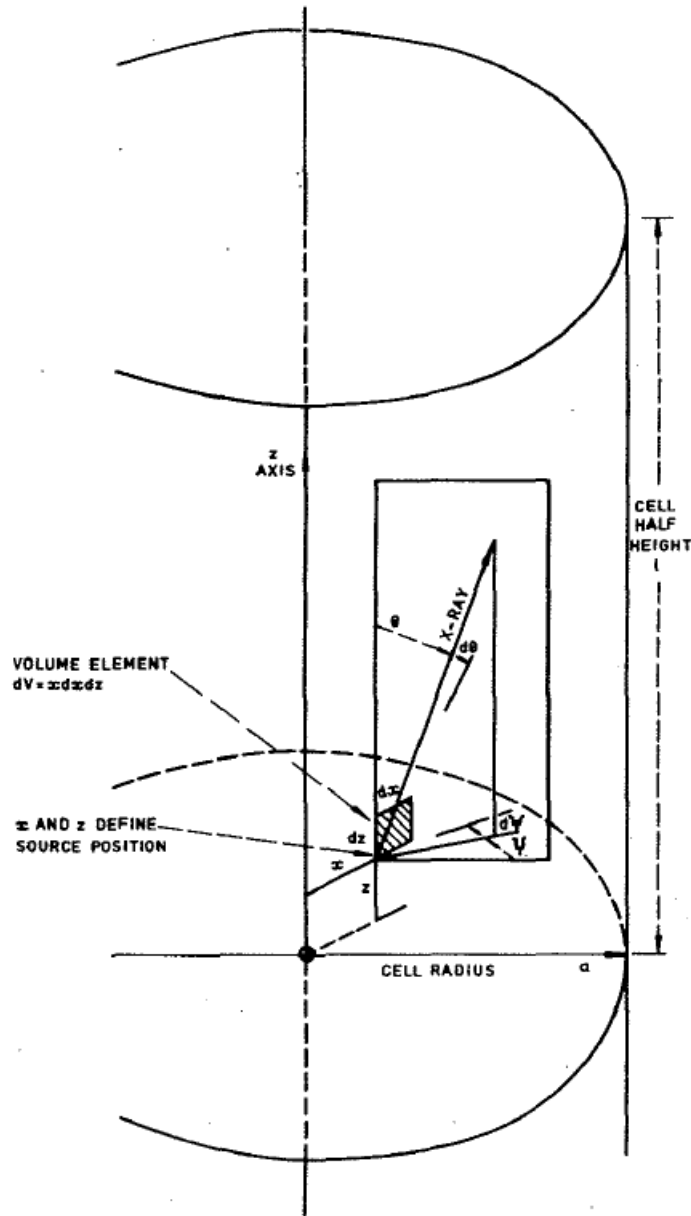


**Figure 15 — Geometry used in calculating the escape of photon radiation from the scintillator cell [195] (courtesy Pergamon Press Ltd., Oxford).**

The limits for  $\Psi$  are 0 to  $\pi$ , for  $x$  from 0 to  $a$  and for  $z$  from 0 to 1. The function  $f$  above is given by

$$f = (a^2 - x^2 \sin^2 \Psi)^{1/2}.$$

The value of  $1 - J(E)$  for a  $15 \text{ cm}^3$  volume with  $a = 10.5 \text{ mm}$  and  $l = 21.75 \text{ mm}$  is plotted as function of energy in Figure 16 and shows that this correction is important above about 2 keV. The efficiency for counting Auger electrons is also shown in this figure for two values of the figure of merit,  $\eta_0 = 0.5$  and 1.0 photoelectron/keV ( $\eta_0/2$  for each phototube).



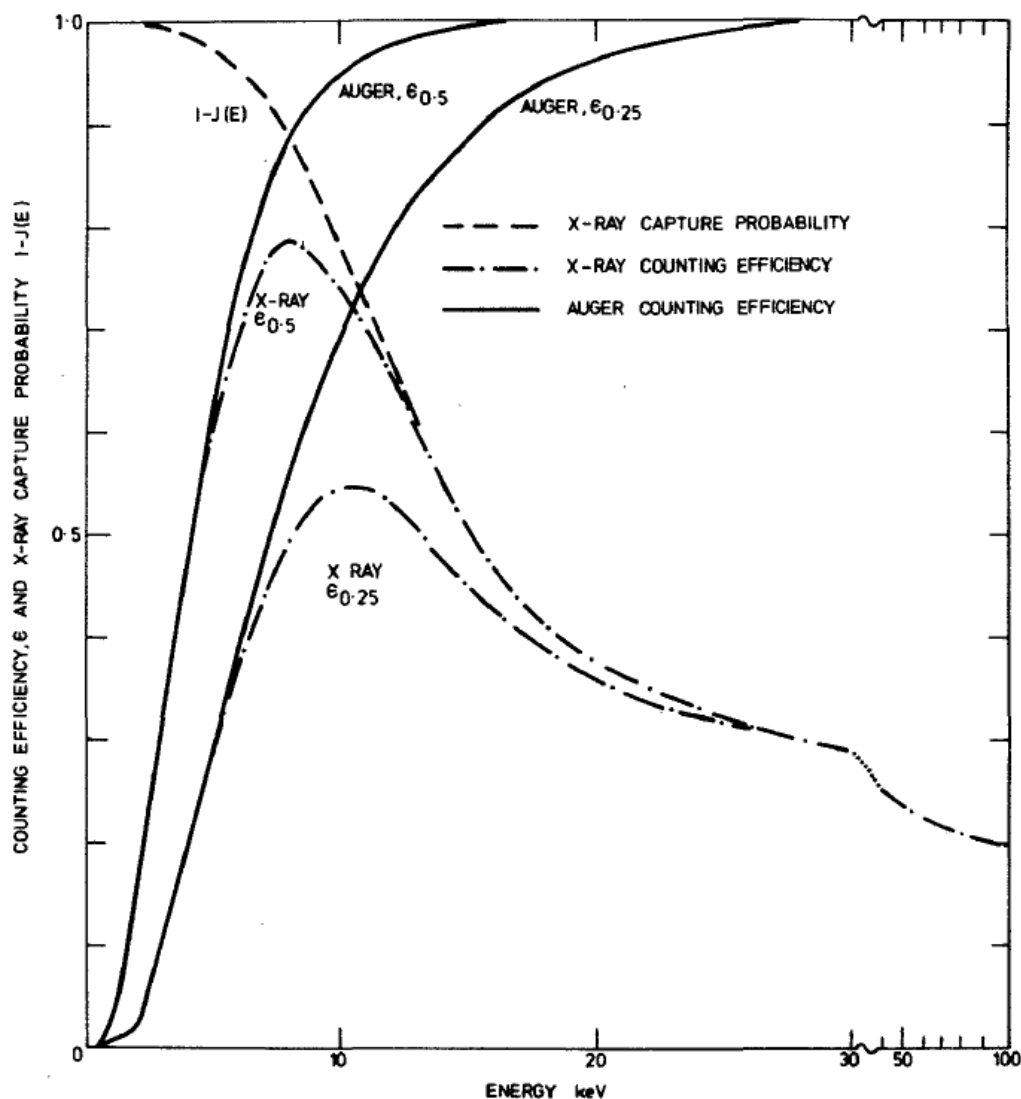


Figure 16 — Counting efficiency for X rays and Auger electrons, and X-ray capture probabilities [195] (courtesy Pergamon Press Ltd., Oxford).

#### 5.4.4. Other effects

There are many minor effects which can distort the spectrum and hence lead to a loss of counting efficiency. Starting with the scintillator and vial, it is important to ensure complete solubility with no plating out on to the vial walls. Colour and chemical quenching distort the spectra in different ways. In the case of chemical quenching the effect is equivalent to a gain change such that

$$g = (1 + kw)^{-1},$$

where  $k$  is the rate constant in the Stern-Volmer [1] equation and  $w$  is the concentration of the quenching agent per unit volume of the scintillator [113]. Thus the figure of merit,  $\eta_0$ , is reduced to  $g\eta_0$ . Colour quenching introduces a more subtle distortion because light produced close to the photocathode is not absorbed but that from deeper in the scintillator may be lost completely. It is better to reduce quenching to a minimum in direct counting, but checks must still be made to make sure this objective is achieved. The vials should be as uniform as possible

so that the light escapes equally to both phototubes in a coincidence system. The vial should be well coupled optically to the phototubes to avoid internal reflections.

The photocathode may be non-uniform as shown by Stanley and Malcolm [277] and it may be necessary to limit the area used to avoid distortions in its response. The collection efficiency of the first dynode needs to be as good as possible and inhomogeneities in all dynodes should be minimised. Coates [149] has demonstrated that edge effects in the dynodes are the major source of spectral distortion with the RCA tube and must be allowed for in calculating the pulse-height distribution. Photoemission from the first dynode is unimportant with a phototube of the RCA type. Instrumental effects due to a poor high-frequency response in the electronics or to poor layout of phototube on other connectors giving rise to ringing or reflections must be avoided. Dead times in excess of 100 ns may be required to avoid this problem.

Afterpulses in the phototube can cause problems but this will be discussed in a later chapter. Equally, long decay times in the scintillator may produce similar effects and should be avoided. In general a careful survey of the system is required on setting up and at regular intervals to ensure that ageing effects do not change any of the parameters or introduce interfering effects.

## 5.5. System design and testing

Most commercial instruments for coincidence counting are designed to minimise the user interaction with the parameters of the system. However modification of a commercial instrument may prove to be the most economical way of setting up a system for direct counting. The choice of phototubes is restricted to the special RCA 8850 phototube with the first dynode of GaP(Cs) with a high gain ( $>30$ ). These phototubes should be carefully selected with a high peak-to-valley ratio ( $>5$ ), with low noise and a similar gain. The photocathodes should be uniform. The dynode chain, connectors and electronics should be designed to reduce after pulses and ringing. The phototubes should be tested with a light source and with  $^{55}\text{Fe}$  in a liquid scintillator. Both phototubes should be set to count monos. It is necessary to provide outputs to a pulse-height analyser for both tubes singly and summed in coincidence if proper analysis is to be performed.

The liquid scintillator needs to be chosen with equal care to ensure adequate solubility for the radionuclide to be standardised and to reduce quenching to a minimum. Studies of the effect of colour and chemical quenching should be made using an external-source method (e.g. [256], see p. 96) and the sample channel-ratio method. The source is ideally positioned at the side of the counting vial to reduce effects due to variations in the thickness of the vial wall. The “H number” concept of Horrocks [256] is independent of such an effect and measures the changes in scintillation efficiency directly.

Having chosen the system and the scintillator, it is then necessary to determine the figure of merit as a function of energy by using EC nuclides, IC transitions and the Compton-edge position. Supplementary information can be obtained from measurements of the resolution of the peaks provided corrections are made for multiple decays of similar energy. The measured data can then be used to determine the ionization quenching constant  $kB$  in Equation (15). Any changes in the system or the scintillator will involve a remeasurement of  $kB$ .

The decay scheme of the radionuclide under investigation should be considered, and in the case of a  $\beta$ -ray emitter it is necessary to know the spectral shape. Any X or  $\gamma$  radiation associated with the decay should be included and the interaction probability within the

scintillator calculated. Finally the full pulse-height-distribution should be calculated for comparison with the measured value. It is then possible to integrate the area under the distribution and so determine the total count rate. The efficiency can be calculated from the theoretical pulse-height distribution. This is the only really effective method for low-energy emitters as any form of extrapolation will involve assumptions of linearity which are difficult to justify in practice and no tests of the method proposed by Kolarov et al. [157] have been reported.

Finally it is necessary to assess the uncertainties in the measurement. These will be less than the zero-detection probability,  $Z$ , and will depend upon the systematic uncertainties in the ionization-quenching constant,  $kB$ , and the high-energy figure of merit,  $\eta_0$ . Some uncertainty must be placed upon the knowledge of the spectrum and on calculations of the escape probabilities of photon radiation. Counting statistics are to be included in the random uncertainty as must any corrections for afterpulses, background and accidental coincidences due to chemiluminescence. Normally these can be reduced to an uncertainty much less than 0.5%.

A simple demonstration of the analysis of uncertainty can be given, as follows. The zero-detection probability  $Z$  is approximately equal to  $e^{-\bar{r}}$ , where  $\bar{r} = \eta E$ . Thus  $dZ/Z = -d\bar{r} = -d\eta \cdot E$  or the fractional uncertainty in  $Z$  is proportional to the uncertainty in  $\eta$ , the figure of merit. Also the fractional uncertainty in the counting efficiency  $\varepsilon$ , is  $dZ/\varepsilon$  so that, if a 5-keV electron in the scintillator produces three photoelectrons at the first dynode ( $\eta_0 Q(E) = 1 \times 0.63$ ), assuming that  $\eta$  is measured to  $\pm 10\%$  (standard deviation), then

$$\frac{dZ}{\varepsilon} = \frac{0.1 \cdot 3 \cdot e^{-3}}{1 - e^{-3}} = 1.6\%.$$

This corresponds, very approximately, to the accuracy obtainable for a direct measurement of tritium [194]. A more precise calculation would involve the use of the whole spectrum to produce a weighted value of  $dZ/E$  and also a better assessment of  $d\eta$  and the other variables.

## 5.6. Conclusions

Precise measurements of nuclides emitting low-energy radiations are possible with an uncertainty of about 3% at the 95% confidence level. However these measurements do rely upon models of light conversion in the scintillator and a simple statistical approach based upon the Poisson distribution. By using phototubes with a high gain ( $>30$ ) at the first stage, such models are probably adequate at this confidence level and the uncertainty could be reduced if the approach proposed above is applied carefully. It is very important to emphasise that extrapolation methods for radionuclides emitting low-energy radiations cannot be justified theoretically. The fact that agreement is reached with other independent methods is not a justification. Essentially, it is necessary to justify theoretically each direct method independently, and then finally to make an intercomparison in order to confirm that agreement to within the calculated uncertainties has been achieved. In the case of the LS counter this justification means a careful study of the system so as to produce the parameters for calculating the pulse-height distribution and hence determine the counting efficiency. Full justification and taking the method to its limits will need further research.

## 6. The Use of Liquid Scintillators in Radionuclide Metrology

R. Vatin<sup>(1)</sup>

<sup>(1)</sup> Laboratoire de  
Metrologie des  
Rayonnements Ionisants,  
CEN Saclay, France.

### 6.1. Introduction

In the following pages we review the situation concerning the use of LS counting in measuring radioactivity standards without, however, dealing with the problems related to obtaining stable solutions, the phenomenon of adsorption and the existence of multiple pulses, these questions being the subject of other parts of this Monograph. Although a special study will be devoted to the statistical phenomena involved in the detection process, we will deal briefly with the subject of measuring radionuclides of the pure  $\beta$ -emission type.

We will examine the various problems raised in activity measurements of nuclides decaying by pure  $\beta$ -particle emission,  $\beta$ - $\gamma$  emission, and those disintegrating by electron capture without, however, seeking to provide an exhaustive list of the published work. After describing the various characteristics of equipment meeting metrological standards we will review the different methods used.

From the beginning of 1950 it appeared that it was possible to introduce small quantities of a radionuclide into a fluorescent solution without destroying its properties of luminous emission. This fact made it possible to envisage a new method of measuring radioactivity, which, as a result of the intimate mixing of the radionuclide with the detecting medium, overcame the loss of efficiency in detection caused by the absorption of part of the radiation by the solid source and its support during measurements with a gas counter. This aspect appeared particularly interesting in the measurement of the activity of radionuclides of the low-energy pure  $\beta$ -particle emitters. However the values reported in the scientific literature at that time showed very low detection efficiencies—only a few per cent in the case of tritium. The method exhibited many inadequacies, low luminous output, parasitic pulses, instability of the solutions, etc., and much work was necessary to reach metrological levels.

### 6.2. Characteristics of metrology equipment

#### 6.2.1. Experimental arrangement

1. **The cell and collection of the light**—The object is to collect the maximum of the light created by the scintillator. Various authors have used one or more electron-multiplier phototubes. In arrangements using a single phototube the cell, or vial, containing the scintillator is arranged vertically above the photocathode of the phototube with an optical joint of silicone grease and a reflecting or diffusing cover which directs the light towards the photocathode [13], [19], [23], [36], [46], [49], [95], [114]. Amongst other advantages, the arrangement with two coaxial phototubes allows better collection of the light. Many types of cells have been used with two phototubes. The authors who use standard vials generally improve the collection of the light by using a silicone bath or by a light duct with a silicone joint [36], [46], [49], [95], [114], [185]. Certain authors have used a sphere in

<sup>(1)</sup> Sometimes called afterpulses or spurious pulses (see Chapter 7).

a silicone oil bath [120]. Others have employed glass cylindrical cells, the axis of which coincides with that of the phototube [26], [123]; see also Section 4.4.

2. **The electron-multiplier phototubes**—Much progress has been made in the development of phototubes, particularly in the quantum efficiency which is nearly 0.32 photoelectron per photon at 385 nm for a bialkali photocathode. The photoelectron collection efficiency has also been improved by using highly sophisticated electron optics. Dynodes activated with gallium phosphide (GaP), which are used in the first stage of certain recent phototubes (RCA 8850), have a very high gain which can reach 40, and this has the effect of greatly reducing fluctuations in low-amplitude pulses. Improved construction has also eliminated ion build-up on the photocathode, so reducing one of the principal sources of parasitic pulses<sup>(1)</sup>. The new photocathodes, with increased sensitivity, have a reduced dark current, and this means that it is no longer necessary to work at low temperatures to achieve low levels of noise.

### 6.2.2. The scintillating solution

1. **The solvent**—The solvent most widely used in LS metrology is still toluene. For diluting inorganic salts in aqueous solution, as is the normal case when measuring standards, ethanol or methanol are most frequently used as the intermediate solvent. Dioxane is little used in metrology because of the chemiluminescence that it exhibits when it comes into contact with water, as has been pointed out by many authors, and also because of its lower luminous output. Furthermore the standards to be measured generally have such high radioactivity concentrations that it is possible to introduce only very small quantities of the radioactive solution into the scintillator (less than 1%). Few authors carry out systematic degassing of the solvent.
2. **The scintillating solution**—Most laboratories still use the PPO-POPOP system, even with the bialkaline photocathode. The reason for this is that the properties of this scintillator are perfectly known, and that it remains very effective even in the presence of quenching elements. Certain workers use PBD or t-butyl-PBD. When measuring toluene labelled with  $^{14}\text{C}$  or  $^3\text{H}$  it is advantageous to use BIBUQ [157]. Chemical formulae for these and other scintillators are given in Table 2.
3. **Preparation of the sources**—Two source-preparation procedures are possible. In certain laboratories a small aliquot of the active solution is placed in each vial to be used in the measurement. Other authors prefer to dissolve a larger aliquot in a large quantity of scintillator (50 to 100 cm<sup>3</sup>) and then to fill the measuring vials with the ready-prepared solution. Obviously, the measurement of the aliquots is carried out by weighing, usually by difference weighing of a polythene pycnometer or using a calibrated micropipette [284]. The first method involves the measurement of small masses, usually a few milligrams, the second procedure allows easier and more accurate weighing since the masses are greater, generally of the order of a few hundred milligrams. Furthermore, homogenisation of the active-solution—scintillator mixture is more easily achieved in a flask of larger dimensions than the measuring cell. We should note that the weighing of volatile solutions does present special difficulties [90].

### 6.2.3. The counting electronics

At the present time charge-sensitive preamplifiers using field-effect transistors completely solve the problem of background noise in the amplification chain. Nevertheless care must be taken not to allow saturation from pile-up in the preamplifier before the first differentiation. In the same way transistor amplifiers are easily protected against overloads so that there is no difficulty in working at very high gains and high-overload levels in count-rate measurements, for example, of pure  $\beta$ -particle emitters. Differentiating amplifiers with a single delay line with base-line restoration give particularly good performance in this field. The discrimination and dead-time circuits should be carefully chosen; for example, the dead time should be non-extending, in order to reduce the dead-time correction uncertainty. No comment needs to be made about scalers, except that provision be made for obtaining the data in a form that is convenient for subsequent computer processing. The electronic clock which controls the counting interval should, in general, have an accuracy of 1 in  $10^5$ . When it is necessary to carry out extrapolation as a function of the discriminator level it is possible, in the case of  $\beta$ -particle emitters of reasonably high maximum energy, to repeat the measurements by varying the discriminator voltage setting each time [157], or by recording count rates at several levels of discrimination simultaneously [123], [246].

### 6.2.4. Measurements using $\beta$ – $\gamma$ coincidences

In the case where coincident  $\gamma$  rays are detected many arrangements of the NaI(Tl) crystal or crystals are possible [26], [49], [95], [114], [120], [123], [185]. In order to obtain a high  $\gamma$ -ray efficiency it is possible to use NaI(Tl) crystals which completely enclose the sample vial and the  $\beta$ -detecting phototube. The  $\gamma$ -channel amplifiers are of the conventional type. The single-channel analyzer should be designed to give precise time information and to impose a well-defined dead time so as to make exact corrections possible.

## 6.3. The methods

### 6.3.1. Measuring radionuclides which disintegrate by pure $\beta$ -particle emission

The  $\beta$ -ray spectra show a non-zero emission probability density down to and including zero energy. Part of the spectrum is situated in the region of the background noise of the detector and the amplifier. It is therefore necessary to have recourse to extrapolation of the rate of integral counting to zero value of the energy. The shapes of the  $\beta$ -ray spectra are very different, and the detection procedure considerably modifies them. For those of high maximum energy it is possible [19], [23], [36], [46], [49], [95], using adequate amplification, to obtain a flat region of the spectrum; this justifies linear extrapolation, although no theoretical reason can be advanced to explain this fact. Many workers have also observed a build-up of the differential spectrum towards the lower energies without being able to attribute this to the background noise of the amplifier or the detector background [8], [13], [19]. This phenomenon, attributed to multiple pulses arising from the detector or the amplifier, can be eliminated by a dead-time circuit preceding the counting scaler [8], [19].

Comparison of these results with those obtained by other methods shows, in the case of radionuclides of maximum energy lower than 200 keV, a detection efficiency which is less than 100% [10], [29], [91] ( $^{14}\text{C}$ ,  $^{35}\text{S}$ ,  $^{63}\text{Ni}$ ,  $^{106}\text{Ru}$ ,  $^{241}\text{Pu}$  and, in particular,  $^3\text{H}$ ). This is

attributed to statistical fluctuations in the number of photoelectrons emitted by the cathode of the phototube, and the non-vanishing probability that a low-energy event results in no photoelectron being emitted (see Chapter 5, see p. 41).

Basing his work on the hypothesis of the Poisson distribution of the electronic emission of the photocathode Wright [14] calculated the zero-detection probability (ZDP) in the case of monoenergetic ionising particles. Tissen [33] extended this calculation to continuous  $\beta$ -ray spectra in the cases of detection by a single phototube, and by two phototubes in coincidence. He characterized the quality of the detection assembly—scintillator and photocathode—by the mean number of photoelectrons obtained for unit loss of energy of the primary particle in the scintillator, and showed that, approximating to the allowed form of the decay of radionuclides of low atomic number, and on the hypothesis of linear response of the scintillator, the efficiency of detection depends only on the quality parameter and the maximum energy of the continuous spectrum. Values calculated in this way for  $^3\text{H}$  and  $^{14}\text{C}$  are found to be in good agreement with current experimental results.

Horrocks and Studier [53] showed that, for a given spectrum, the ratio of the detection efficiencies with a single phototube and two in coincidence depends only on the quality parameter (figure of merit). They obtained excellent agreement between their experimental measurements and theoretical values calculated on the basis of an average of one photoelectron per 1.5 keV of energy dissipated in the scintillator.

The high ionization densities created by low-energy electrons reduce the luminous output of organic scintillators. This results in a non-linear response for energies less than about 100 keV. Birks [3] has given a formula describing the phenomenon where the luminous output varies with the loss of specific energy of the particle. In their article Gibson and Gale [133] take this effect into account by the introduction of a term dependent on the energy,  $Q(E)$ , when calculating the detection efficiency (see Chapter 5). According to them the uncertainty in respect to the coefficients does not introduce an error of more than 3% in the value of  $Q(E)$  for an energy of 5 keV. The quality parameter measured on their installation is 0.45 photoelectron/keV. From this they deduce a detection efficiency with a single phototube of 62.9% for  $^3\text{H}$  and, by comparison with a Radiochemical Centre standard, they observe a difference of—2.4%. With the phototubes in coincidence, they calculate an efficiency of 43% with a difference, in respect to an NBS standard, of +2.7%. For  $^{14}\text{C}$  the calculated values are 96.4% and 93.7%, respectively (1971 revised values) [171], with differences of +3.5% and +2.5% in respect of the standards.

These calculations assume that the quality parameter is known. In the method of Kolarov et al. [157] the quality parameter is determined at the time of the measurement itself by solving the system of non-linear equations which link the efficiency of detection in coincidence, summed and for each phototube separately, with the experimental count rates. In these equations the quality parameter occurs as an unknown in the same way as the activity. When applied to  $^3\text{H}$  this method gives differences of about 4% in excess when compared with an NBS standard (unpublished results).

The accuracy of all these methods obviously depends on the accuracy of the theories and of the values of the parameters occurring in them, since they all lead to an a priori calculation of the detection efficiencies. The principal sources of systematic error are due to the theory of the energy loss of the electrons in matter (Bethe), to the theory of ionization quenching (Birks, Voltz), to the theory of the form of spectra (Fermi), and to the calculation of the deformation of the spectra by wall effects.

Let us examine these various points:

1. The Bethe formula is not very accurate and is almost certainly inaccurate below 0.5 keV for organic solvents. This results in an error which is difficult to quantify but which is certainly less than 0.1% in the case of  $^{14}\text{C}$ . At the present time there is no accurate theory in this field of energy [76].
2. Two different theories [3], [76], [96], [133], [171] giving numerically very similar results make it possible to calculate the yield of organic scintillators [122], [174]. Gibson [133] has estimated that the uncertainty in respect of the coefficient in the Birks formula was likely to introduce an error of  $\pm 2\%$  in the detection efficiency in the case of  $^3\text{H}$ , but less than 0.1% in the case of  $^{14}\text{C}$ . Experimental determination of the luminous response of organic scintillators [80] is inaccurate, particularly below 20 units/ml(keV). There are, in fact, few references to energies in this range and, furthermore, resolution of the peaks is poor.
3. A formula due to Benjamin [55] has been used up to the present time to take account of the wall effect. Actually, this only gives the proportion of particles which encounter the wall. It is however preferable to calculate precisely the deformed spectrum. The method of Snidov and Warren [121] can be used. This effect is considerable in the case of high-energy emitters, since it causes the appearance of a large number of small pulses for which the zero-detection probability is considerable.
4. The exact form of the  $\beta$ -ray spectra themselves is not always well known. Only rarely does theory make it possible to forecast the nature of the transition, and few factors relating to the experimental shape have been published. Furthermore theoreticians have introduced new correction terms (radiative, polarization, etc.) [37], [116], [165], the practical calculation of which has been found to be difficult.

**Methods not requiring a priori calculations**—The guiding idea here is to make the non-detection probability increase and to carry out extrapolation for a zero non-detection probability. Several procedures are possible: inhibition of the luminescence of the scintillator, modification of the optical coupling by interposing optical absorbing filters [169], defocussing of the phototube [172]. It is enough to know simply the attenuation ratios, and this can easily be achieved by using an external  $\gamma$ -ray source or, better, using an internal monoenergetic source (e.g. of conversion electrons or  $\alpha$  particles). The only source of systematic error is then the uncertainty of the extrapolation. In the communication already cited, Flynn and his co-authors carry out a linear extrapolation. They estimate their maximum error as  $\pm 2\%$  for  $^3\text{H}$ . It should be possible to improve the method by increasing the number of points, and this is easily done by defocussing and by carrying out a non-linear extrapolation.

### 6.3.2. Measurements on $\beta$ – $\gamma$ emitters

In the method of activity measurement using  $\beta$ – $\gamma$  coincidences it is very advantageous if at least one of the detectors has a high detection efficiency. Detectors using liquid scintillators for the detection of  $\beta$  radiation satisfactorily meet this condition, but in addition to this the intimate mixing of the radionuclide and the scintillator means that the sensitivity is more or less constant throughout the whole volume of the source (if there is no adsorption at the boundaries), this property also being very favorable to the quality of measuring by coincidence.



The elementary theory of the method of  $\beta$ – $\gamma$  coincidences assumes that the detectors have zero detection efficiency for the type of radiation for which they are not intended.

This is only true as a first approximation, particularly for the  $\beta$  detector. Whilst for a proportional counter this sensitivity  $\varepsilon_{\beta\gamma}$  is several parts in a thousand, it reaches several percent and varies with the level of filling of the cell in an LS counter. Under these conditions it is preferable to use an extrapolation method [256]. However with a liquid scintillator, which preserves the general form of the  $\beta$ -ray spectrum reasonably well, one can easily make the efficiency of detection vary by simple modification of the counting threshold. For the same reasons the method is equally suitable for measuring the activities of emitters with a complex decay scheme [60], [97].

It has been shown that the method of extrapolation in coincidence involves an error if certain conditions are not satisfied [87], [125], [108], [138]. The systematic error arises from the difference in the forms of the spectra of the various  $\beta$  branches, from the lack of homogeneity of the source, and the escape of part of the radiation. Obviously this error becomes smaller as the detection efficiencies which are achieved become greater. With LS the detection efficiency is greater than 95% for  $\beta$  radiation of energy greater than about 5 keV, and this is a very distinct advantage when compared with measurements with counters using a solid source. One way of detecting the systematic error in extrapolation is to repeat the measurement with different  $\gamma$ -ray gates [108]. Spahr and Binkert [187] have recently reported results on measuring  $^{134}\text{Cs}$  with different  $\gamma$ -ray gates:  $\gamma_9$  (1365 keV) in coincidence with  $\beta$ 's of lower energy,  $\gamma_5$  (796 keV) in coincidence with  $\beta$ 's of high energy. They obtained in these cases extrapolated values 0.04% higher and 0.33% lower in relation to the value found with  $\gamma_4$  (604.7 keV), in coincidence with three  $\beta$  branches. The same authors have carried out a comparison of the results obtained with a proportional counter and with a liquid scintillator in the case of  $^{60}\text{Co}$ . They found a deviation of 0.14% lower with the liquid scintillator, their statistical accuracy being 0.14% (the confidence interval is not given). For more details on  $^{134}\text{Cs}$  measurements, the reader may consult Chapter 8 and [301].

It is necessary in all these very important questions to pursue, in a systematic manner, the theoretical and experimental study of the accuracy of the methods obtained by the extrapolation method.

### 6.3.3. Measurement of pure $\beta$ -particle emitters with a $\beta$ – $\gamma$ tracer

The method of  $\beta$ – $\gamma$  tracing previously used in the assay of pure  $\beta$ -particle emitters with proportional counters [35], [43], [68] has subsequently been used with a LS detector [66]. This can, in fact, be regarded as a variant of the method for measuring  $\beta$ – $\gamma$  emitters with a complex decay scheme, and the general theory [97] can be fully applied. LS detectors allow good mixing of the two radionuclides and high homogeneity of the source. As a result they are not subject to the principal cause of systematic error in detectors with a solid source. Extrapolation can conveniently be carried out by variation of the counting threshold. The systematic error arising from the difference in the  $\beta$  spectra still, obviously, continues to exist. It can be detected and estimated by repeating the measurement with different  $\beta$ – $\gamma$  tracers. In this way Spahr and Binkert [187] have assayed  $^{35}\text{S}$  using  $^{60}\text{Co}$ ,  $^{134}\text{Cs}$  and  $^{203}\text{Hg}$  as tracers. Their results expressed as ratios to the result obtained with  $^{134}\text{Cs}$  ( $\gamma$ -ray gate unspecified) were

$$1.0039 \pm 0.0012 \text{ with } ^{60}\text{Co}$$

and

$$0.9989 \pm 0.0012 \text{ with } ^{203}\text{Hg}$$

It can be seen that the difference between these ratios (0.50%) is higher than the random errors in the ratios. It is interesting to note that, in a measurement of  $^{35}\text{S}$  by tracers with a proportional counter, Williams and Goodier [125] found a larger difference in the opposite direction.

The complementarity of these two methods can be clearly seen, and it is reasonable to assume that systematic comparisons would make it possible to detect and reduce the errors.

An accurate extrapolation could be made if it were known how the ratio of the counting efficiencies for the two radionuclides varied as the counting threshold is varied. A novel solution to this problem was developed by Bryant et al. [109], [156] in which an opto-mechanical device simulated the scintillations produced by  $\beta$  particles in the scintillator taking into account the theoretical  $\beta$  spectra and the variation of scintillator efficiency with  $\beta$ -particle energy. Tests showed that this system accurately reproduced the shapes of known efficiency functions. A modification of this method in which the opto-mechanical device has been replaced by a computer simulation is routinely used for the standardization of pure  $\beta$ -particle emitters [298].

#### 6.3.4. Measurement of radionuclides disintegrating by electron capture

In a liquid scintillator the Auger electrons are detected with high efficiency and good reproducibility [123]. X rays of low energy have a short path in the liquid scintillator, and escape is not of great importance with the volumes of scintillator normally used (a few milliliters). Cascades of X and Auger events make it possible to collect all the energy of the vacancy created by a capture. All these reasons lead to high detection efficiency—80% for  $^{54}\text{Mn}$ —for radio-nuclides which disintegrate by electron capture.

Steyn [122] has applied the extrapolation method in coincidence to the measurement of the activity of emitters which disintegrate by electron capture followed by  $\gamma$  emission. In this way he measured  $^{51}\text{Cr}$ ,  $^{54}\text{Mn}$ ,  $^{65}\text{Zn}$  and  $^{57}\text{Co}$  with small differences with respect to measurements made with a proportional counter, except for  $^{51}\text{Cr}$  where he observed a difference of -2.8%. The maximum efficiency obtained with  $^{57}\text{Co}$  was  $(89.1 \pm 0.1)\%$  with the liquid scintillator, whilst it varied from 39% to 62% according to the sources when using a proportional counter. This high reproducibility of liquid-scintillator efficiency makes it possible to envisage the measurement of radionuclides which disintegrate by electron capture without  $\gamma$ -ray emission, the detection efficiency being known by interpolation of the efficiencies obtained with other radionuclides (it must obviously be assumed that the quenching remains small). With radionuclides of high atomic number, that part of the efficiency resulting from the escape of part of the X radiation constitutes a geometrical effect which may involve a systematic error in the extrapolation by variation of the counting threshold [138].

One can therefore envisage the measurement of emitters disintegrating by pure electron capture by using, as the tracer, a radionuclide which disintegrates with electron capture followed by  $\gamma$ -ray emission. If the atomic numbers of the two elements do not differ greatly, the method of extrapolation should not introduce an excessive error.

If the electron capture is in competition with positron emission the situation becomes more complex. A report dealing with this subject is by Steyn and de Jesus [107] who, however, used a plastic instead of a liquid scintillator.

### 6.3.5. Measurement of $\alpha$ emitters

The resolution of  $\alpha$ -particle spectra obtained by LS systems is of the order of 20 to 30% (in terms of full width of the peak at half maximum divided by  $\alpha$ -particle energy). This dispersion arises from the location of light emission in the scintillator, rather than from statistical fluctuations in the number of photoelectrons in the phototube. The boundary effect results in the formation of a “tail” between the peak and zero energy. This tail normally represents less than 1% of all the pulses. Therefore, under these conditions, together with low-noise electronics, the only source of error being that inherent in the extrapolation, it is possible to obtain high accuracy. Ihle [114] has shown that underlight-collecting conditions which had deliberately been made poor, the resultant error remains small ( $\approx 0.1\%$ ).

## 6.4. Conclusion

As a result of many improvements, mainly in electron-multiplier phototubes, liquid-scintillator detectors have become an effective and reliable method for measuring activity in the preparation of radioactivity standards. They now offer an attractive alternative to detectors using gas multiplication. Their intrinsic properties of homogeneity and sensitivity make it possible to achieve low systematic errors, and it cannot be doubted that increasing recourse will be made to them in the metrology of radioactivity standards.

For the measurement of pure  $\beta$ -particle emitters, with the exception of certain difficult cases, the accuracy is a few parts in a thousand. The method of extrapolation, which is very easy with a liquid scintillator, only gives differences of the order of one part in a thousand between the values obtained with different  $\gamma$ -ray gates. These detectors are also very advantageous when measuring emitters which decay by electron capture. Systematic study, both theoretical and experimental, would make it possible to reduce still further the uncertainties in measurement.

## 7. The Problem of Afterpulses

D. Smith<sup>(1)</sup>

<sup>(1)</sup> Division of Radiation  
Science and Acoustics,  
National Physical  
Laboratory, Teddington,  
UK.

### 7.1. Introduction

This part on the subject of afterpulses is principally a review of the literature, but also incorporates and describes experimental work carried out at the National Physical Laboratory (NPL), including some quantitative afterpulse measurements under conditions appropriate to radioactivity standardisation.

### 7.2. Afterpulses in electron-multiplier phototubes

Considerable work was done in the early 1950's [4], [5], [6], [7], [11], [12], [15], [19] on afterpulsing in electron-multiplier phototubes, but since that time fabrication techniques have greatly reduced afterpulses from most phototubes. This, together with the fact that the presence of a slow component in liquid-scintillator emission [69] was not recognised, casts doubt on the relevance of much of the early work to modern phototubes.

The useful gain of a phototube is limited by feedback processes, mainly optical and ionic, which create afterpulses, although even in normal operation well below this limit, such effects do give rise to spurious pulses following the main pulse.

Typical afterpulse distributions are shown in Figure 17 and Figure 18, taken at NPL with a Philips 56 DUVP and an RCA 31000D tube. Similar curves were obtained by White [124], Delaney [110] and Shin [136]. The distributions shown were taken with a time-to-amplitude converter and found to be the same in this time region, irrespective of whether the main pulse is produced by a radioactive source in a scintillator or by a gallium-phosphide nanosecond light pulser. Morton [119] found that in modern tubes, most afterpulses in the region below one microsecond are due to the ionisation of gas molecules in the volume between the cathode and first dynode; the positive ions so formed strike the cathode and cause the release of secondary electrons.

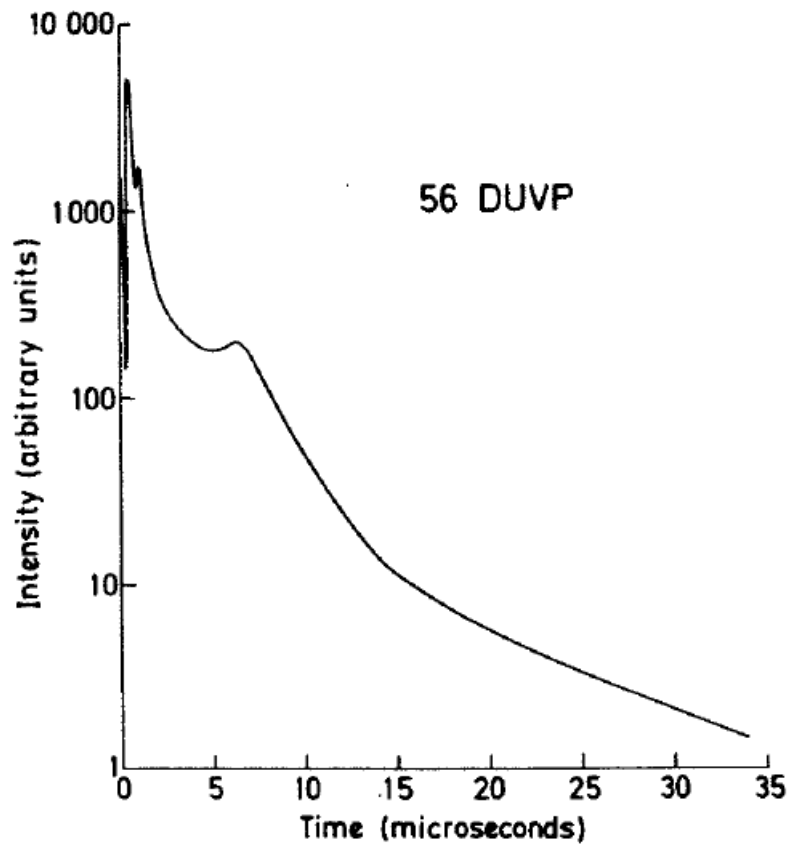


Figure 17 — Typical time distribution of afterpulses from 56 DUVP tube.

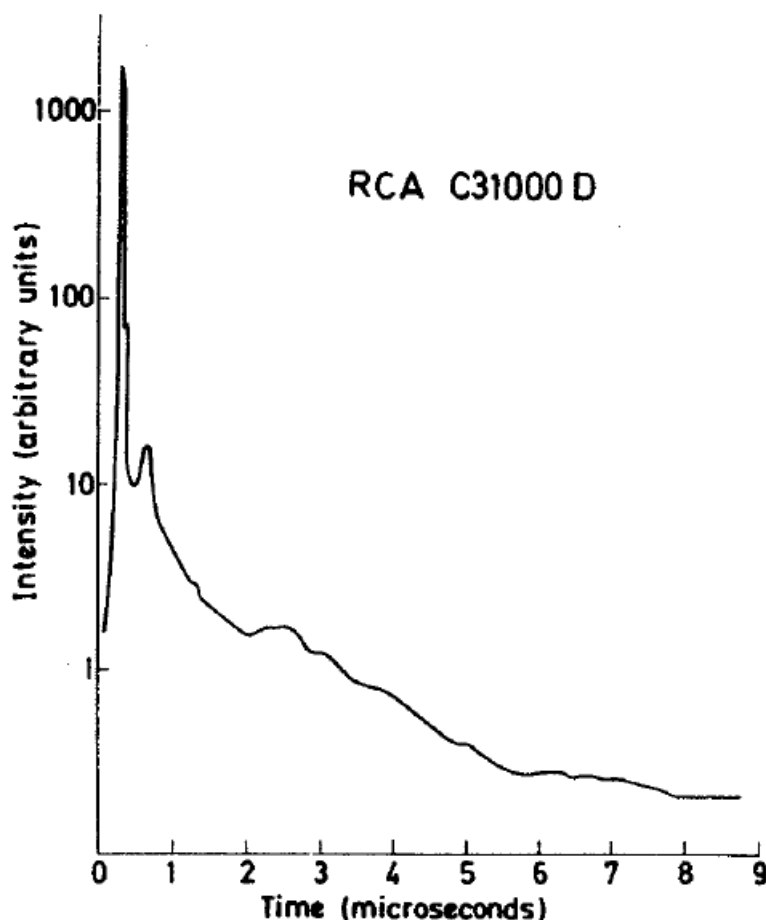


Figure 18 — Typical time distribution of afterpulses from RCA 31000D tube.

The sharpness of the peaks in the afterpulse distribution below  $1\ \mu\text{s}$  has been shown to be due to a combination of the effect of the isochronous transit time [119] for the ions in the cathode-first-dynode space, irrespective of their exact point of origin, and the effect of the variation, with energy, of the collision cross section for ionisation by electrons [167]. Kuchnir [135] found that tubes especially aged by RCA showed a marked reduction in this type of afterpulsing.

By connecting phototubes to a gas-handling system, Morton [119] verified that the early afterpulses were due to gaseous ions and that the  $\text{H}_2^+$  ion, possibly the result of water vapour being absorbed before sealing, is responsible for the prompt afterpulse (at about  $0.3\ \mu\text{s}$  at typical voltages) which is observed in most tubes. Some gases caused afterpulses equivalent in amplitude to only a single photoelectron, and it is interesting to note that oxygen apparently produced no afterpulses. Shin [136] also observed afterpulses in the region below  $1\ \mu\text{s}$  from a 58 AVP and 60 AVP tube, ascribing the various peaks to  $\text{H}_2^+$  ions and other residual gases. White [124], using a focussing-type phototube, observed afterpulses at  $0.8$  and  $4\ \mu\text{s}$ , following single photoelectron events, and suggested they may be due to the movement of ions from an early dynode.

Staupert [164] observed afterpulses in 53 AVP, 54 AVP and EMI 9583B tubes, up to  $15\ \mu\text{s}$  after the main pulse, with an intensity correlated to the main pulse, although an RCA 6810A tube was claimed not to show any afterpulses.

The cathode can be an important element in the process of forming afterpulses. Morton [119] found that tubes with cathodes containing caesium or potassium all exhibited afterpulses, but that a baryum cathode did not for any residual gas composition.

Morton [119] found that for single photoelectron events, an afterpulse was equivalent, on average, to four photoelectrons (for a caesium-containing cathode), although Delaney [110] using a venetian-blind-type tube, found afterpulses only occurred for main pulses greater than about three photoelectrons. At NPL, using a 56 AVP, 56 DUVP and RCA 31000D tubes, it was observed that the probability of afterpulsing was very dependent on the main pulse height, and to a lesser extent, on pulse width. Further, by using a light pulser, a gating system and a variable discriminator, it was found that if any region (above about 1  $\mu$ s) of the afterpulse time distribution was selected, then the general shape (but not the intensity) of the afterpulse amplitude distribution within that selected region did not change significantly with main pulse height over the range from one photoelectron up to many photoelectrons. The majority of afterpulses was equivalent in size to one photoelectron, but there were also many larger afterpulses, and above about four photoelectrons the probability of afterpulsing decreased only linearly with afterpulse amplitude, so that large-amplitude afterpulses are quite possible.

Krall [117] studied extraneous light emission from phototubes, and at high amplification ( $> 10^9$ ) an electrode glow due to electron bombardment of the later dynodes was found, which occurred about 40 and 80 ns after the main pulse. In a single-phototube counting system this is inconsequential, due to the normal dead times employed, but in coincidence counting, this light could activate an adjacent phototube to give a spurious coincidence, although most modern tubes have optical baffles and a constriction in the envelope near the cathode which minimises this effect. Normally however, phototubes are operated at lower gains where this effect is absent, but there is some evidence [117] that light is produced by the recombination radiation of the residual gas ions formed in the manner described by Morton [119], which could also cause spurious coincidences in a two-phototube set-up. Electroluminescence of the tube envelope [117] is also a possible source of extraneous light which is, however, normally avoided with positive high-voltage supplies, whereby the faceplate region is near ground potential.

### 7.3. The effect of $\gamma$ rays on electron-multiplier phototubes

Work by Jerde [115] and Dressier [111] has indicated that high-energy radiation incident upon a phototube can produce pulses of two types. Jerde observed that a  $\gamma$  ray from the decay of  $^{60}\text{Co}$ , passing through the faceplate on an RCA 7265 phototube, produced one large pulse with an amplitude equivalent to about ten photoelectrons, along with about ten afterpulses. Similar studies by Dressier on EMR phototubes recorded afterpulses decaying with a lifetime of up to 2 ms and from one to three afterpulses per main pulse with bialkali or Sb-Cs cathodes with glass faceplates. The main pulse can be explained by the Čerenkov radiation from the Compton-scattered electrons, or for low-energy  $\gamma$  rays, by the production of visible photons in the glass by fluorescence or scintillation [155]. For the afterpulses Jerde suggests that phosphorescence in the glass could be excited by ultra-violet photons produced by the Čerenkov radiation, although later work by Dressier casts doubt on this and suggests that the afterpulses are due to direct excitation of electrons in the sol id. The work indicated that afterpulsing increased with  $\gamma$ -ray energy, suggesting a correlation between the afterpulse and the energy of the recoil electron.

At NPL the effect of  $\gamma$  rays from the decay of  $^{60}\text{Co}$  on an RCA 31000D phototube has been measured. A liquid-scintillator bottle containing  $^{60}\text{Co}$ , enclosed in aluminium foil, did produce numerous afterpulses in the millisecond region, but only at discrimination levels below those normally used for counting purposes.

## 7.4. The decay of excited liquid scintillation

Dupont [112] studied the luminescence decay curves of organic scintillators, excited by  $^{60}\text{Co}$ , and observed a slow component of order  $0.1\ \mu\text{s}$  for toluene or phenylcyclohexane solvents with TP, PBD or PPD solutes<sup>(1)</sup> and found that the presence of dissolved oxygen greatly reduced the strength and probably the lifetime of this component. Using a  $^{137}\text{Cs}$  or  $^{65}\text{Zn}$   $\gamma$ -ray source to excite Nuclear Enterprises liquid scintillators, Kuchnir [135] observed slow components of order  $0.5\ \mu\text{s}$ , after taking into account the effect of phototube afterpulses in this region. Early work by Harrison [11] using X-ray excitation, which showed the slow components to be negligible, was in error presumably as the scintillators contained dissolved oxygen. Vaninbrouckx [95] observed small afterpulses many minutes after irradiation of a phototube and glass sample vial with  $\gamma$  rays from the decay of  $^{60}\text{Co}$ , and pointed out that these small pulses are probably due to phosphorescence and hence consist principally of single-photon events. Therefore a coincidence method would eliminate them, and, in a single phototube, the discriminator level should be so low as to include such single-photon events. Similar experiments at NPL with an RCA 31000D tube confirmed that there was negligible  $\ll 0.1\%$  long-term  $\gamma$ -ray-induced phosphorescence ( $\tau < 30\ \text{s}$ ) at discrimination levels equivalent to one photoelectron.

<sup>(1)</sup> The chemical names of these fluors are given in Chapter 3 of this Monograph.

With electron excitation, Owen [39] observed a slow component in oxygen-free liquid scintillators with a time constant of the order of  $1\ \mu\text{s}$ , and Horrocks [152] gives time constants of about  $0.25\ \mu\text{s}$ . The relative intensities of the fast and slow components differ for different types of particle and is, of course, the basis of pulse-shape discrimination techniques [24], [30], [50].

The prompt emission, whether excited by particles or  $\gamma$  rays is due to emission from primary singlet states formed by direct interaction with the ionising particle [70], [152]. The slow emission is currently explained [69], [112], [152] as being due to a delayed emission from singlet states which result from triplet-triplet interaction between molecule pairs. This mechanism was proposed in 1961 [54], and expanded by King and Voltz [103]. Previous theories which have been abandoned include slow ion-electron recombination [34], [42], long-lived higher excited triplet states [41] and the formation of pairs of excited molecules which had long lifetimes [58].

The shape of the slow decay component is complex and is not described by a simple decay law. However in normal scintillation counting their intensity is small [69] ( $\leq 0.1\%$  that of the main pulse after  $1\ \mu\text{s}$ ) and they can be avoided by employing suitable dead times.

## 7.5. Phosphorescence problems

Electron-multiplier phototubes show long-term phosphorescence after exposure to daylight at ultra-violet light [117] and liquid scintillators or glass containers can fluoresce for days after exposure [25], [62], [95]. Thus all containers and liquids must be handled in darkness or in red light. Chemiluminescence is often associated with biological material and solubilizers and in



particular with dioxanebased scintillators [147], [179], although this is of little importance for standardisation purposes where simpler chemical forms of radioactive material can be chosen.

Because the emission of luminescent light is in the form of single uncorrelated photons, coincidence systems will not be affected, and in a single tube system the discriminator level would eliminate most pulses of this type. Fodor-Csanyi et al. [132], [139] recently observed such phosphorescence and suggested that many early authors attributed non-linear bias curves erroneously to phototube afterpulses.

## 7.6. Some quantitative measurements of afterpulses

The degree of afterpulsing occurring in a LS standardisation of  $^{60}\text{Co}$ , employing an RCA 31000D phototube (which has a GaP first dynode) and a toluene-PPO-POPOP<sup>(1)</sup> scintillator, has been quantitatively measured at NPL. Much of this work, including its mathematical basis, has been published [206], [211], [252].

<sup>(1)</sup> The chemical names are given in Chapter 3 of this Monograph.

In the region below 100  $\mu\text{s}$ , the degree of afterpulsing can be readily observed by variation of the dead time, and such experiments at NPL indicate that a dead time of at least 10  $\mu\text{s}$  is required to reduce these spurious pulses to well below the 0.1% level, even with an electronic threshold (or “discriminator level”) corresponding to modest  $\beta$ -counting efficiencies (say 75% for  $^{60}\text{Co}$ ).

In the 10  $\mu\text{s}$  to 100 ms range a correlation technique [18] has been used [206], [211] to measure the deviations from Poisson statistics in the  $\beta$  channel, in conjunction with the  $4\pi\beta-\gamma$  coincidence method. In this technique, the number of  $\beta$  pulses occurring in a fixed time interval is repeatedly counted, and any difference between the resulting variance and mean of the number in this interval is quantitatively related to the fractional number of afterpulses in that interval. The fraction of afterpulses observed as a function of this sampling time interval at a discriminator level corresponding to a  $\beta$ -counting efficiency of 96.5% for  $^{60}\text{Co}$ , is shown in Figure 19. This shows that most spurious pulses occur within about 10 ms of the main pulse. Figure 20 shows the  $\beta$ -particle count rate as a function of counting efficiency,  $\varepsilon_\beta$ , both with and without this correction for afterpulsing. The deviation from linearity of the corrected curve at the higher efficiencies is mainly due to a fraction of the main pulses being followed by more than one afterpulse.

Afterpulses with lifetimes greater than 100 ms could also occur, but since NPL comparisons of absolute standardisation of  $^{46}\text{Sc}$ ,  $^{51}\text{Cr}$ ,  $^{60}\text{Co}$ ,  $^{86}\text{Rb}$ ,  $^{95}\text{Nb}$ ,  $^{123}\text{I}$ ,  $^{134}\text{Cs}$ ,  $^{139}\text{Ce}$  by  $4\pi\beta(\text{LS})-\gamma$  and  $4\pi\beta(\text{PC})-\gamma$  methods have shown agreement to within 0.2%, they would appear to be negligible.

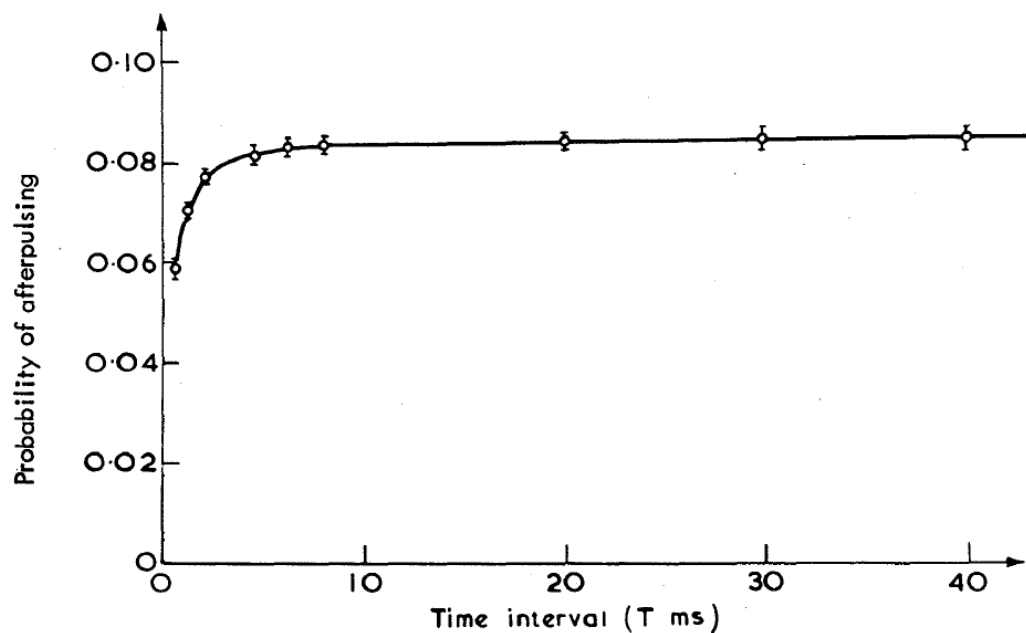


Figure 19 — Fractional number of afterpulses per main pulse as a function of correlation counting interval.

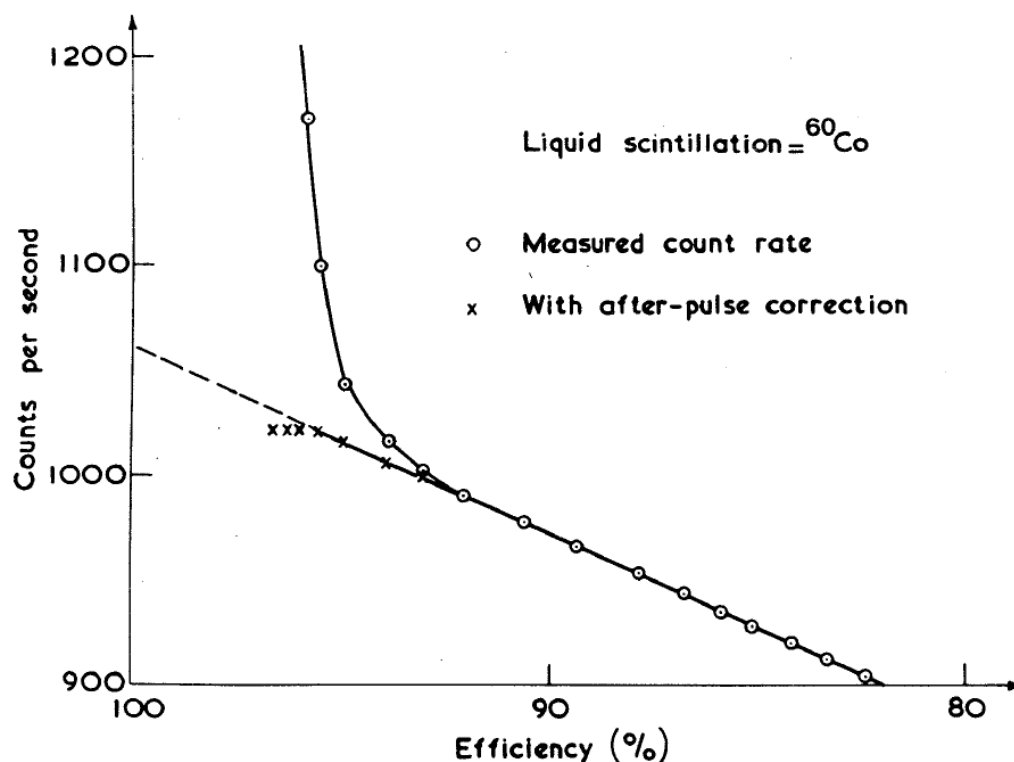


Figure 20 — Observed  $\beta$ -count rate as a function of measured  $\beta$ -counting efficiency, with and without the correction for afterpulsing.

As noted in Section 7.2, the probability of afterpulsing increases with increasing pulse height, so it is to be expected that for  $\beta$  emitters, the larger the end-point energy of the nuclide, the larger the problem of afterpulsing becomes. Indeed, it is found that for  $\beta$ - $\gamma$  emitters with one predominant  $\beta$  branch, the energy threshold of discrimination required to reduce afterpulsing to below say 0.1%, is roughly proportional to the end-point energy, at least for end-point

energies above about 300 keV (which corresponds to a discriminator level in the region of 10 keV). The discriminator level can rarely be reduced much below that corresponding to 10 keV, because to do so would include some pulses corresponding to single photoelectrons, a region in which the probability of afterpulsing is particularly high.

It should be noted that the degree of afterpulsing in two nominally identical phototubes can be significantly different, and also that a slight reduction in the degree of afterpulsing can often be achieved by considerably reducing the cathode-first-dynode voltage below that sometimes recommended, and increasing the amplification elsewhere to compensate.

## 7.7. Conclusion

Although afterpulses arise in electron-multiplier phototubes, and from scintillators and containers, and limit the operating conditions for LS counting, it appears from the above evidence that with modern phototubes, and with readily attainable conditions, afterpulses can be kept below the 0.1% level, at least for medium  $\beta$ -particle energies. Therefore a liquid scintillator should be a feasible substitute for the proportional counter for the metrology of  $\beta$ -particle-emitting nuclides, as far as the problem of afterpulses is concerned.

## 8. Intercomparison of $^{134}\text{Cs}$ by Liquid-Scintillation Counting

### 8.1. Introduction

Following the initial draft of this review of the present position in LS counting, the members of a BIPM working party agreed to arrange an international comparison of measurements of the activity of a solution of  $^{134}\text{Cs}$ , using the method of  $4\pi\beta$  (liquid scintillator)- $\gamma$  efficiency variation. The NPL agreed to act as co-ordinator and provide the ampoules containing the activity. Measurements were carried out by LMRI, NAC, NBS and NPL early in 1977.

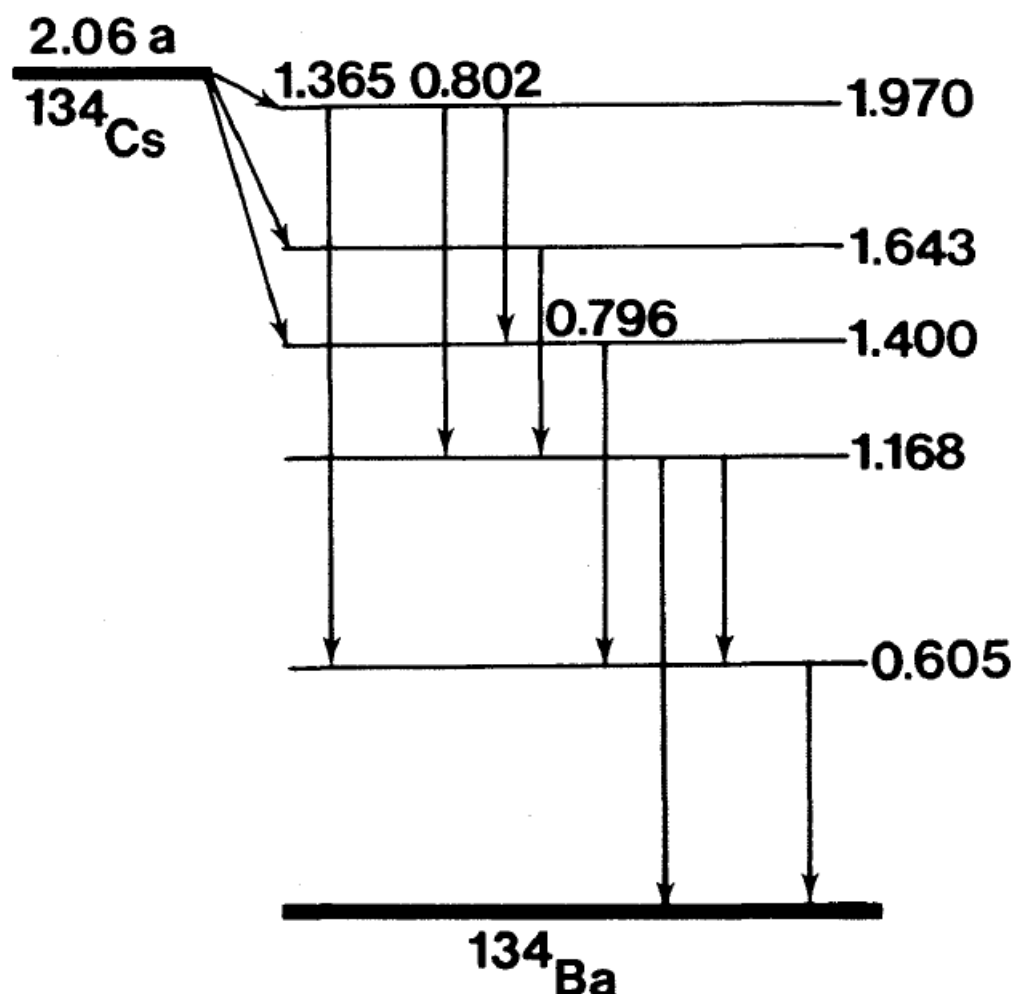


Figure 21 — Decay scheme for  $^{134}\text{Cs}$ .

Gamma-ray spectrometry demonstrated that there was less than 0.1%  $^{137}\text{Cs}$  impurity present in the solution. No other  $\gamma$ -ray-emitting impurities were reported.

Cesium-134 nuclear-decay data from the Oak Ridge Evaluated Nuclear Structure Data File, published in [284], are shown in Table 4 and its decay scheme is illustrated in Figure 21.

**Table 4.** Decay data of  $^{134}\text{Cs}$  (intensities  $\geq 0.10\%$ )  $\beta^-$  decay to  $^{134}\text{Ba}$ ;  
 $T_{1/2} = (2.062 \pm 0.005)a$

Data taken from [284]

Radiation type		Energy and uncertainty (keV)		Intensity and uncertainty (%)	
L shell	Auger electrons	3.67		0.65	0.05
K shell	conversion	531.874	0.015	0.120	0.007
	electrons	567.258	0.015	0.488	0.015
		758.404	0.022	0.224	0.011
$\beta_1^-$	maximum	88.6	0.4		
	average	23.09	0.11	27.40	0.20
$\beta_2^-$	maximum	415.2	0.4		
	average	123.43	0.14	2.47	0.05
$\beta_3^-$	maximum	658.0	0.4		
	average	210.15	0.15	70.1	0.5
total $\beta^-$	average	156.8	0.3	100.0	0.6
X ray	$K\alpha_2$	31.8171	0.0003	0.213	0.009
	$K\alpha_1$	32.1936	0.0003	0.393	0.015
	$K\beta$	36.4		0.143	0.006
$\gamma_3$		475.35	0.05	1.46	0.04
$\gamma_4$		563.227	0.015	8.38	0.05
$\gamma_5$		569.315	0.015	15.43	0.11
$\gamma_6$		604.699	0.015	97.6	0.3
$\gamma_7$		795.845	0.022	85.4	0.4
$\gamma_8$		801.932	0.022	8.73	0.04
$\gamma_9$		1038.57	0.03	1.000	0.010
$\gamma_{10}$		1167.94	0.03	1.80	0.03
$\gamma_{11}$		1365.15	0.03	3.04	0.04

## 8.2. Counting equipment and conditions

Each participant had a  $\beta$ -particle detector consisting of a liquid scintillator coupled to either one or two phototubes and a Na(Tl)  $\gamma$ -ray detector. Details of the equipment and conditions are given in Table 5.

**Table 5.** Counting equipment and conditions

Laboratory	LMRI	NAC	NBS	NPL
Scintillator	20% ethanol + 80% toluene with 12.5 g/l butyl PBD	Insta-Gel (Packard)	PCS (Amersham)	Unisolve 1 (Koch-Light)

Laboratory	LMRI	NAC	NBS	NPL
Volume of scintillator (ml)	3	13	2 to 5.5	6
$\beta$ -channel phototubes	RCA 8850 (two in summation)	EMI 9635QB (two in coincidence)	RCA 8575 (one)	RCA 31000D (one)
$\beta$ -dead time ( $\mu\text{s}\beta$ )	5.0	1.2	live timer used	24.0
$\gamma$ -dead time ( $\mu\text{s}\gamma$ )	5.0	1.1 to 3.7	1.4 to 2.0	1.7 to 4.4
Resolving time $\mu\text{s}$	1.0	0.5	1.8	0.2
Upper limit of correction applied for spurious pulses	presumed negligible	0.4%	0.01%	0.05%
How estimated	-	gating technique [264]	visually by oscilloscope	correlation counting [206]
Method of alternating $\beta$ efficiency	threshold variation		computer discrimination [246]	

### 8.3. Results

Each laboratory took measurements with several different  $\gamma$ -ray windows corresponding to various photopeaks in the spectrum, and two laboratories also took integral measurements above a  $\gamma$ -ray-energy threshold of 500 keV. The usual technique of  $\beta$ -particle detection-efficiency extrapolation [199] was used for each window, i.e. if the count rates per unit mass ( $\text{s}^{-1}\text{mg}^{-1}$ , corrected for dead-time losses, half lives, background, etc.) are  $N_\beta$ ,  $N_\gamma$  and  $N_c$ , then

$$N_\beta/\varepsilon_\beta = N_0 + \alpha_1 (1 - \varepsilon_\beta)/\varepsilon_\beta + \alpha_2 (1 - \varepsilon_\beta)^2/\varepsilon_\beta^2 + \dots,$$

where  $\varepsilon_\beta = N_c/N_\gamma$ , and hence the disintegration rate  $N_0$  is the extrapolated value of  $N_\beta/\varepsilon_\beta$  at  $\varepsilon_\beta = 1$ .

The degree of fit required was usually quadratic, although the actual values of the coefficients  $\alpha_1$  and  $\alpha_2$  obtained for a particular  $\gamma$ -ray window varied greatly from one participant to another, being dependent on the particular apparatus and the exact range of  $\gamma$ -ray energies selected.

The values of  $N_0$  (on 1977-02-01, 00 h UT) with the range of  $\beta$ -detection efficiencies measured for each  $\gamma$ -ray window are quoted in Table 6 and shown graphically in Figure 22.

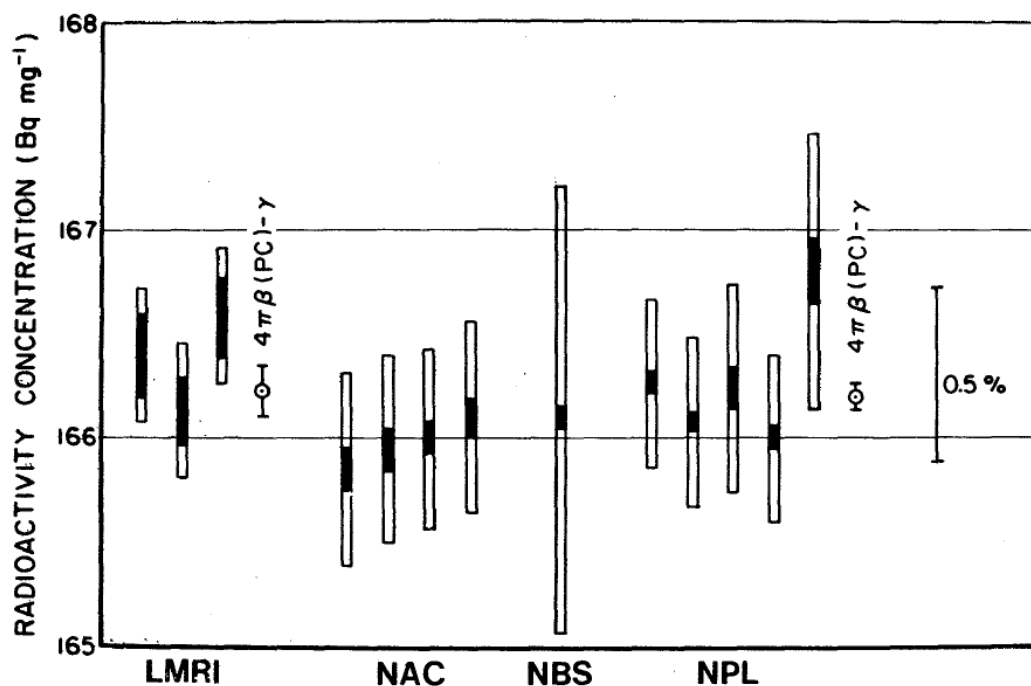


Figure 22 — Activities obtained by  $4\pi\beta(\text{LS})-\gamma$  coincidence counting.

The black (or white) rectangles correspond to the random (or systematic) uncertainties. Two  $4\pi\beta(\text{PC})-\gamma$  results are included for comparison.

## 8.4. Non liquid-scintillation results

Additional measurements were also made by LMRI, NBS and NPL by the conventional  $4\pi\beta$  (gas proportional counter)- $\gamma$  technique of efficiency variation, with various  $\gamma$ -ray windows. The results of these measurements are included in Figure 22 and Table 6.

Table 6. Results

	Coincident $E_\gamma$ or $\Delta E_\gamma$ (MeV)	Range of $N_c/N_\gamma$	$N_0$ ( Bq · mg)	Percent. uncertainty random ( 1 $\sigma$ ) systematic	Degree of fit
LMRI <sup>(a)</sup>	0.6	0.84— 0.94	166.41	0.12 0.19	2
	0.8	0.84— 0.94	166.13	0.07 0.19	2
	1.4	0.80— 0.925	166.58	0.10 0.19	2
$4\pi\beta(\text{PC})-\gamma$			166.23	0.04 0.25	
NAC	0.6	0.78— 0.91	165.85	0.05 0.29	2
	0.8	0.81— 0.92	165.94	0.05 0.29	2
	1.0—1.5	0.71— 0.88	165.97	0.04 0.29	2

	>0.5	0.78— 0.91	166.09	0.05	0.29	2
NBS	0.6					
	0.8	0.3—0.92	166.12	0.02	0.65	2
		(average)				
	1.4					
$4\pi\beta(\text{PPC})-\gamma$			166.02	0.14	0.73	
NPL	0.6	0.75—0.9	166.27	0.03	0.24	2
	0.8	0.71— 0.91	166.08	0.025	0.24	1
	1.4	0.71— 0.87	166.24	0.06	0.30	2
	>0.5	0.71— 0.89	166.00	0.03	0.24	2
	1.97	0.30— 0.71	166.80	0.09	0.40	2
$4\pi\beta(\text{PC})-\gamma$			166.20	0.05	0.29	

(a) The LMRI measurements were made on a solution 8.685 times stronger than that used by other participants. This factor was obtained by weighing during dilution and confirmed by ionization-chamber data. The LMRI results have been divided by this factor.

## 8.5. Conclusion

All the quoted results for  $N_0$  by LS counting are self-consistent within the quoted uncertainties, and are in good agreement with  $N_0$  obtained by  $4\pi\beta(\text{PC})-\gamma$  techniques. The overall spread of 0.50% is comparable with the spread observed in, for example, the recent  $^{139}\text{Ce}$  international comparison [276].



## References

- [1] O. Stern and M. Volmer, Über die Abklingzeit der Fluoreszenz, *Phys. Z. (Leipzig)* **20**, 183.
- [2] W.A. Shureliff and R.C. Jones, The trapping of fluorescent light produced within objects of high geometrical symmetry, *J. Opt. Soc. Am.* **39**, 912.
- [3] J.B. Birks, Scintillations from organic crystals: Specific fluorescence and relative response to different radiations, *Proc. Phys. Soc.* **A64**, 874.
- [4] T.N.K. Godfrey, F.B. Harrison and J.W. Keuffel, Satellite pulses from photomultipliers, *Phys. Rev.* **84**, 1248.
- [5] R.J. Lanter and R.W. Corwin, Spurious pulses from type 5819 photomultiplier tube, *Rev. Sci. Instr.* **23**, 507.
- [6] D.W. Mueller, G. Best, J. Jackson and J. Singletary, Afterpulsing in photomultipliers, *Nucleonics* **10**, 6, 53.
- [7] Latest developments in scintillation counting, Scintillation Counter Symposium, Washington DC, *Nucleonics* **10**, 3, 32.
- [8] F.H. Wells, Fast pulse circuit techniques for scintillation counters, *Nucleonics* **10**, 4, 28.
- [9] H.A. Bethe and J. Ashkin, Passage of radiations through matter, in "Experimental Nuclear Physics", E. Segrè (ed.) (Wiley, New York).
- [10] F.N. Hayes and R. Gordon Gould, Liquid scintillation counting of tritium-labeled water and organic compounds, *Science* **117**, 480.
- [11] F.B. Harrison, Slow component in the decay of fluors, *Nucleonics* **12**, 3, 24.
- [12] K.P. Meyer and A. Maier, Nachimpulse in Scintillationszählern, *Helv. Phys. Acta* **27**, 57.
- [13] D.J. Rosenthal and H.O. Anger, Liquid scintillation counting of tritium and  $^{14}\text{C}$  labelled compounds, *Rev. Sci. Instr.* **25**, 670.
- [14] G.T. Wright, Low energy measurements with the photomultiplier scintillation counter, *J. Sei. Instr.* **31**, 462.
- [15] E. Breitenberger, Scintillation spectrometer statistics, *Prog. in Nucl. Phys.* **4**, 56.
- [16] R.D. Evans, *The Atomic Nucleus* (McGraw-Hill, New York) 536-566.
- [17] M. Furst, H. Kallmann and F.H. Brown, Increasing fluorescence efficiency of liquid scintillation solutions, *Nucleonics* **13**, 58.
- [18] V.I. Goldansky and M.I. Podgoretsky, On a possible application of correlation functions to the study of nuclear transformations (in Russian), *Doklady Akad. Nauk.* **100**, 237.

- [19] J.C. Roucayrol and E. Oberhausen, Measurement of activity of compounds traced with low-energy beta emitters, *Science* **122**, 201.
- [20] J.K. Basson, Absolute alpha counting of astatine-211, *Anal. Chem.* **28**, 1472.
- [21] F.N. Hayes, D.G. Ott and V.N. Kerr, Pulse-height comparison of secondary solutes, *Nucleonics* **1**, 1, 42.
- [22] A.T. Nelms, Energy loss and range of electrons and positrons, National Bureau of Standards Circular 577 (also supplement to NBS Circular 577, 1958) (GPO, Washington, DC).
- [23] J. Steyn, Absolute standardization of beta-emitting isotopes with a liquid scintillation counter, *Proc. Roy. Soc.* **A69**, 865.
- [24] G. T. Wright, Scintillation decay times of organic crystals, *Proc. Phys. Soc.* **B49**, 358.
- [25] J.D. Davidson and P. Feigelson, Practical aspects of internal-sample liquid-scintillation counting, *Int. J. Appl. Rad. and Isotopes* **2**, 1.
- [26] B.N. Audric, Liquid scintillation counting of low energy  $\beta$ -emitters, in "Liquid Scintillation Counting" (Pergamon, Oxford), p. 288.
- [27] C.G. Bell and F.N. Hayes (eds.), *Liquid Scintillation Counting* (Pergamon, New York).
- [28] W. Bernstein, C. Bjerknes and R. Steele, Single phototube liquid scintillation counting of  $^{14}\text{C}$ , in "Liquid Scintillation Counting", C.G. Bell and F.N. Hayes (eds.) (Pergamon, New York), p. 74.
- [29] D.L. Horrocks and M.H. Studier, Low level plutonium-241 analysis by liquid scintillation techniques, *Anal. Chem.* **30**, 1747.
- [30] R.B. Owen, The decay times of organic scintillators and their application to the discrimination between particles of differing specific ionization, *IEE Trans. Nucl. Sci.* **NS-5**, 3, 198.
- [31] J. Steyn and F.J. Haasbroek, The application of internal liquid scintillation counting to a  $4\pi\beta-\gamma$  coincidence method for the absolute standardization of radioactive nuclides, Conference on the peaceful use of atomic energy Conf. P/1104 (International Atomic Energy Agency, Vienna).
- [32] R.K. Swank, Limits of sensitivity of liquid scintillation counters, in "Liquid Scintillation Counting", C.G. Bell and F.N. Hayes (eds.) (Pergamon, New York), p. 23.
- [33] M. Yu. Tissen, Counting loss due to the statistical nature of the photoeffect in  $4\pi$  scintillation counters for  $\beta$ -radiation, *Sov. Phys.-Tech. Phys.* **3**, 1489.
- [34] F.D. Brooks, A scintillation counter with neutron and gamma-ray discriminations, *Nucl. Instr. and Meth.* **4**, 151.
- [35] P.J. Campion, J.G.V. Taylor and J.S. Merritt, Standardization of Radionuclides (International Atomic Energy Agency, Vienna), p. 227.

- [36] K.F. Flynn and L.E. Glendenin, Half-life and beta spectrum of  $^{87}\text{Rb}$ , *Phys. Rev.* **116**, 744.
- [37] T. Kinoshita and A. Sirlin, Radiative corrections to Fermi interactions, *Phys. Rev.* **113**, 1652.
- [38] L. Lutwak, Estimation of radioactive calcium-45 by liquid scintillation counting, *Anal. Chem.* **31**, 340.
- [39] R.B. Owen, Pulse-shape discrimination identifies particle types, *Nucleonics* **17**, 92.
- [40] A.R. Ronzio, Metal loaded scintillator solutions, *Int. J. Appl. Rad. and Isotopes* **4**, 196.
- [41] J.B. Birks, The scintillation process in organic systems, *IEE Trans. NS-7*, 2-3, 2.
- [42] W.L. Buck, The origin of scintillations in organic materials, *IEE Trans. NS-7*, 2-3, 11.
- [43] P.J. Campion, J.G.V. Taylor and J.S. Merritt, The efficiency tracing technique for eliminating self-absorption errors in the  $4\pi\beta$ -counting, *Int. J. Appl. Rad. and Isotopes* **8**, 8.
- [44] W.J. Kaufman, A. Nir, G. Parks and R.M. Hours, Studies of low-level scintillation counting of tritium, in US Atomic Energy Commission Report TID 7612, p. 239.
- [45] J.D. Ludwick, Liquid scintillation spectrometry for the analysis of zirconium-95-niobium-95 mixtures and coincidence standardization of these isotopes, *Anal. Chem.* **32**, 607.
- [46] H.H. Seliger, Liquid scintillation counting of  $\alpha$ -particles and energy resolution of the liquid scintillation for  $\alpha$ - and  $\beta$ -particles, *Int. J. Appl. Rad. and Isotopes* **8**, 29.
- [47] J. Steyn and F.W.E. Strelow, The determination of the half-life of  $^{238}\text{U}$  by absolute counting of  $\alpha$ -particles in a  $4\pi$ -liquid scintillation counter, in "Metrology of Radionuclides" (International Atomic Energy Agency, Vienna), p. 155.
- [48] J. Steyn, The comparative accuracy of the  $4\pi$  liquid scintillation counting method of radioisotope standardization, in "Metrology of Radionuclides" (International Atomic Energy Agency, Vienna), p. 279.
- [49] G.A. Brinkman, Standardization of radioisotopes (Thesis, Amsterdam).
- [50] W. Dachnick and R. Sherr, Pulse shape discrimination in stilbene scintillator, *Rev. Sci. Instr.* **32**, 666.
- [51] L.E. Glendenin, The present status of the decay constant of  $^{232}\text{Th}$ , *Annals New York Acad. Sci.* **91**, 166.
- [52] B.E. Gordon, H.R. Lukens and W. ten Hove, Liquid scintillation counting of  $\text{H}_2\text{S}^{35}$ , *Int. J. Appl. Rad. and Isotopes* **12**, 145.

- [53] D.L. Horrocks and M.H. Studier, Determination of the absolute disintegration rates of low-energy beta emitters in a liquid scintillation spectrometer, *Anal. Chem.* **33**, 615.
- [54] C.A. Parker and C.G. Hatchard, Delayed fluorescence from solutions of anthracene and phenanthrene, *Proc. Roy. Soc.* **A269**, 574, also in *Trans. Faraday Soc.* **57**, 1894 (1962).
- [55] P.W. Benjamin, C.D. Kemshall and D.L.E. Smith, Atomic Weapons Research Establishment Report No. NR/A-2/62.
- [56] D.W. Engelkemeir, K.F. Flynn and L.E. Glendenin, Positron emission in the decay of  $^{40}\text{K}$ , *Phys. Rev.* **126**, 1818.
- [57] D.G. Fleishman and V.V. Glazunov, Determination of the  $\beta$ -decay constant of  $^{40}\text{K}$ , *Sov. J. At. Energy* **12**, 320; (*At. Energiya* **12**, 338).
- [58] P.E. Gibbons, D.C. Northrop and O. Simpson, The scintillation phenomenon in anthracene: II. Scintillation pulse shape, *Proc. Phys. Soc.* **79**, 373.
- [59] D.L. Horrocks and A.L. Harkness, Half-life of nickel-63, *Phys. Rev.* **125**, 1619.
- [60] H. Houtermans and M. Miguel,  $4\pi\beta-\gamma$  coincidence counting for the calibration of nuclides with complex decay schemes, *Int. J. Appl. Rad. and Isotopes* **13**, 137.
- [61] W.J. Kaufman, A. Nir, G. Parks and R.M. Hours, Recent advances in low-level scintillation counting of tritium, in "Tritium in the Physical and Biological Sciences", Vol. I (International Atomic Energy Agency, Vienna), p. 249.
- [62] R.A. Lloyd, S.C. Ellis and K.H. Hallows, Phosphorescence in liquid scintillation counting, in "Tritium in the Physical and Biological Sciences", Vol. I (International Atomic Energy Agency, Vienna), p. 263.
- [63] D.A. Constanzo and R.E. Biggers, A study of the polymerization, depolymerization and precipitation of tetravalent plutonium as function of temperature and acidity by spectrophotometric methods, Oak Ridge National laboratory, Preliminary Report ORNL-TM-585.
- [64] D.G. Fleishman, I.V. Burovina and V.P. Nesterov, Half-life of  $^{137}\text{Cs}$ , *Sov. J. At. Energy* **13**, 1224 (1963); (*At. Energiya* **13**, 592 (1962)).
- [65] J.W. Hastings and G. Weber, Total quantum flux of isotropic sources, *J. Opt. Soc. Am.* **53**, 1410.
- [66] J. Steyn and F.J.W. Hahne, Absolute disintegration rate measurement of beta-emitters by application of efficiency tracing to  $4\pi$ -liquid scintillation counting, *Proc. Nat. Conf. Nucl. Energy*, Pretoria.
- [67] R.E. Yerick and H.H. Ross, Liquid scintillation counting of iodine-129 and iodine-125, *Proc. Oak Ridge Radioisotope Conference Res. Appl. Phys. Sci. Eng.* (Gatlinburg, Te), p. 20.
- [68] A.P. Baerg, S. Meghir and G.C. Bowes, Extension of the efficiency tracing method for the calibration of pure  $\beta$ -emitters, *Int. J. Appl. Rad. and Isotopes* **15**, 279.

- [69] J.B. Birks, *The Theory and Practice of Scintillation Counting* (Pergamon, Oxford), p. 185.
- [70] J.B. Birks, C.L. Braga and M.D. Lumb, A comparison of the scintillation and photofluorescence spectra of organic solutions, *Brit. J. Appl. Phys.* **15**, 399.
- [71] R.L. Brodzinski, J.R. Finkel and D.C. Conway,  $\beta$ -spectrum of  $^{32}\text{Si}$ , *J. Inorg. Nucl. Chem.* **26**, 677.
- [72] F.E. Butler, Assessment of tritium in production workers, *Proc. Symposium of the assessment of radioactive body burdens in man* (International Atomic Energy Agency, Vienna), p. 431.
- [73] D. Donhoff, Bestimmung der Halbwertszeiten der in der Natur vorkommenden radioaktiven Nuklide  $^{147}\text{Sm}$  und  $^{176}\text{Lu}$  mittels flüssiger Szintillatoren *Nucl. Phys.* **50**, 489.
- [74] A. Dyer, J. M. Fawcett and D.U. Potts, The measurement of aqueous solutions of metallic radioisotopes by liquid scintillation methods, *Int. J. Appl. Rad. and Isotopes* **15**, 377.
- [75] G. Erdtmann, Zählverluste bei der Zählung von Metall-Nukliden in flüssigen Szintillatoren, *Radiochimica Acta* **2**, 215.
- [76] U. Fano, A list of currently unsolved problems, *Nat. Acad. Sci. Nat. Res. Council Report* 1133, p. 281.
- [77] K.F. Flynn, L.E. Glendenin, E.P. Steinberg and P.M. Wright, Pulse height-energy relations for electrons and alpha particles in a liquid scintillator, *Nucl. Instr. and Meth.* **27**, 13.
- [78] G. Goldstein, Absolute counting of beta emitters by the liquid scintillation method, *Anal. Chem. Div. Progr. Report ORNL-3750*, p. 51.
- [79] D.L. Horrocks and M.H. Studier, Determination of radioactive noble gases with a liquid scintillator, *Anal. Chem.* **36**, 2077.
- [80] D.L. Horrocks, Pulse height-energy relationship of a liquid scintillator for electrons of energy less than 100 keV, *Nucl. Instr. and Meth.* **30**, 157.
- [81] D.L. Horrocks, Alpha particle energy resolution in a liquid scintillator, *Rev. Sci. Instr.* **35**, 334.
- [82] J.D. Ludwick, Liquid scintillation counting of promethium-147, bioassay procedure, *Anal. Chem.* **36**, 1104.
- [83] E. Rapkin, Liquid scintillation counting 1957-1963: a review, *Int. J. Appl. Rad. and Isotopes* **15**, 69.
- [84] A. Rytz, Rapport sur la comparaison internationale de  $^{241}\text{Am}$ , Juillet 1963, Bureau International des Poids et Mesures, Sèvres, also in Comité Consultatif pour les Etalons de Mesure des Radiations Ionisantes, 5<sup>e</sup> session, Gauthier-Villars, Paris (1965).

- [85] G. von Wangermann, Eine neue Methode zur absoluten Bestimmung der Aktivität energiearmer  $\beta$ -Strahler mit dem Flüssigkeitsszintillationszähler, Atomkernenergie 9-25, H. 5/6, 187.
- [86] G. von Wangermann, Bestimmung der Aktivität energiearmer  $\beta$ -Strahler mit dem Flüssigkeitsszintillationszähler nach einer spektrometrischen Methode, Kernenergie 7, 6/7, 531.
- [87] A. Williams, An estimation of the inherent accuracy of the tracer technique for measurements of disintegration rate, Int. J. Appl. Rad. and Isotopes **15**, 709.
- [88] G. Erdtmann and H. Herrmann, Absolutzählung von Radionukliden durch die Beta-Gamma-Koinzidenzmethode mit einem flüssigen Szintillator als innerem Beta-Detektor, Int. J. Appl. Rad. and Isotopes **16**, 301.
- [89] H.J. Gale and J.A.B. Gibson, Methods of calculating the pulse height distribution of the output of a scintillation counter, Atomic Energy Research Establishment Report AERE-R 5067, Harwell, Berkshire.
- [90] S.B. Garfinkel, W.B. Mann, R.W. Medlock and O. Yura, The calibration of the National Bureau of Standards' tritiated-toluene standard of radioactivity, Int. J. Appl. Rad. and Isotopes **16**, 27.
- [91] G. Goldstein, Absolute liquid scintillation counting of beta emitters, Nucleonics **23**, 3, 67.
- [92] B.A. Rhodes, Liquid scintillation counting of radioiodine, Anal. Chem. **37**, 995.
- [93] L.L. Thatcher and B.R. Payne, The distribution of tritium in precipitation over continents and its significance to ground-water dating, in "Proc. 6th Int. Conf. Radiocarbon and Tritium Dating" (Pullman, Washington), p. 604.
- [94] G.S. Uyesugi and A.E. Greenberg, Simultaneous assay of strontium-90-yttrium-90 by liquid scintillation spectrometry, Int. J. Appl. Rad. and Isotopes **16**, 581.
- [95] R. Vaninbrouckx and A. Spornol, High precision  $4\pi$  liquid scintillation counting, Int. J. Appl. Rad. and Isotopes **16**, 289.
- [96] R. Voltz, Contribution à l'étude de la radioluminescence des scintillateurs organiques (Thesis, Strasbourg).
- [97] A. P. Baerg, Measurement of radioactive disintegration rate by the coincidence method, Metrologia **2**, 23.
- [98] M.L. Curtiss, S.L. Ness and L.L. Bentz, Simple technique for rapid analysis of radioactive gases by liquid scintillation counting, Anal. Chem. **38**, 636.
- [99] J.D. Eakins and D.A. Brown, An improved method for the simultaneous determination of iron-55 and iron-59 in blood by liquid scintillation counting, Int. J. Appl. Rad. and Isotopes **17**, 391.
- [100] M.K. Ellis, S.N. Wampler and R.H. Yager, Liquid scintillation method for determination of solvent-extracted phosphorous-32 in foods, Anal. Chim. Acta **34**, 169.

- [101] H.J. Gale and J.A.B. Gibson, Methods of calculating the pulse height distribution at the output of a scintillation counter, *J. Sci. Instr.* **43**, 224.
- [102] G. Goldstein, unpublished results, Oak Ridge National Laboratory.
- [103] T.A. King and R. Voltz, The time dependence of scintillation intensity in aromatic materials, *Proc. Roy. Soc.* **A289**, 424.
- [104] J.R. Prescott, A statistical model for photomultiplier single-electron statistics, *Nucl. Instr. and Meth.* **39**, 173.
- [105] C. Ronzani and M.A. Tamers, Low-level chlorine-36 detection with liquid scintillation techniques, *Radiochimica Acta* **6**, 206
- [106] E. Schwerdtel, Glasgefäße mit rauher Oberfläche für die Messung niederenergetischer  $\beta$ -Strahlung in flüssigen Szintillatoren, *Int. J. Appl. Rad. and Isotopes* **17**, 479.
- [107] J. Steyn and A.S.M. de Jesus, Coincidence measurements on nuclides decaying by electron-capture, CSIR Special Report FIS 15 (Council for Scientific and Industrial Research, Pretoria), 19 p.
- [108] A.P. Baerg, Absolute measurement of radioactivity, *Metrologia* **3**, 105.
- [109] J. Bryant, D.G. Jones and A. McNair, Development of a  $4\pi$  liquid scintillation counting method for the absolute standardization of radioactive solutions with particular reference to efficiency tracing measurements, in "Standardization of Radionuclides" (International Atomic Energy Agency, Vienna), p. 47.
- [110] C.F.G. Delaney and J.A. Harwood, Some aspects of single electron response and afterpulsing in photo- and electron multipliers, *Sci. Proc. Roy. Dublin Soc.* **A3**, 5, 57.
- [111] K. Dressier and L. Spitzer, Photomultiplier tube pulses induced by  $\gamma$  rays, *Rev. Sci. Instr.* **38**, 436.
- [112] H. Dupont, G. Pfeffer, G. Laustriat and A. Coche, Décroissance de l'intensité lumineuse des scintillateurs organiques, *Nucl. Instr. and Meth.* **47**, 93.
- [113] J.A.B. Gibson and H.J. Gale, A fundamental approach to quenching in liquid scintillators, *Int. J. Appl. Rad. and Isotopes* **18**, 681.
- [114] H.R. Ihle, A. P. Murrenhoff and M. Karayannis, Standardization of alpha emitters by liquid scintillation counting, in "Standardization of Radionuclides" (International Atomic Energy Agency, Vienna), p. 69.
- [115] R.L. Jerde, L.E. Peterson and W. Stein, Effects of high energy radiations on noise pulses from photomultiplier tubes, *Rev. Sci. Instr.* **38**, 1387.
- [116] G. Källén, Radiative corrections to  $\beta$ -decay and nucleon form factors, *Nucl. Phys.* **B1**, 225.
- [117] H.R. Krall, Extraneous light-emission from photomultipliers, *IEEE Trans.* **NS-14**, 1, 455.

- [118] J.D. van der Laarse, Experience with emulsion counting of tritium, *Int. J. Appl. Rad. and Isotopes* **18**, 485.
- [119] G.A. Morton, H.M. Smith and R. Wassehnan, Afterpulses in photomultipliers, *IEEE Trans. NS-14*, 1, 443.
- [120] D. Paligorić, L. Dobrilović and Dj. Bek-Uzarov, Efficiency of a liquid scintillation counter (in Russian), in “Standardization of Radionuclides” (International Atomic Energy Agency, Vienna), p. 57.
- [121] N.L. Snidow and H.D. Warren, Wall effect corrections in proportional counter spectrometers, *Nucl. Instr. and Meth.* **51**, 109.
- [122] J. Steyn, Internal liquid scintillation counting applied to the absolute disintegration-rate measurements of electron capture nuclides, in “Standardization of Radionuclides” (International Atomic Energy Agency, Vienna), p. 35.
- [123] J. Steyn, Coincidence standardization of electron-capture nuclides utilizing a  $4\pi$ -internal liquid scintillation counter, CSIR Research Report 253 (Council for Scientific and Industrial Research, Pretoria).
- [124] G. White, A multi-stop time-of-flight encoder, *Nucl. Instr. and Meth.* **55**, 157.
- [125] A. Williams and I.W. Goodier, Systematic errors of the efficiency tracer technique for measuring the absolute disintegration rates of pure beta emitters, in “Standardization of Radionuclides” (International Atomic Energy Agency, Vienna), p. 153.
- [126] A. Aziz, S.J. Lyle and S.J. Naqvi, Chemical equilibrium in americium and curium sulphate and oxalate systems and an application of a liquid scintillation counting method, *J. Inorg. Nucl. Chem.* **30**, 1013.
- [127] H. Bennet, J.L. Bishop and M. F. Wulkinghoff (eds.), *Practical Emulsions*, 2 vols. (Chemical Publishing Company, New York).
- [128] F.J. Cosolito, N. Cohen and H.G. Petrov, Simultaneous determination of iron-55 and stable iron by liquid scintillation counting, *Anal. Chem.* **40**, 213.
- [129] B. Denecke, A. Spornol and B. Vaninbroukx, Monitoring of  $^{241}\text{Pu}$ , *Int. J. Appl. Rad. and Isotopes* **19**, 812.
- [130] R.D. Evans, X-ray and  $\gamma$ -ray interactions, in “Radiation Dosimetry”, Vol. I, F.H. Attix and W.C. Roesch, (eds.) (Academic Press, New York), p. 93.
- [131] W.D. Fairman and J. Sedlet, Direct determination of lead-210 by liquid scintillation counting, *Anal. Chem.* **40**, 2004.
- [132] P. Fodor-Csányi and E. Szilágyi-Györi, Considerations on the disturbing of phosphorescence and that of afterpulsing in measuring the absolute activity of low energy beta isotopes, *Int. J. Appl. Rad. and Isotopes* **19**, 712.
- [133] J.A.B. Gibson and H.J. Gale, Absolute standardization with liquid scintillation counters, *J. Phys. E. Sci. Instr.* **1**, 2, 99.



- [134] B.E. Gordon and R.M. Curtis, The anti-quench shift in liquid scintillation counting, *Anal. Chem.* **40**, 1486.
- [135] F.T. Kuchnir and F.J. Lynch, Time dependence of scintillations and the effects on pulse-shape discrimination, *IEEE Trans. Nucl. Sci.* **NS-15**, 3, 107.
- [136] Y.M. Shin, S.H. Ku, C. Glavina and J.A. Rawlins, Satellite pulses from Philips 58 AVP photomultiplier and their effect on ( $\gamma$ ,  $n$ ) time-of-flight spectroscopy, *Nucl. Instr. and Meth.* **58**, 353.
- [137] P. Skarstad, R. Ma and S. Lipsky, The scintillation efficiency of benzene, in "Molecular Crystals", Vol. 4 (Gordon and Breach, New York), p. 3.
- [138] A. Williams, F.A. Hughes and P.J. Campion, Systematic errors in  $4\pi\beta-\gamma$  coincidence measurements, *Metrologia* **4**, 178.
- [139] P. Fodor-Csányi and B. Levay, A new phenomenon to be taken into consideration when investigating phosphorescence by liquid scintillation method, *Int. J. Appl. Rod. and Isotopes* **20**, 223.
- [140] A. Lindenbaum and C. Lund, Alpha counting by liquid scintillation spectrometry of plutonium-239 in animal tissues, *Can. J. Rod. Res.* **37**, 131.
- [141] A.A. Moghissi, H.L. Kelley, J.E. Regnier and M.W. Carter, Low-level counting by liquid scintillation—I. Tritium measurements in homogeneous systems, *Int. J. Appl. Rod. and Isotopes* **20**, 149.
- [142] J.H. Parmentier and F.E.L. ten Hoof, Developments in liquid scintillation counting since 1963, *Int. J. Appl. Rod. and Isotopes* **20**, 305.
- [143] R.E. Shuping, C.R. Phillips and A.A. Moghissi, Low-level counting on environmental krypton-85 by liquid scintillation, *Anal. Chem.* **41**, 2082.
- [144] R. Voltz, Radioluminescence des milieux organiques, in "Actions Chimiques et Biologiques des Radiations", M. Haissinsky, (ed.) (Masson, Paris), p.1.
- [145] Ashcroft, Gamma counting of iodine-125 using a metal-loaded liquid scintillator, *J. Anal. Biochem.* **37**, 268.
- [146] J.B. Birks, Physics of the liquid scintillation process, in "The Current Status of liquid Scintillation Counting", E.D. Bransome Jr. (ed.) (Grune and Stratton, New York), p. 3.
- [147] E.D. Bransome Jr. (ed.), The Current Status of Liquid Scintillation Counting (Grune and Stratton, New York).
- [148] G.A. Bray, Determination of radioactivity in aqueous samples, in "The Current Status of Liquid Scintillation Counting", E.D. Bransome Jr. (ed.) (Grune and Stratton, New York), p. 170.
- [149] P.B. Coates, The edge effect in electron multiplier statistics, *J. Phys. D* **3**, 1290.
- [150] D.M. Hercules, Physical basis of chemiluminescence, in "The Current Status of liquid Scintillation Counting", E.D. Bransome Jr. (ed.) (Grune and Stratton, New York), p. 315.

- [151] J.H. Hildebrand, J.M. Prausnitz and R.L. Scatt, *Regular and Related Solutions* (Van Nostrand, New York), p. 130.
- [152] D.L. Horrocks, Pulse shape discrimination with organic liquid scintillator solutions, *Appl. Spectros. USA* **24**, 397.
- [153] D.L. Horrocks, The scintillator solute, in “The Current Status of Liquid Scintillation Counting”, E.D. Bransome Jr. (ed.) (Grune and Stratton, New York), p. 25.
- [154] W.D. Jeschke, Der Influx von Kaliumionen bei Blättern von *Elodea densa*, Abhängigkeit vom Licht, von der Kaliumkonzentration und von der Temperatur, *Planta* **91**, 111.
- [155] F.A. Johnson, Investigation of source-dependent contribution to photo-multiplier noise, *Nucl. Instr. and Meth.* **87**, 215.
- [156] D.G. Jones and A. McNair, Standardization of radionuclides by efficiency-tracing methods using a liquid-scintillation counter, in “Radioactivity Calibration Standards”, W.B. Mann and S.B. Garfinkel (eds.), NBS Special Publication 331, p. 37.
- [157] V. Kolarov, Y. Le Gallic and R. Vatin, Mesure absolue directe de l’activite des émetteurs bêta purs par scintillation liquide, *Int. J. Appl. Rad. and Isotopes* **21**, 443.
- [158] G. Laustriat, R. Voltz and J. Klein, Influence of the solvent on scintillation yield, in “The Current Status of Liquid Scintillation Counting”, E.D. Bransome Jr. (ed.) (Grune and Stratton, New York), p. 13.
- [159] R. Lieberman and A.A. Moghissi, Low-level counting by liquid scintillation—II. Applications of emulsions in tritium counting, *Int. J. Appl. Rad. and Isotopes* **21**, 319.
- [160] M. Marshall, J.A.B. Gibson and P.D. Holt, An analysis of the target theory of Tea with modern data, *Int. J. Rad. Biol.* **18**, 127.
- [161] M. Marshall, P.D. Holt and J.A.B. Gibson, Physical parameters of radiation determined from the inactivation of ribonuclease, *Int. J. Rad. Biol.* **18**, 139.
- [162] D.E. Persyk, Computer simulation of photomultiplier-tube operation (RCA Corp., Lancaster, Penn.).
- [163] H.H. Ross, Čerenkov radiation: photon yield application to ( $^{14}\text{C}$ ) assay, in “The Current Status of Liquid Scintillation Counting”, E.D. Bransome Jr. (ed.) (Grune and Stratton, New York), p. 123.
- [164] R. Staubert, E. Böhm, K. Hein, K. Sauerland and J. Trumper, Possible effects of photomultiplier afterpulses on scintillation counter measurements, *Nucl. Instr. and Meth.* **84**, 297.
- [165] D.H. Wilkinson and B.E.F. Macefield, The numerical evaluation of radiative corrections of order  $\alpha$  to allowed nuclear  $\beta$ -decay, *Nucl. Phys.* **A158**, 110.
- [166] I.B. Berlman, *Handbook of Fluorescent Spectra of Aromatic Molecules* (Academic Press, New York).

- [167] P.B. Coates, Noise sources in the C31000D photomultiplier, *J. Phys.* **E4**, 201.
- [168] A. Dyer (ed.), *Liquid Scintillation Counting*, Vol. I (Heyden, London).
- [169] K.F. Flynn, L.E. Glendenin and V. Prodi, Absolute counting of low energy beta emitters using liquid scintillation counting techniques, in “Organic Scintillators and Liquid Scintillation Counting”, D.L. Horrocks and C.T. Peng (eds.) (Academic Press, New York), p. 687.
- [170] C. Fuchs, F. Heisel, R. Voltz and A. Coche, Scintillation decay and absolute efficiencies in organic liquid scintillators, in “Organic Scintillators and Liquid Scintillation Counting”, D. L. Horrocks and C. T. Peng (eds.) (Academic Press, New York), p. 171.
- [171] J.A.B. Gibson, Communication to the Symposium on Liquid Scintillation Counting, Brighton, Sept. 1971.
- [172] J.A.B. Gibson, Statistics of the scintillation process and determination of zero probability, Atomic Energy Research Establishment Report AERE-R6919, Harwell, Berkshire.
- [173] J.A.B. Gibson and A E. Lally, Liquid scintillation counting as an analytical tool: a review, *The Analyst* **96**, 681.
- [174] D. L. Horrocks, Obtaining the possible maximum of 90 percent efficiency for counting of  $^{55}\text{Fe}$  in liquid scintillator solutions, *Int. J. Appl. Rad. and Isotopes* **22**, 258.
- [175] D.L. Horrocks and C.T. Peng (eds.), *Organic Scintillators and Liquid Scintillation Counting* (Academic Press, New York).
- [176] D.L. Horrocks, Techniques for the study of eximers, in “Organic Scintillators and Liquid Scintillation Counting”, D.L. Horrocks and C.T. Peng (eds.) (Academic Press, New York), p. 75.
- [177] H.R. Ihle, M. Karayannis and A. P. Murrenhoff, Discrimination between different alpha- and beta-emitters in liquid scintillation counting systems, in “Organic Scintillators and Liquid Scintillation Counting”, D.L. Horrocks and C. T. Peng (eds.) (Academic Press, New York), p. 879.
- [178] P. Jordan, On the statistics of coincidence detection efficiency in liquid scintillation spectrometry, *Nucl. Instr. and Meth.* **97**, 107.
- [179] D.S. Kearns, Reduction of chemiluminescence in both refrigerated and ambient temperature liquid scintillation counting, *Int. J. Appl. Rad. and Isotopes* **23**, 73.
- [180] T.K. Kim and M.B. MacInnis, Combination of liquid scintillation counting and solvent extraction, in “Organic Scintillators and Liquid Scintillation Counting”, D.L. Horrocks and C.T. Peng (eds.) (Academic Press, New York), p. 925.
- [181] K.E. Kirkham and W.M. Hunter (eds.), *Radioimmunoassay Methods* (Churchill, Livingstone, England).
- [182] A. Lindenbaum and M.A. Smyth, Determination of  $^{239}\text{Pu}$  and  $^{241}\text{Am}$  in animal tissues by liquid scintillation spectrometry, in “Organic Scintillators and Liquid

- Scintillation Counting”, D.L. Horrocks and C.T. Peng (eds.) (Academic Press, New York), p. 951.
- [183] W.J. McDowell, Sample preparation in liquid scintillation counting, in “Organic Scintillators and Liquid Scintillation Counting”, D.L. Horrocks and C.T. Peng (eds.) (Academic Press, New York), p. 587.
- [184] W.D. McTaggart and D. Cardus, Tritium oxide movement in body water of healthy and paralytic men, in “Organic Scintillators and Liquid Scintillation Counting”, D.L. Horrocks and C.T. Peng (eds.) (Academic Press, New York).
- [185] T. Radoszewski, The absolute method of measurement of  $^{14}\text{C}$  activity by  $4\pi$  liquid scintillator counting, in “Liquid Scintillation Counting”, Vol. I, A. Dyer (ed.) (Heyden, London), p. 15.
- [186] G. Sheppard and C.G. Marlow, The simultaneous measurement of  $^{51}\text{Cr}$  and  $^{14}\text{C}$  by liquid scintillation counting, *Int. J. Appl. Rad. and Isotopes* **22**, 125.
- [187] J. Spahr and T. Binkert, Zur Absolutmessung der Radioaktivität reiner  $\beta$ -Strahler mit flüssigen Szintillatoren, *Z. f. angew. Math. und Phys.* **22**, 472.
- [188] J.C. Turner, Review number 6: sample preparation for liquid scintillation counting (The Radiochemical Centre, Amersham).
- [189] B. Vaninbrouckx, Absolute high accuracy counting of alpha particles in the presence of beta radiation, in “Organic Scintillators and Liquid Scintillation Counting”, D.L. Horrocks and C.T. Peng (eds.) (Academic Press, New York), p. 913.
- [190] O. Yura, Absolute activity measurement of tritium by liquid scintillation counting, *Radioisotopes* **20**, 17.
- [191] O. Yura, Disintegration rate of americium-241 by liquid scintillation counting, *Radioisotopes* **20**, 31.
- [192] M.A. Crook, P. Johnson and B. Scales (eds.), *An Introduction to Liquid Scintillation Counting* (Heyden, London).
- [193] A. Dyer, Methods of sample preparation of inorganic materials including Čerenkov counting, in “Liquid Scintillation Counting”, Vol. II, M.A. Crook, P. Johnson and B. Scales (eds.) (Heyden, London), chapter 9.
- [194] J.A.B. Gibson, Liquid scintillation counting as an absolute method, in “An Introduction to Liquid Scintillation Counting”, M.A. Crook, P. Johnson and B. Scales (eds.) (Heyden, London), Vol. II, p. 23.
- [195] J.A.B. Gibson and M. Marshall, The counting efficiency for  $^{55}\text{Fe}$  and other E.C. nuclides in liquid scintillator solutions, *Int. J. Appl. Rad. and Isotopes* **23**, 321.
- [196] IEEE standard test procedures for photomultipliers for scintillation counting and glossary for scintillation counting field, IEEE-398.
- [197] J. Klumpar, An improved method for absolute liquid scintillation counting of beta emitters, *Czech. J. Phys.* **B22**, 103.

- [198] H.R. Krall and D.E. Persyk, Recent work on fast photomultipliers utilizing GaP(Cs) dynodes, *IEEE Trans. Nucl. Sci.* **NS19**, 3, 45.
- [199] A.P. Baerg, The efficiency extrapolation method in coincidence counting, *Nucl. Instr. and Meth.* **112**, 143.
- [200] E. Brumix, Mesure de la période de  $^{37}\text{Ar}$ , *Int. J. Appl. Rad. and Isotopes* **24**, 359.
- [201] R. Evans, A tritium tracer technique for the measurement of oil consumption in gasoline and diesel engines, *Int. J. Appl. Rad. and Isotopes* **24**, 19.
- [202] L.H. Handler and J.A. Romberger, The use of a solubilizer-scintillator mixture for counting aqueous systems containing high- and low-energy radionuclides, *Int. J. Appl. Rad. and Isotopes* **24**, 129.
- [203] D.L. Horrock, Energy calibration of a liquid scintillation counter, *Int. J. Appl. Rad. and Isotopes* **24**, 49.
- [204] H. Houtermans, Probability of non-detection in liquid scintillation counting, *Nucl. Instr. and Meth.* **112**, 121.
- [205] H. Ishikawa and M. Takiue, liquid scintillation measurement for beta-ray emitters followed by gamma-rays, *Nucl. Instr. and Meth.* **112**, 437.
- [206] V.E. Lewis, D. Smith and A. Williams, Correlation counting applied to the determination of absolute disintegration rates in nuclides with delayed states, *Metrologia* **9**, 14.
- [207] J.S. Merritt, Present status in quantitative source preparation, *Nucl. Instr. and Meth.* **112**, 325.
- [208] L. W. Price, Practical course in liquid scintillation counting (3 parts), *Laboratory Practice* **22**, pp. 110, 181, 194.
- [209] E. Rapkin, Guide to preparation of samples for liquid scintillation counting (New England Nuclear, Boston, Mass.).
- [210] J. Steyn, Special problems involved in liquid scintillation counting: standardization of  $^{87}\text{Y}$  and  $^{67}\text{Ga}$ , *Nucl. Instr. and Meth.* **112**, 137.
- [211] A. Williams and D. Smith, Afterpulses in liquid scintillation counters, *Nucl. Instr. and Meth.* **112**, 131.
- [212] M. Wolf, Benzolsynthese über Essigsäure zur low-level-Messung von Tritium, *Int. J. Appl. Rad. and Isotopes* **24**, 299.
- [213] E.D. Bransome Jr. and S.E. Sharpe, Measurement of  $^{125}\text{I}$ ,  $^{131}\text{I}$  and other  $\gamma$ -emitting nuclides by liquid scintillation counting, in "Liquid Scintillation Counting: Recent Developments", P.E. Stanley and B.A. Scoggins (eds.) (Academic Press, New York), p. 103.
- [214] M.A. Crook and P. Johnson (eds.), *An Introduction to Liquid Scintillation Counting* (Heyden, London), Vol. III.

- [215] A. Dyer, in "An Introduction to liquid Scintillation Counting", M.A. Crook and P. Johnson (eds.) (Heyden, London), Vol. III.
- [216] B.W. Fox, General criteria for radioassays by colloid scintillation counting under optimal conditions, *Int. J. Appl. Rad. and Isotopes* **25**, 209.
- [217] B.W. Fox, Optimization in colloid scintillation counting, in "An Introduction to Liquid Scintillation Counting", M.A. Crook and P. Johnson (eds.) (Heyden, London), Vol. III, p. 202.
- [218] B. Francois and M. Ghizzo, Liquid scintillation counting of hard  $\beta$ - and  $\gamma$ -emitting radionuclides in biological samples, *J. Nucl. Med. and Biol.* **1**, 147.
- [219] H.J. Gale, Approximations to the pulse height distribution at the output of a scintillation counter, *J. Phys.* **E7**, 258.
- [220] A.M. Herbland and J.F. Bois, Assimilation et minéralisation de la matière organique dissoute dans la mer: méthode par comptage en scintillation liquide, *Marine Biology* **24**, 203.
- [221] D.L. Horrocks, Measurement of low-levels of normal uranium in water and urine by liquid scintillation alpha counting, *Nucl. Instr. and Meth.* **117**, 589.
- [222] D.L. Horrocks, Measurement of  $^{129}\text{I}$  by liquid scintillation and NaI(Tl) scintillation methods, *Nucl. Instr. and Meth.* **120**, 345.
- [223] D.L. Horrocks, Counting vials, in "Applications of Liquid Scintillation Counting" (Academic Press, New York), p. 188.
- [224] Y. Kobayashi and D. V. Maudsley, Recent advances in sample preparation, in "Liquid Scintillation Counting: Recent Developments", P.E. Stanley and B.A. Scoggins (eds.) (Academic Press, New York), p. 189.
- [225] H. Lefeore and A. Godement, Liquid scintillation counting of alpha emitters, *Radioanal. Lett.* **17**, No. 3, 197.
- [226] K.J. Lissant (ed.), Emulsions and Emulsion Technology, in two parts (Marcel Decker, New York).
- [227] G.C. Lowenthal, Comments on aspects of absolute activity measurement obtained by liquid scintillation counting, in "Liquid Scintillation Counting: Recent Developments", P.E. Stanley and B.A. Scoggins (eds.) (Academic Press, New York), p. 349.
- [228] P.J. Malcolm and P.E. Stanley, A stochastic model of the liquid scintillation counting process, in "Liquid Scintillation Counting: Recent Developments", P.E. Stanley and B.A. Scoggins (eds.) (Academic Press, New York), p. 77.
- [229] K. Painter and M. Gezing, The purity of commercial liquid scintillation fluors and the effects of impurities on performance, in "Liquid Scintillation Counting: Recent Developments", P.E. Stanley and B.A. Scoggins (eds.) (Academic Press, New York), p. 183.

- [230] D.E. Persyk and T.T. Lewis, Recent developments in photomultipliers for liquid scintillation counting, in "An Introduction to Liquid Scintillation Counting", M.A. Crook and P. Johnson (eds.) (Heyden, London), Vol. III, p. 21.
- [231] S.E. Sharpe and E.D. Bransome Jr., Surfactants behave as scintillators in liquid scintillation counting, in "Liquid Scintillation Counting: Recent Developments", P.E. Stanley and B.A. Scoggins (eds.) (Academic Press, New York), p. 113.
- [232] B. Sipp and J.A. Miehe, Fluorescence self-absorption effect and time resolution in scintillator counters, Nucl. Instr. and Meth. **114**, 255.
- [233] P.E. Stanley and B.A. Scoggins (eds.), Liquid Scintillation Counting: Recent Developments (Academic Press, New York).
- [234] P.E. Stanley, Fundamental approaches for the assessment of chemical and colour quenching in background and samples, in "An Introduction to liquid Scintillation Counting", M.A. Crook and P. Johnson (eds.) (Heyden, London), Vol. III, p. 65.
- [235] V.R. Switsur, R. Burleigh, N. Meeks and J.M. Cleland, A new sample combustion bomb for radiocarbon dating, Int. J. Appl. Rad. and Isotopes **25**, 113.
- [236] J.H. Thorngate, W.J. McDowell and D.J. Christian, An application of pulse shape discrimination to liquid scintillation alpha spectroscopy, Health Physics **27**, 123.
- [237] BIPM, Procedures for accurately diluting and dispensing radioactive solutions, P.J. Campion (ed.) (Bureau International des Poids et Mesures, F-92310 Sèvres), Monographie BIPM- 1.
- [238] J.B. Birks, An introduction to liquid scintillation counting and solutes and solvents for liquid scintillation counting (Koch-Light Laboratories, Colnbrook, Buckinghamshire).
- [239] A. Chylinski and T. Radoszewski,  $4\pi\beta-\gamma$  and  $4\pi(x, e)-\gamma$  coincidence method with liquid scintillation counter for counting  $\beta$ -particles, Auger electrons or X rays, Nukleonika **20**, 469.
- [240] D.L. Horrocks, Measurement of radioactive noble gases by liquid scintillation techniques, in "Noble Gases", Proc. Symp: Las Vegas, Nevada, 1973, R.E. Stanley and A.A. Moghissi (eds.), p. 199.
- [241] F. B. Johns, Portable apparatus and procedure for the separation of krypton, xenon and methane in air, in "Noble Gases", Proc. Symp. Las Vegas, Nevada, 1973, R.E. Stanley and A.A. Moghissi (eds.), p. 225.
- [242] C. T. Peng, Liquid scintillation and Čerenkov counting, in "Radiochemical Methods in Analysis", D.I. Coomber (ed.) (Plenum Press, London), p. 79.
- [243] R. B. Randolph, Determination of strontium-90 and strontium-89 by Čerenkov and liquid scintillation counting, Int. J. Appl. Rad. and Isotopes **26**, 9.
- [244] T. Smith, How much light from rectangular scintillation counters?, Phys. Med. Biol. **20**, 282.
- [245] D. Smith and L.E.H. Stuart, An extension of the  $4\pi\beta-\gamma$  coincidence technique: two dimensional extrapolation, Metrologia **11**, 67.

- [246] D. Smith, An improved method of data collection for  $4\pi\beta-\gamma$  coincidence measurements, *Metrologia* **11**, 73.
- [247] R.E. Stanley and A.A. Moghissi (eds.), *Noble Gases*, Proc. Symp. Las Vegas, Nevada, 1973.
- [248] M.A. Tamers, Chemical yield optimization of the benzene synthesis for radiocarbon dating, *Int. J. Appl. Rad. and Isotopes* **26**, 676.
- [249] M. Alessio, L. Allegri, F. Bello and S. Improta, Study of the background characteristics by means of a high efficiency liquid scintillation counter, *Nucl. Instr. and Meth.* **137**, 537.
- [250] Alpha Division of the Ventron Corporation (Danvers, Massachusetts), *Organometallics for electronics; Atomic absorption spectrometry standards*, 55K277.
- [251] R.H. Benson, Characteristics of solgel scintillators for liquid scintillation counting of aqueous and non-aqueous samples, *Int. J. Appl. Rad. and Isotopes* **27**, 667.
- [252] BIPM, The detection and estimation of spurious pulses, P.J. Campion (ed.), (Bureau International des Poids et Mesures, F-92310 Sèvres), Monographie BIPM-2.
- [253] B.W. Fox, Specialist periodical report, in “Radiochemistry” (Chemical Society, UK), Vol. 3, p. 108.
- [254] B.W. Fox, Techniques of sample preparation for liquid scintillation counting, in “Laboratory Techniques”, T.S. Work and E. Work (eds.) (North Holland, Amsterdam).
- [255] J.A.B. Gibson, Liquid scintillation counting of novel radionuclides, in “Liquid Scintillation: Science and Technology”, A.A. Noujaim, C. Ediss and L.I. Weibe (eds.) (Academic Press, New York), p. 153.
- [256] D.L. Horrocks, Absolute disintegration rate determination of beta-emitting radionuclides by the pulse height shift-extrapolation method, in “Liquid Scintillation: Science and Technology”, A.A. Noujaim, C. Ediss and L.I. Weibe (eds.) (Academic Press, New York), p. 185.
- [257] D.L. Horrocks, Measurement of  $^{125}\text{I}$  by liquid scintillation methods, *Nucl. Instr. and Meth.* **133**, 293.
- [258] H. Lundquist, K. J. Johanson and G. Jonsson, Improved separation of  $^3\text{H}$  and  $^{125}\text{I}$  spectra in liquid scintillation counting by doping with thallium and lead, *Int. J. Appl. Rad. and Isotopes* **27**, 233.
- [259] P.J. Malcolm and P.E. Stanley, A unified approach to the liquid scintillation counting process—I. A comprehensive stochastic model, *Int. J. Appl. Rad. and Isotopes* **27**, 397.
- [260] P.J. Malcolm and P.E. Stanley, A unified approach to the liquid scintillation counting process—II. Optimising optical design, *Int. J. Appl. Rad. and Isotopes* **27**, 415.



- [261] G. W. Mason, D.N. Metta and D.F. Peppard, The extraction of selected M(III) metals by bis-2 ethylhexyl phosphoric acid in n-heptane, *J. Inorg. Nucl. Chem.* **38**, 2077.
- [262] W.J. McDowell and J. F. Weiss, liquid scintillation alpha counting and spectrometry and its application to bone and tissue samples, in “Liquid Scintillation: Science and Technology”, A.A. Noujaim, C. Ediss and L.I. Weibe (eds.) (Academic Press, New York), p. 17.
- [263] A.A. Noujaim, C. Ediss and L.I. Weibe (eds.), *Liquid Scintillation: Science and Technology* (Academic Press, New York).
- [264] J. Steyn and S.M. Botha, International comparison of the radioactivity of a  $^{139}\text{Ce}$  solution (March 1976): the effect of spurious pulses on the accuracy of the final result, NPRL Research Report FIS 102.
- [265] M.A. Crook and P. Johnson (eds.), *An Introduction to Liquid Scintillation Counting* (Heyden, London), Vol. IV.
- [266] F.E.L. ten Haaf and M.L. Vereijke, A simple mathematical model of a liquid scintillation counter, in “An Introduction to Liquid Scintillation Counting”, M.A. Crook and P. Johnson (eds.) (Heyden, London), chapter 4.
- [267] N.G.L. Harding and J. Dixon, Micellar-based technique for recycling liquid scintillation glass vials, in “An Introduction to Liquid Scintillation Counting”, M.A. Crook and P. Johnson (eds.) (Heyden, London), Vol. IV, p. 85.
- [268] A. Herbland, The prevention of radiocarbon loss in liquid scintillation counting of solutions containing  $^{14}\text{C}$ - $\text{NaHCO}_3$ , *Int. J. Appl. Rad. and Isotopes* **28**, 795.
- [269] International Electrotechnical Commission, Dimensions of vials for liquid scintillation counting (in French and English), IEC-582, Technical Committee 45 (International Electrotechnical Commission, Geneva).
- [270] L.L. Lucas, W.B. Mann and B.M. Coursey, Standardization of  $^{134}\text{Cs}$  by the method of  $4\pi\beta(\text{LS})-\gamma$  coincidence counting, in “Proc. of Septuagenarian Tribute to Professor Dr. A.H.W. Aten”.
- [271] P.J. Malcolm and P.E. Stanley, Systematically understanding the liquid scintillation counting process: A stochastic computer model, in “An Introduction to Liquid Scintillation Counting”, M.A. Crook and P. Johnson (eds.) (Heyden, London), Vol. IV, chapter 2.
- [272] P.J. Malcolm and P.E. Stanley, Liquid scintillation spectrometry: Organizing a methodology, in “An Introduction to Liquid Scintillation Counting”, M.A. Crook and P. Johnson (eds.) (Heyden, London), Vol. IV, chapter 3.
- [273] P.J. Malcolm and P.E. Stanley, Low level counting using liquid scintillation spectrometry: Optimizing optical design, in “Proc. International Conference on Low-Radioactivity Measurements and applications”, P. Provinec and S. Usacev (eds.) (Slovenske Pedagogicke Nakladatelstvo, Bratislava), p. 123.
- [274] G.W. Mason, Private communication (April 1977).

- [275] C.T. Peng, Sample preparation in liquid scintillation counting, Review 17 (The Radiochemical Centre Ltd., Amersham).
- [276] A. Rytz, Report on the international comparison of activity measurements of a solution of  $^{139}\text{Ce}$  (March 1976) (BIPM, F-92310 Sèvres), Rapport BIPM-77/4.
- [277] P.E. Stanley and P.J. Malcolm, Practical liquid scintillation spectrometry: Organizing a methodology, in "An Introduction to Liquid Scintillation Counting", M.A. Crook and P. Johnson (eds.) (Heyden, London), Vol. IV, p. 44.
- [278] A. Szörényi and J. Vágvolgyi, Spetsialnye elektronnye bloki dlia etalonnykh ustanovok izmereniia aktivnosti, vystavka, in "Simposium Metrologia, Moscow".
- [279] M. Alessio, L. Allegri, F. Bella and S. Improta, Influence of quenching on the background of liquid scintillation counters, Nucl. Instr. and Meth. **157**, 579.
- [280] N. S. Huskisson and P. F. V. Ward, A reliable method for scintillation counting of  $^{14}\text{CO}_2$  trapped in solutions of sodium hydroxide, using a scintillant suitable for general use, Int. J. Appl. Rad. and Isotopes **29**, 729.
- [281] J.M.R. Hutchinson, F.J. Schima and B.M. Coursey, Decay of  $^{121}\text{Sn}^m$ , Phys. Rev. **C18**, 400.
- [282] E.F. Joy, Application of liquid scintillation counting (LSC) to isotopes other than carbon-14 and tritium, Chemist-Analyst **67**, 4.
- [283] J.J. Miglio, The determination of americium, curium and californium in biological samples by combined solvent extraction-liquid scintillation counting, Int. J. Appl. Rad. and Isotopes **29**, 581.
- [284] NCRP-58, A Handbook of Radioactivity Measurements Procedures (NCRP Publications, Washington).
- [285] K.D. Neame, Sources of error in the channels ratio method for efficiency determination in liquid scintillation counting, Anal. Biochem. **91**, 323.
- [286] N.J. Parks and K.K. Tsuboi, Emulsion scintillation counting of radium and radon, Int. J. Appl. Rad. and Isotopes **29**, 77.
- [287] J.F. Patterson, B.J.L. Sauerbrunn and L. Battist, A comparison of instrument performance for six liquid scintillation counters, Anal. Biochem. **86**, 707.
- [288] J.G. Ring, A.R. Reich, J.J. Marcec and D.H. Moore, The performance of liquid scintillation counters using large and small vials, in "An Introduction to liquid Scintillation Counting", M.A. Crook and P. Johnson (eds.), Vol. V.
- [289] L.I. Wiebe, Čerenkov counting and Čerenkov-scintillation counting with high refractive index organic liquids using a liquid scintillation counter, Int. J. Appl. Rad. and Isotopes **29**, 391.
- [290] Dow Corning, Selection guide to Dow Corning silicone fluids (Dow Corning Corp., Midland, Mich.).
- [291] J.A.B. Gibson, Private communication (July 1979).

- 
- [292] D.E. Persyk, Personal communication.
- [293] K. Pochwalski and T. Radoszewski, Disintegration rate determination by liquid scintillation counting using the triple to double coincidence ratio (TDCR) method, Institute of Nuclear Research Report INR 1848/OPIDI/E/A, Warsaw, Poland.
- [294] K. Pochwalski, Scintillation quenching by a simple spring diaphragm, Institute of Nuclear Research Report INR 1847/OPIDI/E/A, Warsaw, Poland.
- [295] RCA photomultiplier 8850, RCA photodetector 4501/V4. Electro optics and devices (Solid State Division, Lancaster, Penn.)
- [296] W.B. Whitten and H. H. Ross, Fiber optic waveguides for time-of-flight optical spectrometry, *Anal. Chem.* **51**, 417.
- [297] ANSI, American national standard for specifications of sealed radioactivity check sources for liquid-scintillation counters, Subcommittee N42.2.
- [298] A. McNair, Private communication to the editors.
- [299] National Institute of Metrology, An outline of the Ionizing Radiation Laboratory of the NIM, Peking, Peoples Republic of China.
- [300] R.A. Pacer, Evaluation of counting efficiency, possible container sorption, and quenching characteristics in the liquid scintillation counting of technetium-99, *Int. J. Appl. Rad. and Isotopes*, in press.
- [301] A. Rytz,  $^{134}\text{Cs}$ , Report of an international comparison of activity measurements (October 1978), Rapport BIPM-80/2.





